SYNTHESIS AND CHIROPTICAL PROPERTIES OF α-CHIRAL 2,5-DIAMINOTEREPHTHALATES

A THESIS SUBMITTED TO
THE GRADUATE SCHOOL OF NATURAL AND APPLIED SCIENCES
OF
MIDDLE EAST TECHNICAL UNIVERSITY

BY

DORUK BAYKAL

IN PARTIAL FULFILLMENT OF THE REQUIREMENTS
FOR
THE DEGREE OF MASTER OF SCIENCE
IN
CHEMISTRY

SEPTEMBER 2022

Approval of the thesis:

SYNTHESIS AND CHIROPTICAL PROPERTIES OF α-CHIRAL 2,5-DIAMINOTEREPHTHALATES

submitted by DORUK BAYKAL in partial fulfillment of the requirements for the degree of Master of Science in Chemistry, Middle East Technical University by,

Prof. Dr. Halil Kalıpçılar
Dean, Graduate School of Natural and Applied Sciences _____

Prof. Dr. Özdemir Doğan
Head of the Department, Chemistry _____

Prof. Dr. Akın Akdağ
Supervisor, Chemistry, METU _____

Examining Committee Members:

Prof. Dr. Metin Zora
Chemistry, METU _____

Prof. Dr. Akın Akdağ
Chemistry, METU _____

Prof. Dr. Adnan Bulut
Chemistry, Kırıkkale University _____

Prof. Dr. Ali Çırpan
Chemistry, METU _____

Assoc. Prof. Dr. Serhan Türkyılmaz
Chemistry, METU _____

Date: 02.09.2022

I hereby declare that all information in this document has been obtained and presented in accordance with academic rules and ethical conduct. I also declare that, as required by these rules and conduct, I have fully cited and referenced all material and results that are not original to this work.

Name Last name : Doruk Baykal

Signature :

ABSTRACT

SYNTHESIS AND CHIROPTICAL PROPERTIES OF α-CHIRAL 2,5-DIAMINOTEREPHTHALATES

Baykal, Doruk
Master of Science, Chemistry
Supervisor : Prof. Dr. Akın Akdağ

September 2022, 77 pages

2,5-Diaminoterephthalates (DATs) are known to be intensely colored and fluorescent compounds that are quite open to functionalization. Even though their conjugated structure is significantly shorter/smaller than that of its popular counterparts such as fluoresceins and BODIPYs, they possess comparable optical properties. Most prominently, DATs have been used as organic linkers for metal-organic framework (MOF) materials, and as fluorescent sensors. Despite the existence of chiral DAT derivatives, their chiroptical properties remain obscure. In this study, 6 novel chiral DAT derivatives were designed and synthesized. The designs were first evaluated *in silico* by DFT calculations. Their optical and chiroptical properties were explored using UV-Vis, fluorescence, and circular dichroism (CD) spectroscopies. In general, their optical properties showed dependence on the hydrogen bonding ability of the solvent, and hence showed promising properties as chiroptical sensors.

Keywords: Diaminoterephthalates, Chiroptics

ÖZ

α-KİRAL 2,5-DİAMİNOTEREFİTALATLARIN SENTEZİ VE KİROPTİK ÖZELLİKLERİ

Baykal, Doruk
Yüksek Lisans, Kimya
Tez Yöneticisi: Prof. Dr. Akın Akdağ

Eylül 2022, 77 sayfa

2,5-Diaminotereftalatların (DAT) yoğun renkli ve fonksiyonelleşmeye oldukça açık floresan bileşikler olduğu bilinmektedir. Konjuge yapıları, floreseinler ve BODIPY'ler gibi popüler muadillerinden önemli ölçüde daha kısa/daha küçük olmasına rağmen, karşılaştırılabilir optik özelliklere sahiptirler. En belirgin şekilde, DAT'ler metal organik çerçeve (MOF) malzemeleri için organik bağlayıcılar ve floresan sensörler olarak kullanılmıştır. Kiral DAT türevlerinin varlığına rağmen, kiroptik özellikleri belirsizliğini korumaktadır. Bu çalışmada 6 yeni kiral DAT türevi tasarlanmış ve sentezlenmiştir. Tasarımlar, ilk olarak DFT hesaplamaları ile değerlendirilmiştir. Optik ve kayroptik özellikleri UV-Vis, floresan ve dairesel dikroizm (CD) spektroskopileri kullanılarak araştırıldı. Genel olarak, bu bileşiklerin optik özelliklerinin, çözücünün hidrojen bağı kurma becerisine bağlı olduğu bulundu ve bu nedenle kiroptik sensörler olarak umut verici özellikler gösterdikleri sonucuna ulaşıldı.

Anahtar kelimeler: Diaminoterefitalatlar, Kiroptik.

To my wonderful mother and grandmother…

ACKNOWLEDGMENTS

First and foremost, I would like to express my gratitude to my supervisor Prof. Dr. Akın Akdağ for his guidance, and for numerous opportunities he provided.

I would like to thank the jury members Prof. Dr. Metin Zora, Prof, Dr. Akın Akdağ, Prof. Dr. Adnan Bulut, Prof. Dr. Ali Çırpan, and Assoc. Prof. Dr. Serhan Türkyılmaz for their time and interest in this study.

I would like to thank Assist. Prof. Dr. Yunus Emre Türkmen and Bilge Banu Yağcı for their most needed help with HRMS measurements.

I would like to express my sincerest gratitude to Perihan Öztürk Düzenli, and Dr. Gizem Ünay for teaching practically everything I know for survival in the laboratory. Without their extensive knowledge, kindness, generosity, and seemingly infinite patience, none of this work would be possible.

I would like to thank Hüseyin Kaç for his hard work and most appreciated help with experimentation.

Special thanks to my amazing partner Ege Hoşgör, for always being there for me, through thick and thin, even when vast distances separated us. I will always be grateful to her for being the endless source of inspiration and happiness that she is.

My brothers Bolkar and Can, my little sister Lila, and our wonderful parents Şükrü and Sema: I thank you for your endless support.

Lastly to my framily; Berna, Can, Elif, Ezgi, Görkem, Mert, Oytun, Selena, Serkan, Tarkan, Uzay, and Yeşim. I thank you for everything.

TABLE OF CONTENTS

LIST OF TABLES

LIST OF FIGURES

LIST OF SCHEMES

CHAPTER 1

INTRODUCTION

1.1 Chirality

Chirality is a symmetry property of 3D objects that defines the superimposability of said object on its mirror image. So that an object is said to be chiral, if it is not superimposable on its mirror image. The term “chirality” is derived from the Greek word “κειρ” (cheir), meaning “hand”, in reference to the chiral shape of human hands. A literal translation of “chirality” to plain English would be “handedness”, which is sometimes used in lieu of the Greek-English term. Thus, objects can be classified as right- or left-handed, in terms of symmetry. Some everyday examples of chiral objects would be hands, earphones, shoes, screws, and so on, depicted in Figure 1.

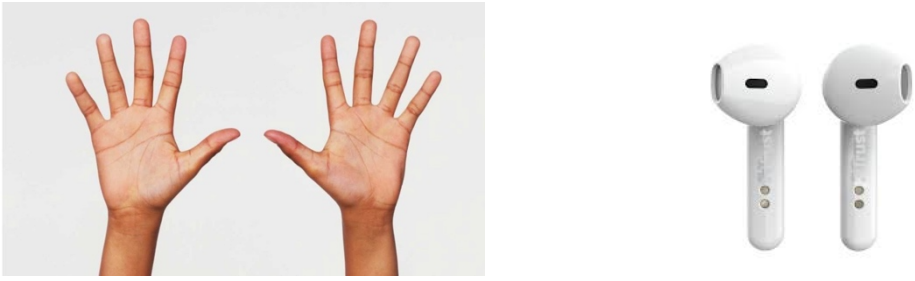

Figure 1 Everyday chiral objects: human hands (left) and earphones (right)

Molecular structures can also exhibit chirality.[1] Pairs of chiral molecules that are non-superimposable mirror images of each other are called “enantiomers”. In fact, most biological structures, such as peptides, carbohydrates, and nucleic acids, are chiral, and their interaction with other chiral structures are crucial in their function.[2]

Many pharmaceuticals also fall to this category due to aforementioned chirality of biological structures.[3] An infamous example would be thalidomide, which was used for the treatment of morning sickness in pregnant women.[4] While one enantiomer works as intended, the "wrongly-handed" counterpart of the drug caused irreversible birth defects in many newborns before being retracted from the market.[5] Even if the correctly handed drug was purely administered, it is partially converted in the body to its maleficent counterpart through the process of "racemization".[6] Structures of the enantiomers of thalidomide are shown in Figure 2. Another example would be the decongestant pharmaceutical *l*-methamphetamine, where its enantiomer *d*-methamphetamine is a potent and addictive central nervous system stimulant, infamously known as "meth".[7]

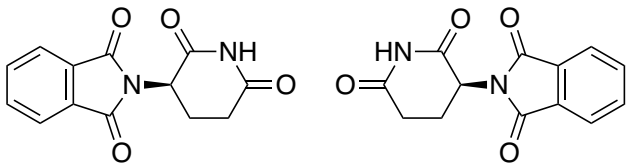

Figure 2 Enantiomers of thalidomide: (R)-thalidomide (left) and (S)-thalidomide (right)

Chiral compounds can be characterized *via* their interaction with plane-polarized light (PPL). For example, a pure solution of a chiral compound such as glucose will rotate the polarization axis of PPL, which can be measured by a polarimeter. The direction of rotation then indicates the handedness of the structure. For instance, (+)-limonene rotates the PPL with a positive angle, whereas its enantiomer (-)-limonene causes a rotation with a negative angle, hence the notation. The chiral properties of light, and interaction of light with chiral compounds will be discussed further in the following section.

1.2 Chiroptical Spectroscopy

1.2.1 Plane-Polarized Light

The wave-particle duality of light is a well-established concept in modern science. From the perspective of its wave-like nature, light consists of oscillations in the electromagnetic field, and has two oscillating vector quantities, an electric and a magnetic component that are perpendicular with respect to each other. This gives light measurable properties such as frequency and wavelength. A beam of light is commonly comprised of many photons, the electric (and thus magnetic) vectors of which are oriented in random directions with respect to each other. Such a light beam is "unpolarized". This unpolarized beam may be "polarized" using a polarization filer. A polarization filter is a material that reflects half of the photons in an unpolarized beam and results in a transmitted polarized beam. All of the electric vectors become aligned in the polarization axis of the filter. It must be noted that, the passage and rejection of randomly oriented photons from a polarization filter is a quantum phenomenon and hence, probabilistic in nature. So that, the filter does not simply reject the photons that are not aligned with the filter; the polarized light beam would be expected to have much less intensity if so. Instead, each photon has a probability of passing or being rejected, depending on their orientation with respect to the filter. This probability, P, is given by *Equation 1* where θ is the angle between the electric vector of the photon and polarization axis of the filter. Regardless of its initial orientation, a photon that passes a polarizing filter will always be aligned with the filter.[8]

$$P = Cos^2(\theta) \qquad \text{Equation 1}$$

1.2.2 Circular and Elliptical polarization of Light, and Optical Rotatory Dispersion

Circularly-polarized (CP) light is a PPL with its electric vector constantly changing in a circular direction. Therefore, CP light may exist in right-handed and left-handed forms, depending on the circular direction in which its electric vector rotates. Theoretically, PPL can be broken down to two CP components that are rotating in opposite directions. If one of these components were to be absorbed (or otherwise eliminated) completely, the remaining beam of light will be CP in a single direction: clockwise (right-handed) or counter-clockwise (left-handed).[9]

When passing through an anisotropic medium, such as an enantiopure solution of a chiral compound, PPL becomes elliptically-polarized (EP). The anisotropy of the medium causes one CP component of PPL to be slowed down more than its counterpart, due to having different refractive indices. This retardation of one component with respect to the other causes the electric and magnetic vectors to be out-of-phase with each other, causing both a net circular polarization and a component along the propagation axis, causing elliptical polarization. This phenomenon is called "optical rotatory dispersion" (ORD). This effect persists as long as the lagging of one component persists. So that if the beam leaves the anisotropic medium, it becomes PPL once again. The ORD effect is more pronounced when PPL passes through an anisotropic medium such as an enantiopure solution of a chiral chromophore that has an absorption band overlapping with that of the incident PPL beam i.e., in the anomalous dispersion zone. [10]

A PPL beam can be EP in empty space if it had passed through a medium that lengthens the path of one of its CP components by exactly a quarter of its wavelength ($\lambda/4$). Such materials are widely used in chiroptical spectrometers, and appropriately named "quarter-wavelength plates".

Passage through a quarter-wavelength plate once more converts the beam back to PPL. The working principle of such materials are not discussed in this report.

1.2.3 Circular Dichroism

Alongside ORD, a chiral chromophore may absorb one CP component of PPL more intensely than its counterpart. This phenomenon is called "circular dichroism" (CD). Technical advances in the manufacture of optical components and in phase-sensitive detection made it later possible to measure the difference of the absorption coefficient, $\Delta\varepsilon_{CD}$, directly. Equation 2 defines this entity. The first commercial CD spectrometers operating in this fashion became available in the 1960s. CD spectroscopy then developed into a subfield of absorption spectroscopy, where it is now an essential tool for biochemical and chiroptical research. The working principle of a CD spectrometer is explained on the block diagram in Figure 3.[8,9]

$$\Delta\varepsilon_{CD} = \varepsilon_L - \varepsilon_R \qquad \text{Equation 2}$$

Figure 3 Block diagram of a CD spectrometer

1.3 2,5-Diaminoterephthalates

2,5-Diaminoterephthalates, or shortly DATs, are the 2,5-diamino-derivatives of p-benzenedicarboxylates, as indicated by the nomenclature. DATs are known to be intensely colored and fluorescent dyes which are relatively smaller structures as compared to their widely-used counterparts such as fluoresceins and BODIPYs. The DAT scaffold is depicted in Figure 4.

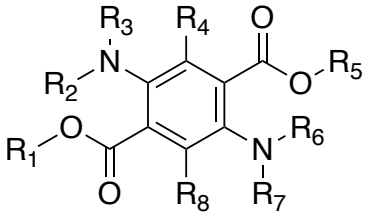

Figure 4 The DAT scaffold

Due to their structure, DATs are quite open to derivatization and thus, their optical properties can be fine-tuned as desired.[11] With 4 on the nitrogens, 2 on the aromatic ring, and 2 on the carboxylates, the DAT scaffold can take up to 8 different functional groups that are in conjugation with the core chromophore. This tunability property of DATs makes them quite viable candidates for bio- and chemosensors, multivalent ligands, and optoelectronic materials. All in all, DATs are an interesting and underrated class of compounds.

1.4 Early History

The first instance of a DAT structure and synthesis was described by Adolf von Baeyer in his 1886 paper "Ueber den Succinilobernsteinsäureäther" meaning "On the esters of succinylsuccinate".[12] As the title suggests, von Baeyer investigated the reactivity of succinylsuccinates, and reported the structure of both its "diimine" condensation product with ammonium acetate, and the corresponding aromatized 2,5-diaminoterephthalic acid diethyl ester. Having already discovered other potent fluorescent dyes such as fluorescein, phenolphthalein, and pyoverdine, von Baeyer speculatively overlooked

DATs[13]. However, the era's chemical community -mostly in Germany- took interest on this interesting structure and investigated further.

Hans Liebermann researched the DAT structure in 1914, and published a detailed guide on the synthesis and properties of various esters of symmetrical, N,N'-disubstituted DATs. In this paper named "Über Ester der Succinylobernsteinsäure und ihre Reaktionen gegen Ammoniak und primäre Amine", meaning "On the esters of succinylsuccinate and their reactions with ammonia and primary amines", Liebermann described the synthesis of numerous aryl and alkyl functionalized DAT and *p*-hydroxyaniline-2,5-dicarboxylate derivatives.[14] On a different publication, he described the synthesis and physical properties of many more arylamino-derivatives of terephthalic acid diesters.[15]

Liebermann was also the first to describe the oxidative aromatization of the diimine intermediate using only atmospheric oxygen. von Baeyer had used elemental bromine in concentrated sulfuric acid for this purpose.[12,14–16]

Uhlig reported in 1956 that 2,5-bis(β-hydroxyethylamino)terephthalic acid gives an intensely red colored product upon oxidation with an agent such as $AgNO_3$, $Hg(NO_3)_2$, and $FeCl_3$.[17,18] The reaction with $AgNO_3$ was found to be quite sensitive and therefore, the use of this DAT compound as an indicator for argentometric titrations was proposed studied. The proposed reaction is depicted on Scheme 1.

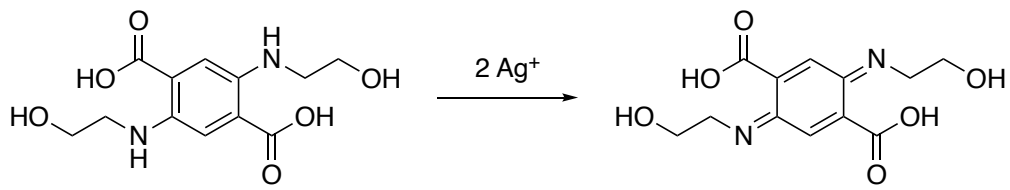

Scheme 1 Oxidation of the indicator with silver cations

Determination of chloride and bromide ions was achieved with an error margin of approximately 1% through titration with standard $AgNO_3$ solution[17–19]. This method was claimed to be advantageous over the other well-established argentometric methods such as the Mohr method by means of easier endpoint detection. Although being promising, this method for argentometric titrations never became a standard like the Mohr, Fajans, and Volhard methods.

Arguably, the most important impact of DATs in history is their use as a precursor to quinacridone class of dyes. Quinacridones are the result of Claisen-type condensation of DATs. They may exist in linear or angular forms as well as cis- and trans-. The first quinacridone was reported in 1896 by Niementowski, who also gave this class of compounds their name.[20] The dye was a result of the reaction between phloroglucinol and anthranilic acid, which was later characterized as an angular trans-quinacridone species.

In 1935, Liebermann was the first to synthesize a linear trans-quinacridone species, and also was the first to do it starting from 2,5-diaminoterephthalic acid.[15,21] Although being underappreciated then, quinacridone dyes are a frequently-used and thus, quite important class of compounds today, especially in the optoelectronics and dye industries. Annually, over 150 derivatives, and over 3400 tons of quinacridones are being prepared in the recent years.[22] Figure 5 shows three example structures for quinacridones.

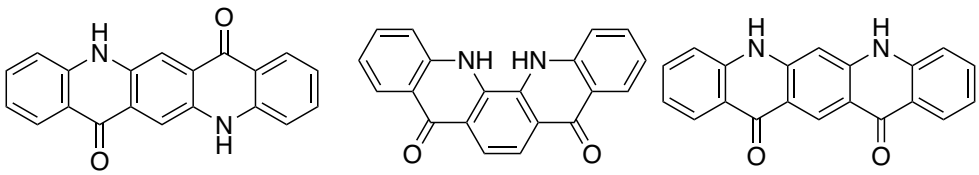

Figure 5 A linear trans-quinacridone (left), an angular cis-quinacridone (mid), and a linear cis-quinacridone (right)

1.5 Synthesis of the DAT Scaffold

1.5.1 From Succinylsuccinates

The two-step synthesis starting from a succinylsuccinate ester and a primary amine is the first described synthesis of the DAT scaffold, and it is still the mostly used one to date[11,12,23–43]. The method is fairly straightforward: two equivalents of a primary amine condense with a succinylsuccinate to form a diimine / double-enamine intermediate. This intermediate is then oxidized into the aromatic final DAT product. The modern conditions that have been utilized for this synthesis are summarized on Table 1. The general reaction scheme is shown on Scheme 2.

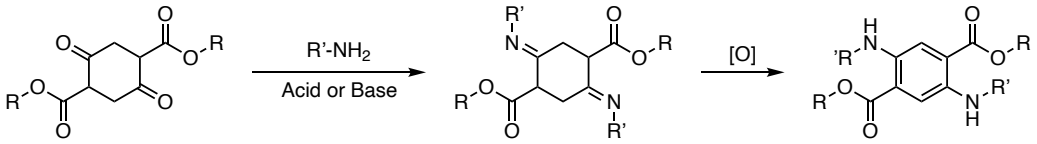

Scheme 2 Synthesis from succinylsuccinates

In addition to these, Huang et al. reported a synthesis of dimethyl 2,5-diaminoterephthalate from the condensation and consecutive elimination of dimethyl succinylsuccinate and phenylhydrazine in acidic medium.[44]

Table 1 Commonly utilized conditions from the literature

Succinylsuccinate	Amine (eq.)	Acid/Base (eq.)	Solvent	Oxidant (%yield)	Ref.
Dimethyl	N-Boc-ethylenediamine (5)	Acetic acid (0.7)	Toluene (Dean-Stark)	Air in DMF (71)	[30]
Benzyl Methyl	Methylamine (20)	Acetic acid (20)	Toluene (Dean-Stark)	Air in toluene (87)	[23]
Benzyl Methyl	Aniline (20)	HCl (4)	Toluene	Air in toluene (85)	[25]
Diethyl	*p*-iodoaniline (20)	HCl (cat.)	Toluene	Air in toluene (86)	[34]
Benzyl Methyl	Ammonia (20)	-	Ethanol	Air in DCM (61)	[11]
Dimethyl	3-chloropropanamine (4)	DMAP (2)	Ethanol	Air in ethanol (85)	[45]
Dimethyl	*p*-(trifluoromethyl)aniline	Acetic acid	Ethanol	Iodine in chloroform (65)	[46]
Diethyl	Alanine ethyl ester (2)	Triethylamine (10)	Ethanol	Bromine in ethanol (25)	This work

1.5.2 From 2,5-Dihaloterephthalates

It is well-known that aromatic halides can give coupling reactions with electrophiles such as amines under catalytic conditions. One example to such reaction would be copper catalyzed Ullmann-type coupling.[47] This strategy is mainly utilized for the synthesis of aza-heteroaromatic derivatives such as 2,5-bis(imidazolyl)- and 2,5-bis(triazolyl)terephthalates.[48–50] The general reaction scheme is shown on Scheme 3.

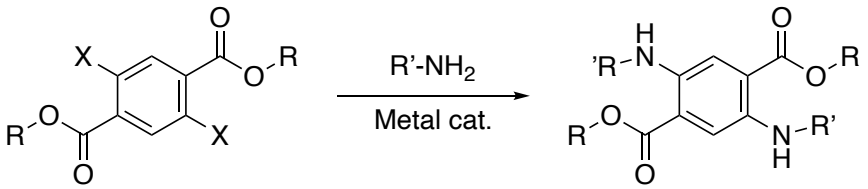

Scheme 3 Synthesis from dihaloterephthalates

1.5.3 From Imidoesters

The rearrangement of an imidoester to an amide is known as Chapman rearrangement. Chapman reported the double rearrangement of a 2,5-bis(imidoester) derivative of a terephthalate diester into a 2,5-bis(amido) terephthalate[51]. This amide can then be hydrolyzed into the free amine. Obviously, if the ester functionality is desired to be maintained, selective amide hydrolysis conditions must be employed. Therefore, this method could be a useful pathway to amide functionalized DATs, instead of the aromatic amine functionality. Synthesis of such imidoesters is not

discussed in this report. The general reaction scheme is shown in Scheme 4.

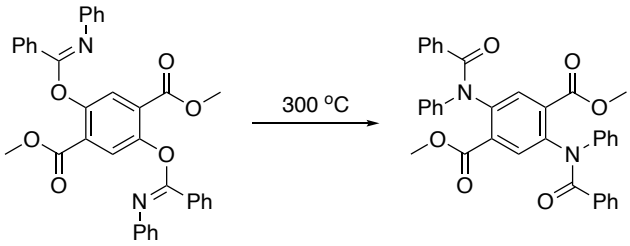

Scheme 4 Synthesis from imidoesters

1.5.4 From Pyromellitimide

It was reported by Hojo *et al*. that pyromellitimide can undergo a double Hoffmann rearrangement to yield 2,5-diaminoterephthalic acid.[52] The reported yields are around 30% which is not quite feasible as compared to succinylsuccinate pathway. The general reaction scheme is shown in Scheme 5.

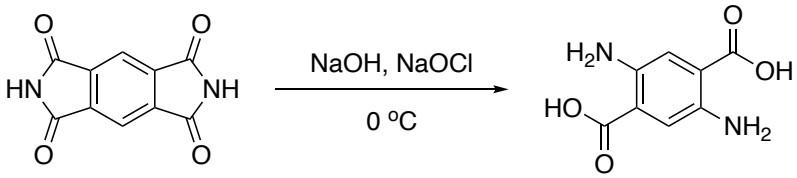

Scheme 5 Synthesis from pyromellitimide

1.6 Applications

These unique properties of the DAT motif make it desirable for several applications in a broad spectrum of chemical research. The most prominent ones of these applications are as multifunctional ligands in metal-organic frameworks, optoelectronics, and as chromophores and fluorophores for chemo- and biosensing applications.

1.6.1 Metal-Organic Frameworks

Metal-organic frameworks (MOFs) are a special type of crystalline organometallic compounds that may exist in one-to-three-dimensional coordination networks. They are generally semiconducting, microporous materials that can have a large surface area. The porosity and the bandgap of these materials can be tailored via adjustments to the ligands and metal coordination centers[53–55]. These properties of MOFs make them desirable for research on gas-storage, semiconductors, photoelectronics, and catalysis.

MOFs with organic ligands that are strong chromophores –such as DATs– studied for their sensing and photocatalytic properties. The most studied application of DATs in MOFs is the photocatalytic transformation of atmospheric CO_2 into useful, energy-dense organic materials i.e., artificial photosynthesis. Many MOF materials into which the DAT scaffold was incorporated were prepared and studied. The preparations, and detailed crystal structures and mechanisms of action of such materials are out of the scope of this report.

1.6.2 DAT Containing MOFs

The bandgap is arguably the most important feature of a MOF photocatalyst. The terephthalate structure has been a popular choice of organic linker for MOFs. It was demonstrated by Usman *et al.* that the bandgap of a MOF material can be reduced by adding electron-donating substituents, such as amines, on the terephthalate linkers, among other strategies. TDDFT calculations by Voort *et al.* confirms and extends on this principle to show the increased effect of doubly substituted terephthalate linkers such as DATs.[56] Guo *et al.* reviewed the principles of bandgap engineering for MOF materials, in detail.[57,58]

1.6.3 Fluorescent Biosensors and Chemosensors

The research on life-sciences depends heavily on optical techniques such as fluorescence microscopy. The tunable absorptive and emissive properties of DATs make them viable candidates for bio- and chemosensors.

1.6.4 Turn-on Sensors for Thiols

By introduction of quenching functional groups, "turn-on" type sensors can be designed. For instance, a maleimide functional group can be utilized in the design of a turn-on sensor for thiols, exploiting the well-known click reaction. This strategy was employed by Christoffers, Sulmann *et al.* in the design of biosensors that are sensitive to the free thiol moieties on proteins.[24,25,30,39,41,43]

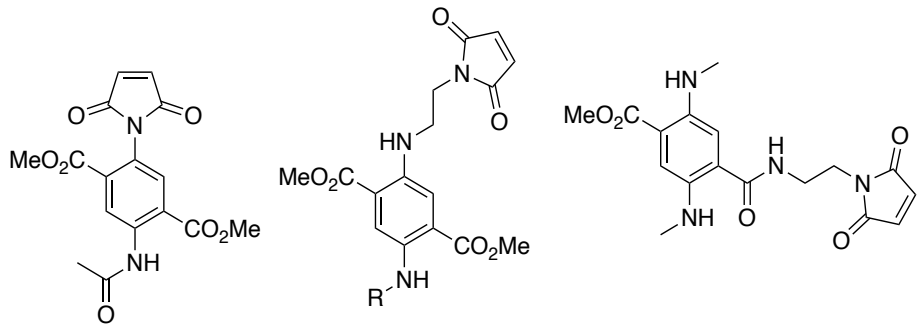

Figure 6 Structures of Compound X, Compound Y, and Compound Z

Figure 6 depicts three generations of maleimide functionalized thiol sensors.[30,43] Compound X is the first generation in which the maleimide group is in direct conjugation with the central ring. Therein, both 2 and 5 positions are of amide functionality instead of amine. This compound is reported to have an absorption maximum ($\lambda_{abs,\ max}$) at 333 nm and shows no fluorescence. Upon click reaction with a thiol, this chromophore becomes emissive with an emission maximum ($\lambda_{em,\ max}$) at 396 nm and with a fluorescence quantum yield (Φ_F) of 0.59.

Compound Y is the second generation on which the 2 and 5 positions are of amine functionality, and the maleimide moiety is out of conjugation with the chromophore core.[39,41,43] This design exploits better -as compared to amides- electron donating properties of amines. Interestingly, Compound Y retains the turn-on property although the

quenching group being out of conjugation, possibly suggesting an intramolecular excited-state energy transfer between the cycles. As expected, the amine groups caused a bathochromic shift on the absorption where $\lambda_{abs, max}$ = 467. Its "activated" counterpart fluoresces with $\lambda_{em, max}$ = 559 nm, and Φ_F = 0.80. This dramatic increase in Φ_F as compared to Compound X may again be attributed to amines being better electron donors than amides. The preparation of this compound suffers from insufficient yields and therefore, a third generation was designed to address this issue.

The third generation of these sensors is Compound Z where the maleimide moiety is attached to one of the "carboxylate" sites, with both methylamino-substituents at positions 2 and 5.[24,25] This compound absorbs with $\lambda_{abs, max}$ = 454 nm and shows a very faint emission with $\lambda_{em, max}$ = 568 nm, Φ_F = 0.001. Nevertheless, Compound Z retains the turn-on property as Φ_F = 0.08 for the "activated" sensor, corresponding to an 80-fold increase in emission.

The mechanism of action of these turn-on thiol probes were explained by the authors through TD-DFT calculations. The proposed mechanism is as follows: The post-click-reaction "activated" structures show regular absorptive and emissive properties where HOMO is the π and LUMO is the π^* orbitals. Whereas for the "inactive" structure, LUMO lies on the maleimide moiety, and the π^* orbital becomes LUMO +1. For the "inactive" structure, HOMO to LUMO transition is symmetry-disallowed and absorption occurs via HOMO to LUMO+1 transition. The excited state energy is then dissipated in a non-radiative fashion. This path is alleviated upon the click reaction through the dissipation of maleimide double-bond, hence the turn-on behavior.

1.6.5 Bifunctional Dyes for Protein Site-Specific Sensing

The first instance of a bifunctional DAT sensor, Compound P, was reported by Freimuth *et al.*, where the DAT scaffold is decorated with both maleimide and alkyne functionalities.[25] The strucures are shown on Figure 7.

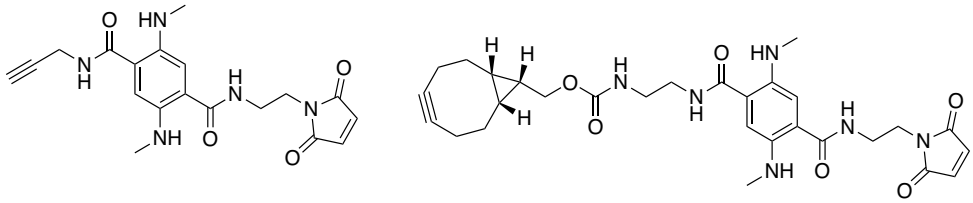

Figure 7 Structures of Compound P (left) and Compound Q (right)

The main idea behind this design is to exploit alkyne-azide type click reaction in addition to the maleimide-thiol strategy. This compound was designed for a specific purpose: to investigate the dimerization behavior of recoverin as a function of matrix Ca^{2+} concentration. The conformation of recoverin is dependent on Ca^{2+} concentration. A myristoyl group is attached to the N-terminus, which is buried in the protein interior at low Ca^{2+} concentration. This myristoyl group may be replaced with an ω-azido analogue, which can then undergo the triazole click reaction and attach to the sensor in this specific site. The maleimide moiety may then attach to another recoverin at the open cysteine residue, triggering the turn-on function.

Compound P could be considered the first generation of such a DAT compound. This compound is reported to show a $\lambda_{abs,\ max}$ = 416 nm, and a faint emission with $\lambda_{em,\ max}$ = 551 nm, Φ_F = 0.003. Upon conjugate addition of a thiol to the maleimide moiety, emission intensity increases 10-fold with Φ_F = 0.03. Compound P suffers from low solubility in aqueous media as well as unsatisfactory yields for the triazole-click reaction, without a catalyst.

Reported by Wallisch *et al.*, Compound Q is considered to be the second generation of such DAT sensors where the terminal alkyne moiety is replaced with the highly strained cyclopropane-fused cyclooctyne group.[35] The high ring strain is known to increase the reactivity of the alkyne towards azides, alleviating the need for a catalyst to give the triazole-click reaction with satisfactory yields.[59] This compound shows an absorption with a $\lambda_{abs, max}$ = 429 nm, and an emission with $\lambda_{em, max}$ = 556 nm, Φ_F = 0.02. Upon conjugate addition of a thiol to the maleimide moiety, emission intensity increases almost 20-fold with Φ_F = 0.41.

1.6.6 A Cysteine-Homocysteine Discriminative Turn-On Sensor

Since cysteine (Cys) and homocysteine (HCys) are quite similar in structure, their chemical reactivity is also similar. This makes them difficult to differentiate for a thiol sensor such as the ones in the previous sections. Instead of a maleimide-thiol reaction, Shimizu *et al.* employed thioester chemistry in the design of a turn-on fluorescent sensor, Compound R, for thiols that can discriminate between Cys and HCys. Figure 8 shows the structure of compound R, which is not fluorescent itself.

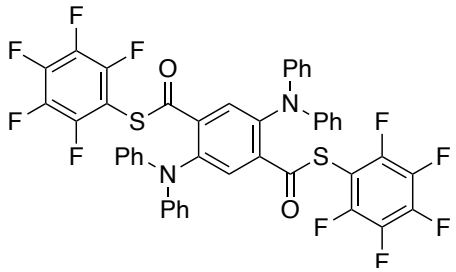

Figure 8 Compound R

This design exploits the different tendencies of β- and γ-aminoalkyl arylthioates towards rearrangement into their respective β- and γ-mercaptoarylamides. Wherein, the γ-amino derivatives rearrange much slowly than their β-amino counterparts. The product of such rearrangement, that is depicted on Scheme 6, is fluorescent unlike its precursor. Hence, the turn-on function.

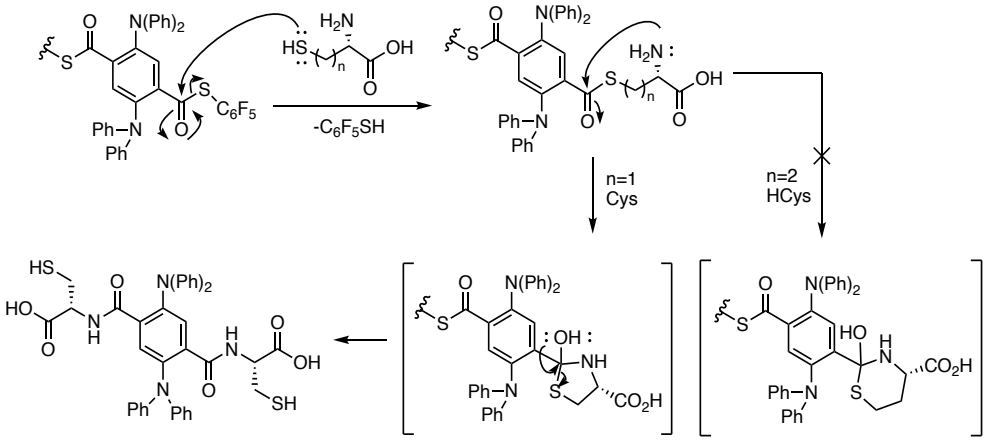

Scheme 6 Mechanism of action of Compound R

1.6.7 A Ratiometric Sensor for Gaseous H_2O_2

A ratiometric fluorescent sensor for gaseous hydrogen peroxide was developed by Zang *et al.*, which exploits the fluorescence resonance energy transfer (FRET) phenomenon.[60]

Figure 9 gives the structure of the sensor, Compound H. It is basically an amine protected analogue of diethyl 2,5-diaminoterephthalate. This sensor takes advantage of the "deprotection" reaction of this type of boronate esters. The product of this reaction is the "free" diethyl 2,5-diaminoterephthalate, which is known to be a strongly fluorescent compound with a $\lambda_{em,\ max}$ = 574 nm. The protected sensor is also fluorescent with and a $\lambda_{em,\ max}$ = 500 nm.

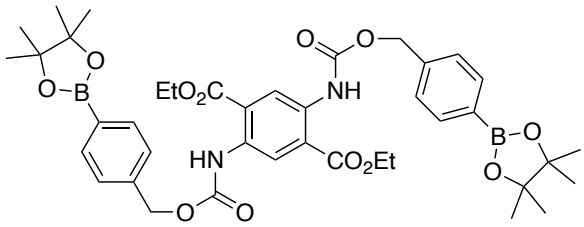

Figure 9 Compound H

The sensory material was prepared by coating a quartz surface with Compound H and probing with a beam of 350 nm wavelength. A dilute gaseous mixture of N_2 and H_2O_2 was then flowed above the surface. As a result, some of the sensor molecules become deprotected. The protected and deprotected fluorophores which are in close proximity then form a FRET pair. This allows an emission at 574 to be observed even though the deprotected sensor has a quite low excitation intensity at 350 nm. The ratio of the detected emission intensities at 500 nm and 575 nm was then used to calculate the concentration of gaseous H_2O_2.

1.7 A DAT-Fullerene (C_{60}) Conjugate for Artificial Photosynthesis

Mimicking the natural process of photosynthesis has been on the agenda of chemical research for decades. Many different strategies were developed, including the utilization of MOFs and organic chromophores as electron capture and transfer agents. Among the energy- and electron-accepting moieties, fullerene (C_{60}) has become the most promising one due to its unique physical and chemical properties. It can be easily ligated to dyes and other larger molecular systems by cycloaddition reactions. Several dye–fullerene conjugates, so called dyads, have been prepared in the past years. One such structure bearing a DAT group, Compound J, was reported by Freimuth, Rozzi, *et al.*, the structure of which is depicted on figure 8. Christoffers and Bushbeck reported a second generation of such dyads, Compound K,

incorporating a retinal moiety in addition to the C_{60}. Figure 10 shows both of their structures.

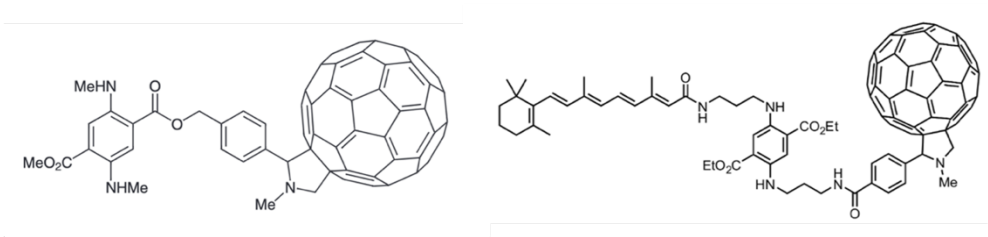

Figure 10 Compound J (left), and Compound K (right)

CHAPTER 2

AIM OF THE STUDY

2,5-diaminoterephthalates (DATs) are known to be intensely colored and fluorescent dyes which are relatively smaller structures as compared to their widely-used counterparts such as fluoresceins and BODIPYs. These properties of DATs make their absorptive and emissive qualities tunable to a desired function. This tunability property of DATs makes them quite viable candidates for bio- and chemosensors, multivalent ligands, and optoelectronic materials. Although chiral derivatives of DATs have been prepared and studied, their chiroptical properties, and their potential for chiral recognition, remain obscure. The aim of this study is to study chiral DAT derivativatives and to explore their chiroptical properties with an emphasis on chiral recognition. For this purpose, three enantiomeric pairs of novel, chiral DAT derivatives were synthesized. Chiral moieties that are attached to the DAT scaffold were chosen to be: (R)- and (S)-methylbenzylamine; D- and L-phenylalanine; D- and L-alanine. Through these designs, that are shown in Figure 11, the effect of benzyl, methyl, and carboxylate moieties on the chiroptical properties of DATs were aimed to be studied.

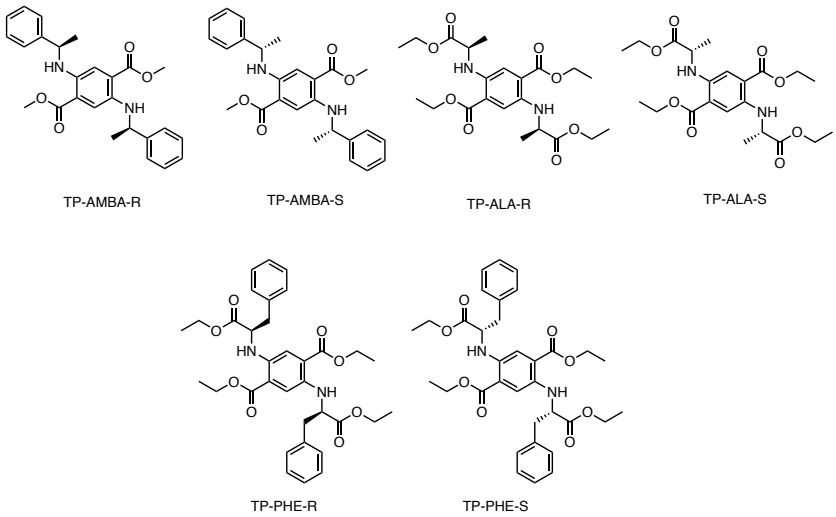

Figure 11 Structures and codenames of the studied DAT derivatives

CHAPTER 3

RESULTS AND DISCUSSION

3.1 Synthesis

At the beginning of this study, we were motivated by the synthesis of **1**. This compound was designed to show singlet fission, in which one singlet state dissociates into two triplet states. This process is the reverse process of triplet-triplet annihilation.[61] Figure 12 shows the structure of **1**.

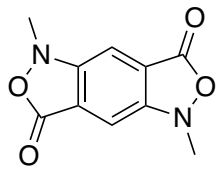

Figure 12 Structure of **1**

Towards synthesis of this compound, we started with bromination of terephthalaldehyde at 2 and 5 positions. The dibromination product **2**, was obtained in 64% yield using N-bromosuccinimide in concentrated sulfuric acid at 65 °C. Oxidation of **2** in basic aqueous medium with $KMnO_4$ to the corresponding dicarboxylic acid **3** was achieved in 71% yield. Resulting **3** was then subjected to Fischer esterification in dry methanol, using $SOCl_2$ as an *in situ* source of HCl.

Esterification resulted in the corresponding dimethyl ester **4**, in 70% yield. The diester **4** was treated with NaN_3 in the presence of CuI and L-proline in DMSO. This reaction resulted in the 2,5-diamino product **5**, in 9% yield. Overall, **5** was obtained

in 4 steps from terephthalaldehyde in 3% yield. The reactions so far are organized on Scheme 7.

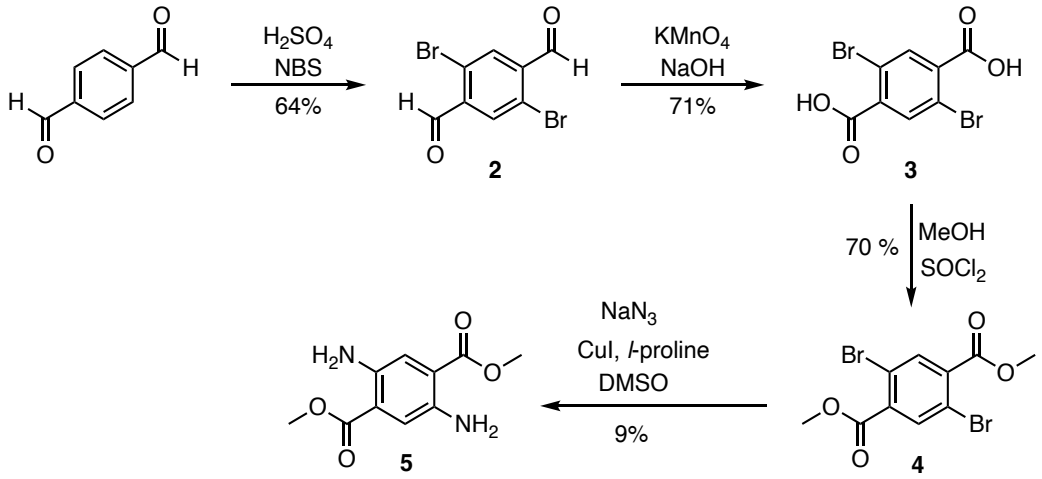

Scheme 7 Synthesis of **5**

Compound **5** piqued our interest immediately as it was found to be intensely colored and strongly fluorescent even to the naked eye. With these results in hand, we decided to further our study focusing the optical and chiroptical properties of chiral 2,5-diaminoterephthalate (DAT) derivatives.

In order to install chiral amines onto the terephthalate skeleton, one might think of Buchwald-Hartwig reaction however, esters being susceptible to amidation in Buchwald-Hartwig conditions was discouraging. With this in mind, we turned our attention to another route.[62,63]This route starts from the Fischer esterification of succinic acid. Synthesis of the diesters of succinic acid was achieved by dissolving succinic acid in the related alcohol and treating with $SOCl_2$, followed by reflux for 2 hours. Both the dimethyl and diethyl esters of succinic acid, **6** and **7** respectively, were obtained with this method in 90-95% yield. The diesters were then subjected to double Claisen condensation in the presence of NaH in THF, resulting both **8** and **9** in 46-48% yield. Overall, succinylsuccinates were synthesized in 2 steps from

succinic acid in approximately 45% yield. The related reactions are organized on Scheme 8.

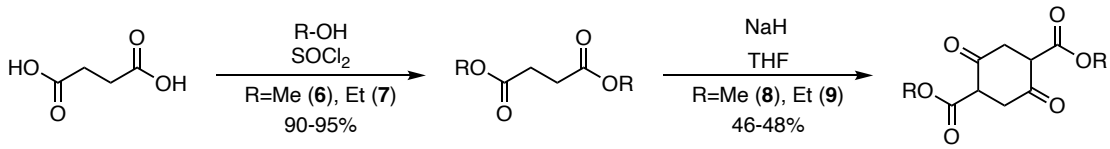

Scheme 8 Synthesis of **8** and **9**

Figure 13 shows the ^{1}H NMR spectrum of **8** which was recrystallized from chloroform over extended period of time. The resultant succinylsuccinates were found to exist in enol-form in chloroform, as indicated by the vinylic OH protons resonating around 12 ppm. The compound should be stored as solid under inert atmosphere. Otherwise, exposure to ambient oxygen aromatizes the compound into **10**. The peaks for **10** can be seen on the spectrum at 4.0, 7.5, and 10.2 ppm on this

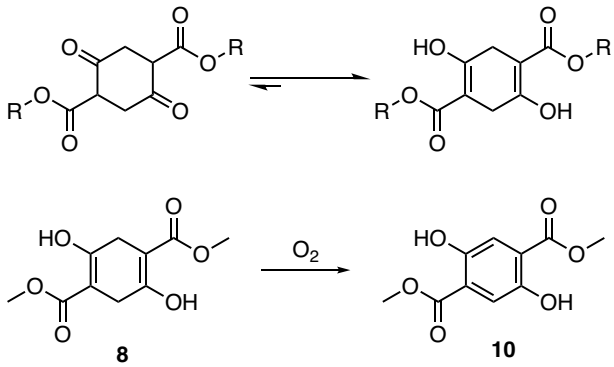

Scheme 9 Keto-enol tautomerization of succinylsuccinates (top), aerobic oxidative aromatization of **8** into **10** (bottom)

contaminated sample of **8** where the integrals suggesting 14% presence of **10**. Scheme 9 shows the related reactions.

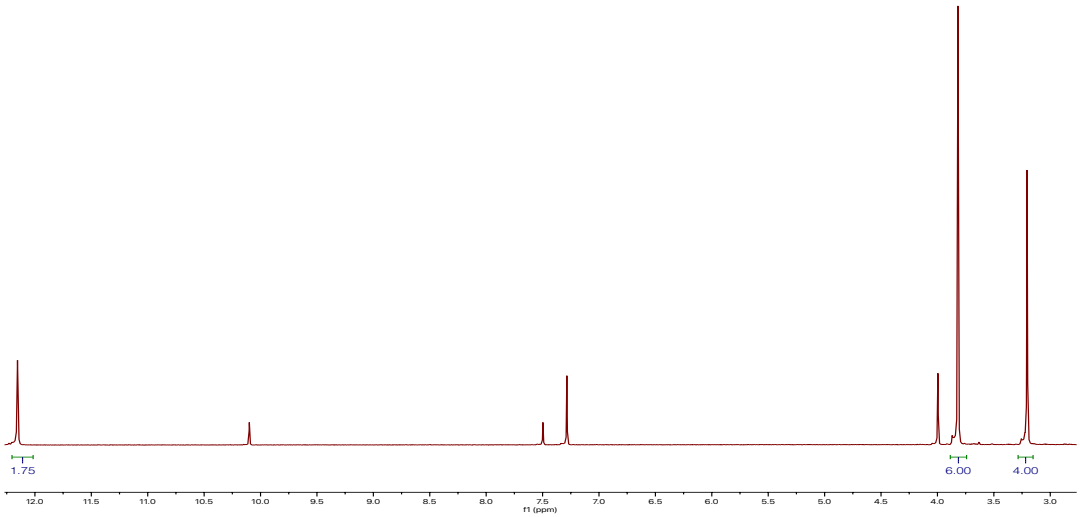

Figure 13 ^{1}H NMR Spectrum of **8** contaminated with **10**. Although the synthesis was carried out under inert atmosphere, recrystallization over extended period of time under air caused **10** to form.

With succinylsuccinates ready as starting materials, the von Baeyer method was used to synthesize **11** in an attempt to replicate the literature.[62,64] A methanolic solution of **9** was treated with a 40% aqueous solution of 10 equivalents of methylamine. After refluxing overnight, the volatile species were evaporated *in vacuo* and the residue was redissolved in ethanol. Consecutive treatment with 0.9 equivalents of elemental bromine resulted in **11** in 17% yield. Scheme 10 shows the synthesis of **11**.

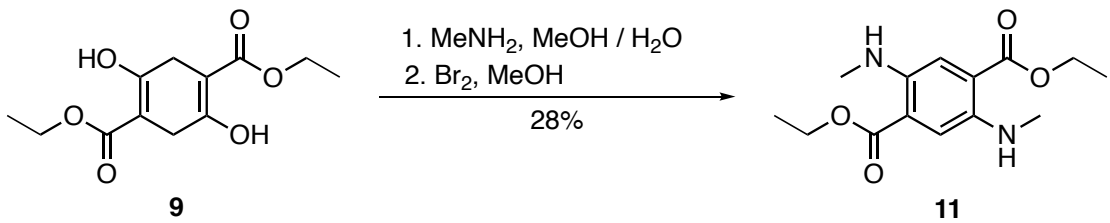

Scheme 10 Synthesis of **11**

In order to evaluate the effect of benzyl group on synthesis, benzylamine substituted **12** was prepared. Treatment of **8** with 10 equivalents of benzylamine following a

similar procedure for the synthesis of **11** did not yield **12** in detectable amounts even though anhydrous conditions were utilized. Alternatively, 2 equivalents of benzylamine were used in the presence of 10 equivalents of triethylamine, in anhydrous ethanol. This method resulted in **12** in 28% yield. Scheme 11 shows the synthesis of **12**.

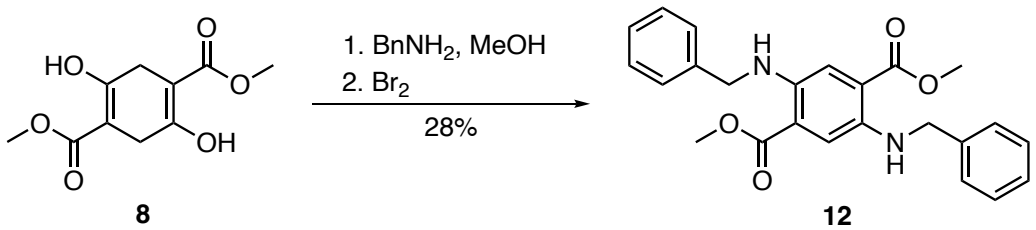

Scheme 11 Synthesis of **12**

Since the preparation of **12** gave the best results, the first chiral DAT derivatives **TP-AMBA-R** and **TP-AMBA-S** were prepared using the same method, with (R)- and (S)-α-methylbenzylamine (MBA) as substituents, respectively. **TP-AMBA-R** and **TP-AMBA-S** were obtained accordingly in 18% and 26% yield. Scheme 12 shows the syntheses of **TP-AMBA-S** and **TP-AMBA-R**.

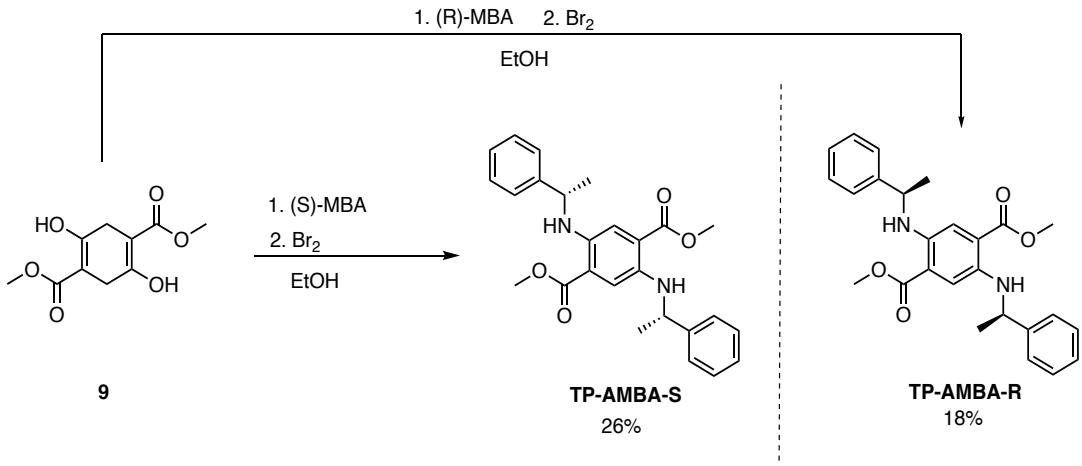

Scheme 12 Synthesis of **TP-AMBA-S** and **TP-AMBA-R**

For the synthesis of aminoacid substituted DATs, the same conditions with that of **TP-AMBA-**and **S TP-AMBA-R** was used. Initially, D-alanine was used as it is for imine formation. Even though imine formation was favored under acidic conditions,

using the bare aminoacid did not yield the desired product. This is arguably due to the sparing solubility of the zwitterionic aminoacid in ethanol. Extending the reaction time did not affect the outcome. For this reason, ethyl esters of alanine and phenylalanine enantiomers were prepared. Esterification of aminoacids were performed by treating a suspension of the related aminoacid in ethanol with $SOCl_2$, followed by reflux for 2 hours. This method gave the ethyl esters of the aminoacids in over 94% yield. Scheme 13 shows the syntheses of **TP-ALA-S** and **TP-ALA-R**.

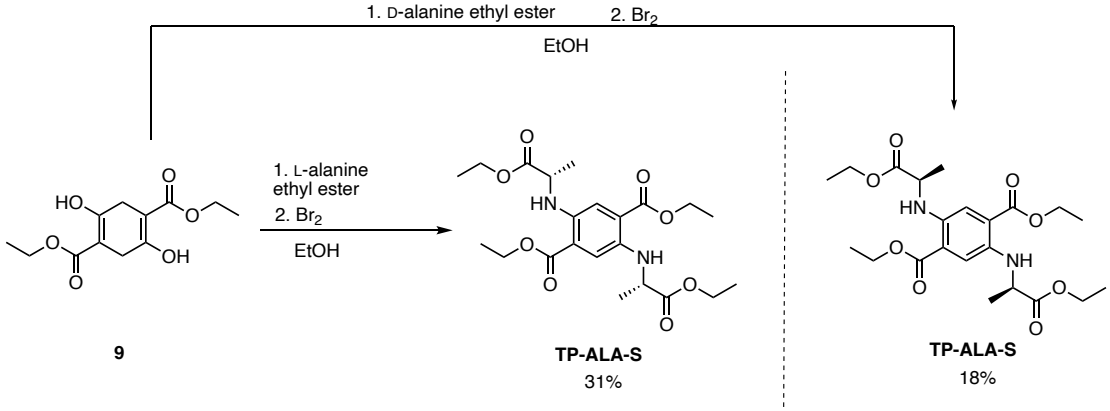

Scheme 13 Synthesis of **TP-ALA-S** and **TP-ALA-R**

Syntheses of alanine and phenylalanine ester substituted DATs were achieved using the same conditions. Alanine ethyl ester substituted **TP-ALA-S** and **TP-ALA-R** were obtained in 31% and 18% yield, respectively. **TP-PHE-S** and **TP-PHE-R** were obtained in 12% and 9% yield, respectively. Scheme 14 shows the related syntheses.

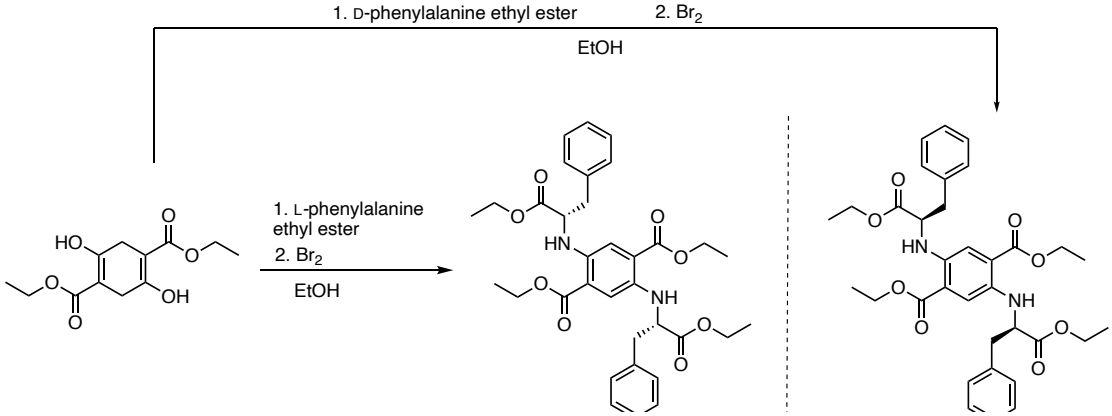

Scheme 14 Synthesis of **TP-PHE-S** and **TP-PHE-R**

Purification of these compounds was quite challenging. For every aminoacid ester substituted species, silica column chromatography was carried out at least twice since some impurities had impractically similar polarities with that of the desired products. In each case, multiple recrystallizations were performed after column chromatography in order to increase the purity. Wherein **13** was detected as well as "asymmetric" products that are the result of the reaction between **9** and only one equivalent of the chiral amine.

3.2 UV-Vis studies

UV-VIS spectrum of **11** was measured in chloroform. λ_{max} was found to be at 485 nm. The UV-VIS spectrum of **12** in chloroform shows a λ_{max} at 480 nm. This shows that such compounds are sensitive to the substituents attached to the amines. Figure 14 shows the superimposed UV-Vis spectra of **11** and **12**.

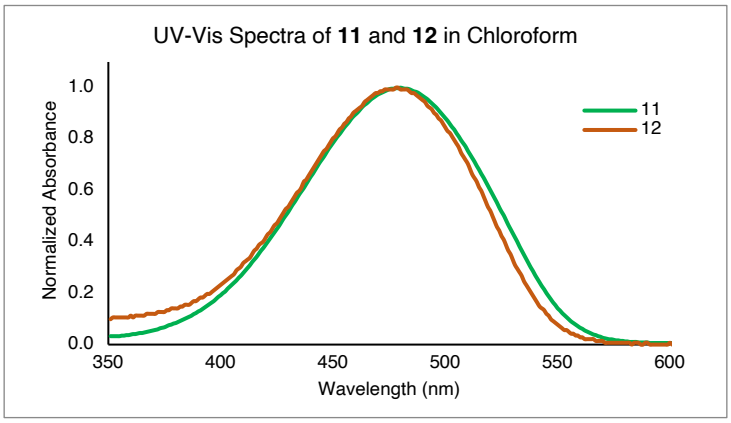

Figure 14 UV-VIS spectra of **11** and **12** in chloroform

This difference is attributed to geometric differences between **11** and **12**. Previously calculated structures in our laboratory showed hydrogen bonding between NH and the carbonyl oxygen gave the lowest energy.[65] Based on these results, the geometries of these compounds were optimized at the level of M06/6-31G(d) as implemented in Gaussian 09 software.[66] Figure 15 shows these structures.

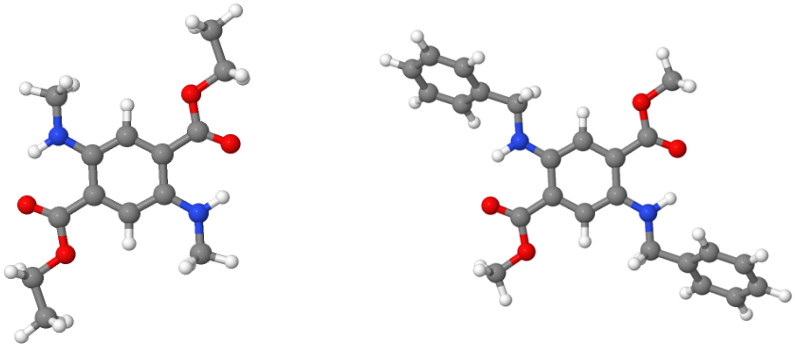

Figure 15 Optimized geometries of **11** (left) and **12** (right)

With these results in hand, we recorded the UV-VIS spectra of **TP-AMBA-S** in different solvents. It was found that, the λ_{max} in solvents that can act as H-bond donor or acceptor, namely in acetonitrile and methanol, was found to be 470 nm. In chloroform, 10 nm of redshift on λ_{max} was observed. This is due to competition of intramolecular H-bonding against molecule-solvent H-bonding. This affects the planarity and hence the overlap of p-orbitals. However, H-bonding between molecule and the solvent brings steric effects, which in turn deviates the molecule from planarity. This molecule was optimized at the level of M06/6-31G(d) as implemented in Gaussian 09 software. HOMO and LUMO of this molecule show that any deviation from the calculated molecular structure will affect the π-delocalization. Figure 19 shows the HOMO and LUMO of **TP-AMBA-R** calculated on its optimized geometry.

As to the aminoacid ester modified DATs, the UV-VIS spectra of **TP-ALA-S** and **TP-PHE-S** was taken in chloroform, acetonitrile, and methanol. The effect of the solvent on the absorption spectrum was found to be less pronounced as compared to that of **TP-AMBA-S**. Figure 16 shows these spectra. For both species, UV-VIS spectra show a λ_{max} at 453 nm in acetonitrile and methanol, whereas in chloroform, 7 nm redshift was observed. The UV-VIS spectra of both species suggests that similar groups attached to the amine results in similar UV-VIS spectra.

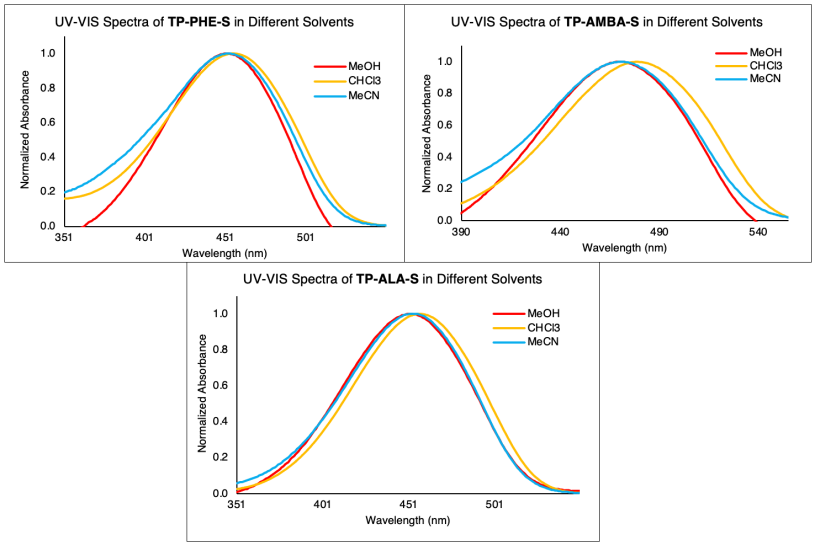

Figure 16 spectra of **TP-ALA-S**, **TP-PHE-S**, and **TP-AMBA-S** in different solvents

The geometry optimization of **TP-ALA-R** and **TP-PHE-R** was performed with abovementioned methods. Similar to the previous calculations, in both cases the most stable conformer includes intramolecular hydrogen bonding between the NH proton and carbonyls. This brings the methyl and benzyl moieties on the same side of the molecular plane. The electronic natures are similar to that of **TP-AMBA-R**. Figures 17, 18, and 19 shows the HOMO and LUMO of these compounds on their optimized structures.

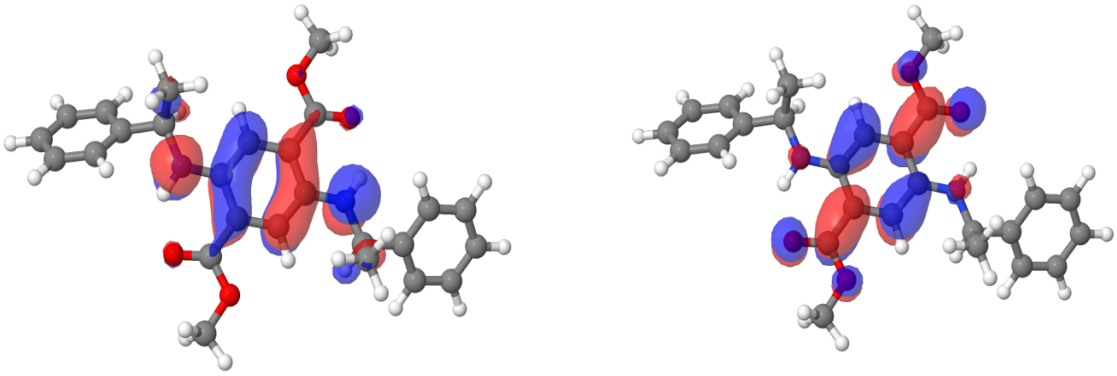

Figure 17 HOMO (left) and LUMO (right) of **TP-AMBA-R**

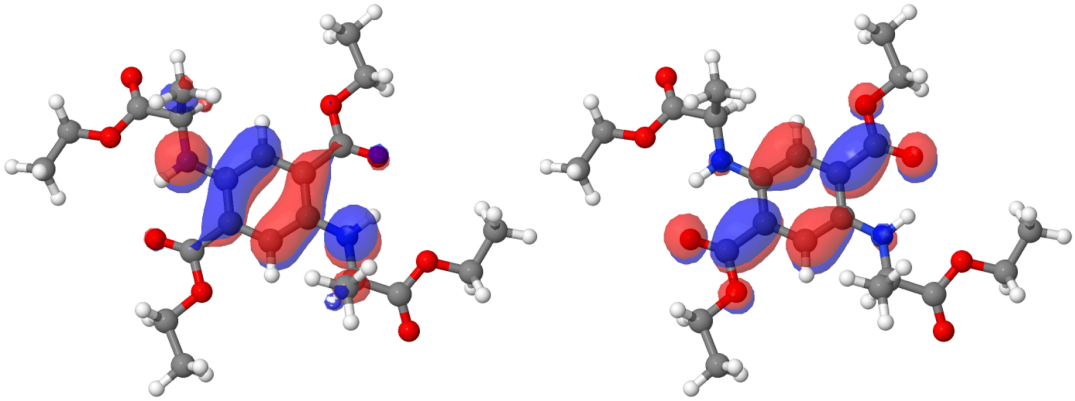

Figure 18 HOMO (left) and LUMO (right) of **TP-ALA-R**

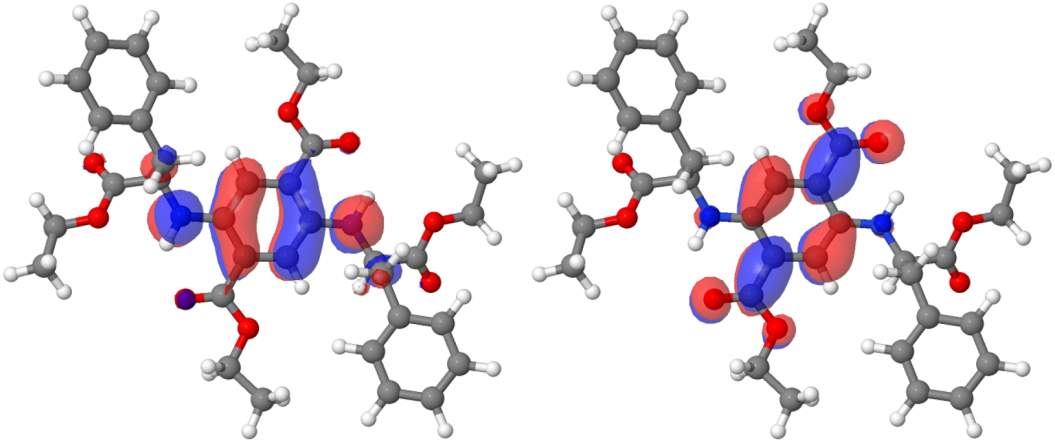

Figure 17 HOMO and LUMO of **TP-PHE-R**

3.3 Fluorescence studies

Solutions of **11** and **12** at 2.0×10^{-4} M concentrations were prepared and their fluorescence emission and excitation spectra were measured. It was already observed in UV-VIS spectra that the chromophore is somewhat sensitive to substituents. **11** in chloroform showed an excitation maximum at 500 nm while **12** shows an excitation maximum at 390 nm. This 110 nm difference is most probably due to a chemical change in the structure of **11**.[67] Zhang et al. suggest that a small chemical change can result in a significant change in the electronic structure of DATs.

As to emission spectra of these compounds, **11** has an emission maximum at 560 while **12** has an emission maximum at 460 nm. These data suggest that, **11** has a Stokes shift of 60 nm while **12** has a Stokes shift of 70 nm. These large Stokes shifts suggest an NH proton interaction with the carbonyl group. Figure 18 shows the fluorescence spectra of **11** and **12**.

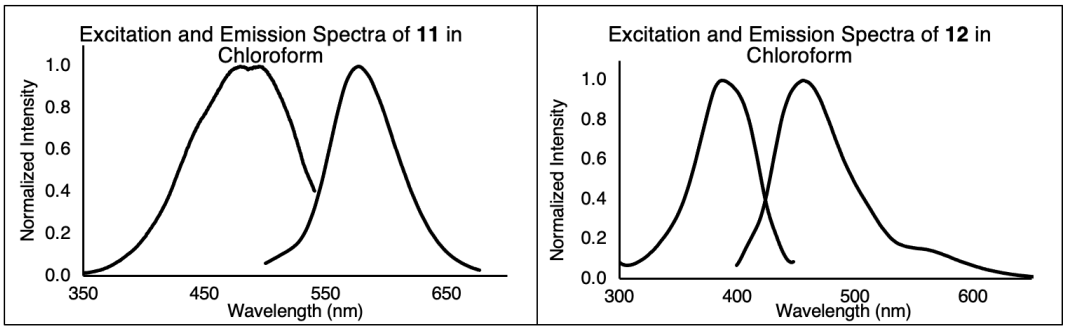

Figure 18 Excitation and emission spectra of **11** and **12** in chloroform

Fluorescence spectra of **TP-AMBA-S**, **TP-ALA-S**, and **TP-PHE-S** were recorded in chloroform, acetonitrile, and methanol, at 2.0×10^{-4} M concentrations. In chloroform, **TP-AMBA-S** shows an excitation maximum at 500 nm while that of emission is around 575 nm, resulting in a 75 nm Stokes shift. In acetonitrile, the excitation maximum is around 475 nm while the emission maximum is again 575 nm, with a Stokes shift of 100 nm. In methanol, however, a significant redshift is observed on both the excitation and emission maxima, 560 and 585 nm, respectively. Excitation band is observed to be significantly sharper, and the Stokes shift observed in methanol is a mere 25 nm. These results suggest an increased structural rigidity of the molecule provided by the methanol solvent cage, along with the alleviation of intramolecular proton transfer process. Figure 19 shows the fluorescence spectra of **TP-AMBA-S**.

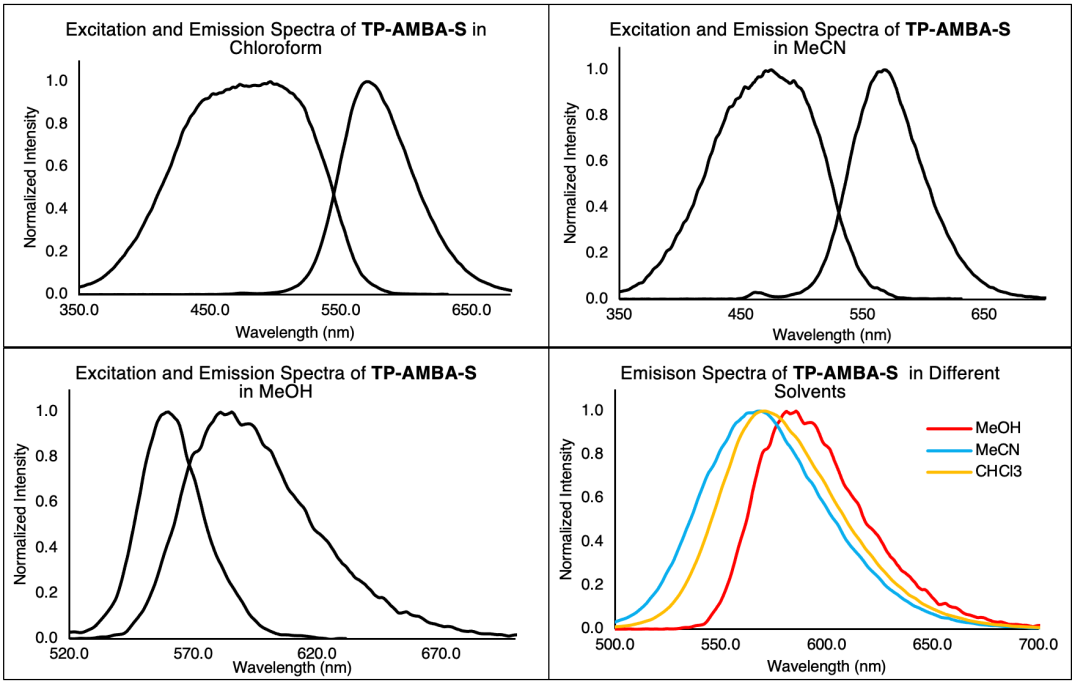

Figure 19 Fluorescence spectra of **TP-AMBA-S** in chloroform, acetonitrile, and methanol

The fluorescence excitation and emission spectra of aminoacid ester substituted DATs were recorded for the (S)-isomers in chloroform, acetonitrile, and methanol. In chloroform the excitation and emission maxima of **TP-ALA-S** are located at 445

nm and 550 nm, respectively, amounting for a 105 nm Stokes shift. The fluorescence spectra of **TP-ALA-S** in acetonitrile is almost exactly the same with that of in chloroform with the same maxima, corresponding to a Stokes shift of 105 nm. In methanol, no shift on the excitation maximum was observed whereas a 7 nm redshift was observed on the emission maximum at 557 nm, increasing the Stokes shift to 112 nm. These results differ from that of **TP-AMBA-S** as the Stokes shift is slightly increased as opposed to a stark decrease in methanol. This may be attributed to the additional carbonyls on the aminoacid ester substituted DATs acting also as H-bond acceptors and hence, disrupting the rigidity that is provided by the methanol solvent cage. Figure 20 shows the fluorescence spectra of **TP-ALA-S**.

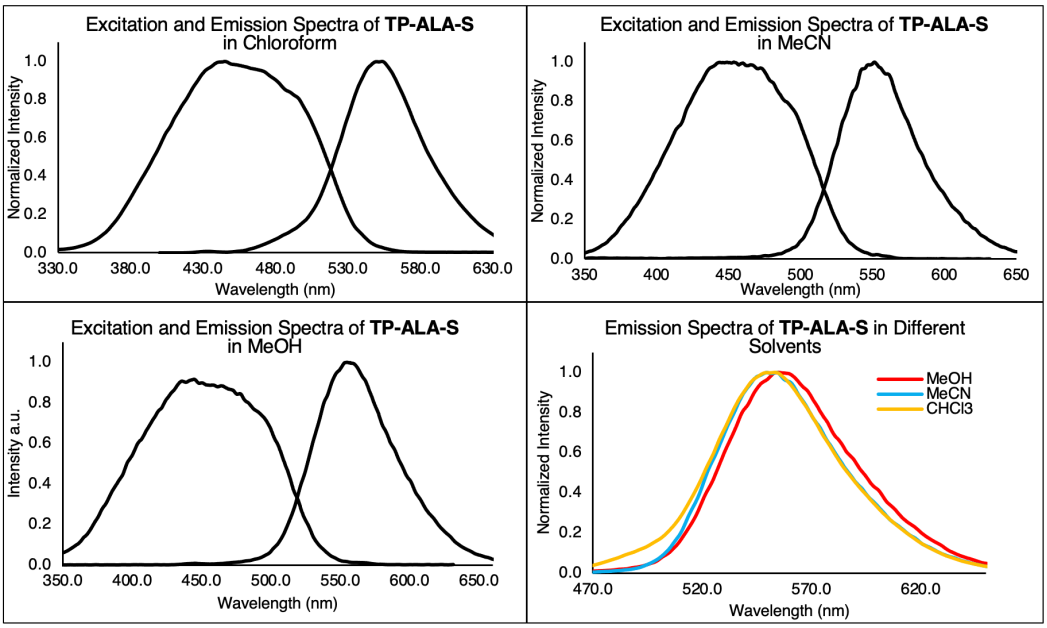

Figure 20 Fluorescence spectra of **TP-ALA-S** in chloroform, acetonitrile, and methanol

The excitation and emission spectra of **TP-PHE-S** in chloroform, acetonitrile, and methanol were recorded. The excitation maximum in all the solvents were found to be located at 460 nm. The emission maxima in both chloroform and acetonitrile were found to be 550 nm, corresponding to a Stokes shift of 90 nm. Whereas in methanol, the emission maximum is located at 557 nm, with a 7 nm redshift as compared to

that in other solvents. Similar to that of **TP-ALA-S**, the stokes shift is increased by 7 nm in methanol. Interestingly, the Stokes shifts are overall larger for **TP-ALA-S** than that of **TP-PHE-S**. Somehow, the non-radiative vibrational and rotational decay paths on the excited state appear to be less prominent for **TP-PHE-S**, which has a larger conformational space compared to **TP-ALA-S**. Figure 21 shows the fluorescence spectra of **TP-PHE-S**.

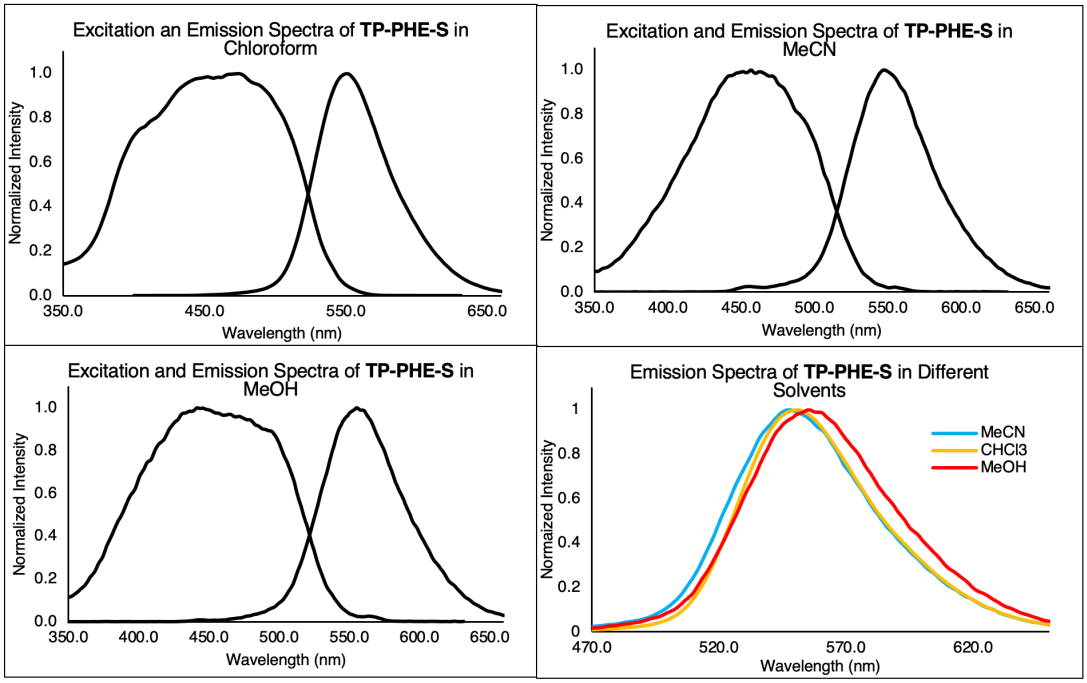

Figure 21 Fluorescence spectra of **TP-PHE-S** in chloroform, acetonitrile, and methanol

3.4 CD Studies

Circular dichroism (CD) spectroscopy is known to be sensitive to any changes in molecular structure. That is why, CD spectroscopy is used for biological samples and supramolecular chiral interactions. Chirality transfer to an achiral dye from chiral substituents results in a CD active signal in the dye-absorbing region. Such studies are used for sensing chiral compounds. With this in mind we started the CD measurements of **TP-AMBA-R** and **TP-AMBA-S** in chloroform, acetonitrile, and methanol. The CD spectra in chloroform showed a chiroptical signal in the dye-absorbing region. CD spectra of the (R)- and (S)-isomers are mirror images of each other. In acetonitrile and methanol, we observed a similar chiroptical signal, except for a new signal around 250 nm. This is attributed to solvent-solute interactions. Figure 22 shows the CD spectra of **TP-AMBA-S** and **TP-AMBA-R**.

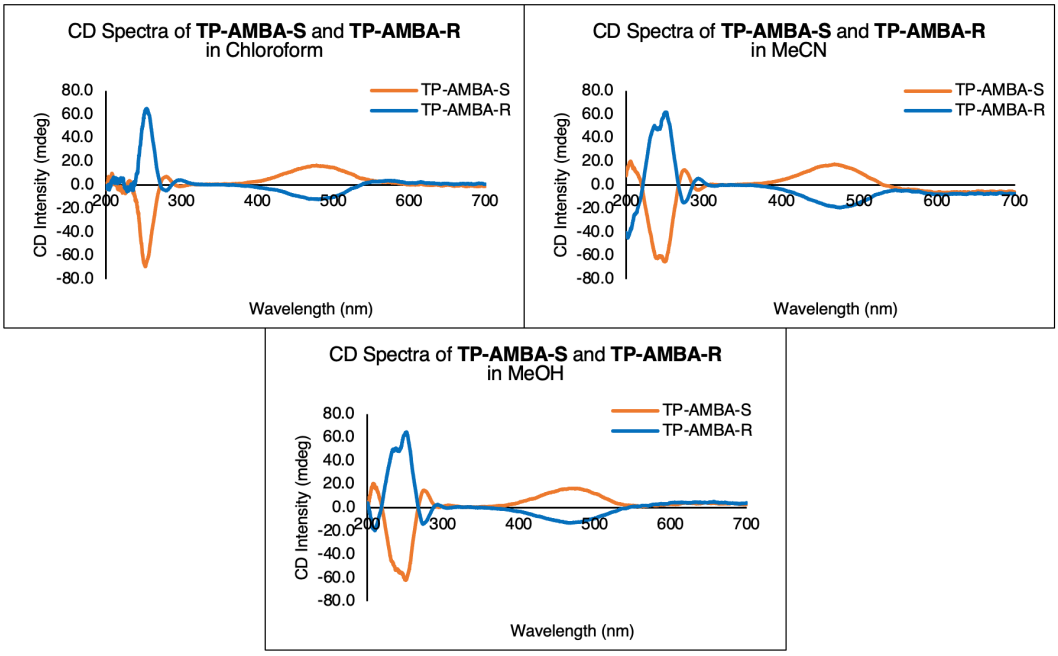

Figure 22 CD spectra of **TP-AMBA-S** and **TP-AMBA-R** in chloroform, acetonitrile, and methanol

The CD spectra of **TP-ALA-S** and **TP-ALA-R** were recorded in chloroform, acetonitrile, and methanol. In chloroform, the CD signal came noisier as compared to that of in acetonitrile and methanol. This is probably due to the conformational space in chloroform being larger than that in acetonitrile and methanol. The conformational space could be affected by solvent-solute interactions through intermolecular H-bonding. The chiroptical signal for the dye diminishes in acetonitrile and methanol as compared to that in chloroform. These results suggest that solvents with H-bonding capacity reduces the CD activity. No qualitative difference between the spectra was observed in all three solvents. Figure 23 shows the CD spectra of **TP-ALA-S** and **TP-ALA-R**.

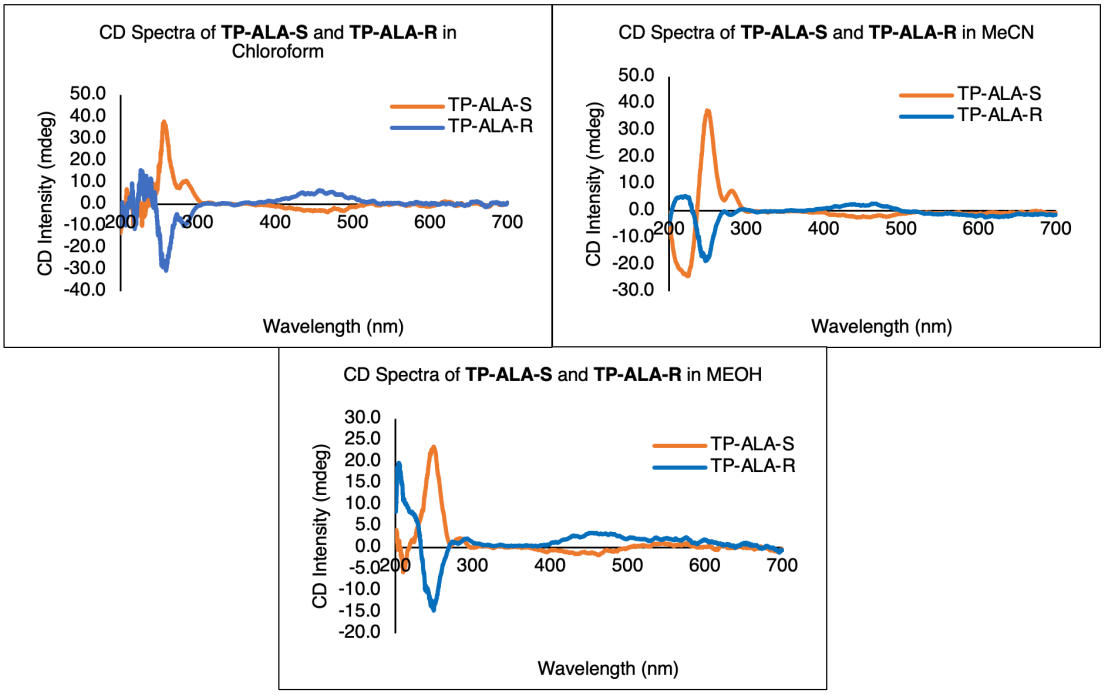

Figure 23 CD spectra of **TP-ALA-S** and **TP-ALA-R** in chloroform, acetonitrile, and methanol

The CD spectra of **TP-PHE-S** and **TP-PHE-R** were recorded in chloroform, acetonitrile, and methanol. Similar to **TP-ALA-S** and **TP-ALA-R**, the chiroptical signal was stronger but noisier in chloroform as compared to that in acetonitrile and methanol. The signal on the high energy region (200-250 nm) in chloroform is exceptionally noisy. This may be caused by the benzyl group creating additional conformational space in chloroform. The benzyl group is known to be hydrophobic and in methanol and acetonitrile, these compounds may have fixed conformers. That could be the reason why we observed sharp signals in acetonitrile and methanol, in the high energy region. Figure 24 shows the CD spectra of **TP-PHE-S** and **TP-PHE-R**.

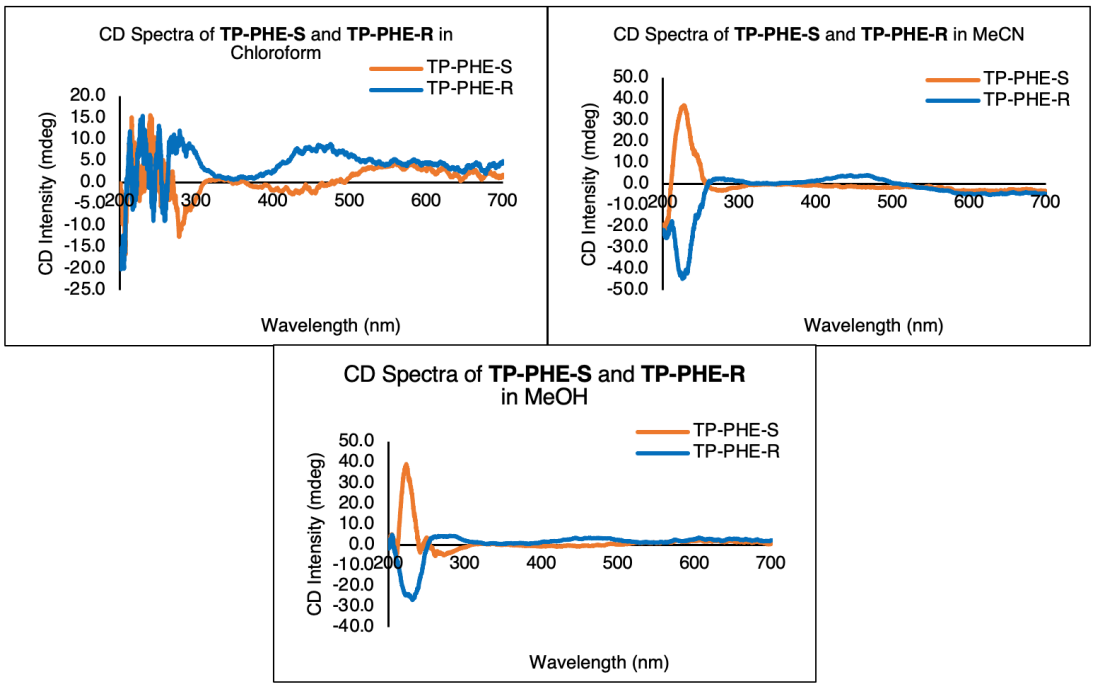

Figure 24 CD spectra of **TP-PHE-R** and **TP-PHE-S** in chloroform, acetonitrile, and methanol

CHAPTER 4

CONCLUSION

2,5-diaminoterephthalates (DATs) are known to be intensely colored and fluorescent compounds that are open to functionalization. They are considerably smaller in their conjugated structure to popular dyes such as fluoresceins and BODIPYs however, they possess comparable optical properties. Most prominently, DATs have been used as organic linkers for metal-organic framework (MOF) materials, and as fluorescent sensors. The chiroptical properties of DATs and hence their potential as chiroptical sensors still remain obscure despite their old history.

In this study, 3 novel enantiomeric pairs of chiral 2,5-diaminoterephthalate derivatives were designed, synthesized, and their optical and chiroptical properties were explored. In the design of these DATs, enantiomers of α-methylbenzylamine, alanine, and phenylalanine were chosen as the substituents.

All the DAT derivatives were synthesized through the same method, starting from succinic acid. The products were purified using silica column chromatography and recrystallization techniques. The products were characterized using ^{1}H and ^{13}C NMR, IR, and HRMS spectroscopies. Their optical properties were investigated using UV-Vis, fluorescence, and circular dichroism (CD) spectroscopies.

The UV-Vis and fluorescence spectra of each compound showed dependence on the solvent's ability to form hydrogen bonds. This is attributed to conformational changes in molecular structure due to competition with intramolecular hydrogen bonding. Overall, UV-Vis absorption, fluorescence excitation, and emission spectra showed redshift on corresponding maxima in acetonitrile and methanol.

Of all the chiral DATs, **TP-AMBA-S** and **TP-AMBA-R** showed the strongest CD activity in the visible region, along with the lowest dependency on the solvent. On the other hand, the CD activity of the aminoacid ester substituted DATs was found to be amplified in chloroform, revealing the importance of conformation and molecular interactions on their chiroptical activity. Overall, increased hydrophobicity on the substituents provided better CD activity in the visible region.

Overall, we conclude that chiral DAT derivatives are viable candidates for stereochemical sensing applications. Even though we laid the groundwork for such applications in this study, more elaborate experiments should be designed and executed.

CHAPTER 5

EXPERIMENTAL

5.1 Methods and Materials

All starting materials and solvent except ethyl acetate and hexane were purchased from Sigma Aldrich and were used without further purifications. Solvents used for Flash Chromatography were distilled prior to use (EtOAc and Hexane over $CaCl_2$). The reactions were monitored by thin layer chromatography (TLC) (Merck Silica Gel 60 F_{254}) and visualized by UV light at 254 nm.

Structural evaluation of the synthesized compounds was accomplished with the instruments stated below. Each spectra were processed using Microsoft Excel unless otherwise stated.

Melting points were measured using Stuart SMP11 instrument. All reported melting points were uncorrected.

^{1}H and ^{13}C nuclear magnetic resonance spectra of the compounds were recorded in $CDCl_3$ with Bruker Avance III Ultrashield 400 Hz NMR spectrometer. The chemical shifts were stated in parts per million (ppm) with tetramethylsilane (TMS) as internal reference. Spin multiplets were indicated as s (singlet), d (doublet), dd (doublet of doublet), t (triplet), tt (triplet of triplet), m (multiplet) and coupling constants (J) were reported as in Hz (Hertz). Raw ^{1}H and ^{13}C NMR spectra of products were given in Appendix A. NMR spectra were processed with MestReNova program.

Infrared (IR) Spectra were recorded with Thermo Scientific Nicolet iS10 ATR-IR spectrometer. Signal locations were reported in reciprocal centimeter (cm^{-1}). The IR spectra of the compounds synthesized are given in Appendix C.

UV-Vis measurements were recorded with Shimadzu UV-2450 spectrophotometer. Spectroscopic measurements were carried out in methanol, chloroform, and acetonitrile.

High Resolution Mass Spectra (HRMS) were processed in positive mode on (ES+) using Time of Flight mass analyzer. The high-resolution mass spectra of compounds synthesized are given in Appendix B.

Fluorescence measurements were recorded with Perkin Elmer LS55 spectrofluorometer. Both the excitation and emission slits were adjusted to 10 nm. 1% Attenuator filter was used after emission slit. Spectroscopic measurements were carried out in methanol, chloroform, acetonitrile of spectroscopic grade.

CD measurements were recorded with Jasco J-1500 CD Spectrometer. Spectroscopic measurements were carried out in methanol, chloroform, and acetonitrile.

5.2 Synthesis

5.2.1 General Procedure for the Synthesis of DATs

In an oven-dried 50 mL round bottom flask, the succinylsuccinate (0.79 mmol) was partially dissolved in 25 mL of alcohol at room temperature. To this suspension, triethylamine (7.90 mmol, 10 eq.) was added and the mixture was stirred for one minute. The related amine (1.58 mmol, 2 eq.) was then added at once. The flask was then fitted with a reflux condenser and the mixture was refluxed overnight. The mixture was then cooled down to room temperature and bromine (0.71 mmol, 0.9 eq.) was added at once. The mixture was then stirred for 30 minutes at room temperature and then quenched with 10 ml of concentrated aqueous $Na_2S_2O_3$ solution. This mixture was then extracted 3 times with each approximately 50 mL portions of DCM. The organic extracts were then dried over anhydrous $MgSO_4$ and concentrated *in vacuo*. The products were isolated using silica gel column chromatography with an appropriate gradient of hexanes and ethyl acetate as the

mobile phase. Further purification by recrystallization yielded the crystalline products. The products were characterized using ^{1}H and ^{13}C NMR, as well as HRMS and IR spectroscopies.

5.2.2 TP-AMBA-R

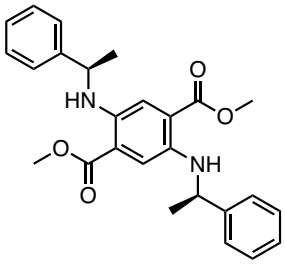

The general procedure for the synthesis of chiral DATs was followed using dimethyl succinylsuccinate (180.3 mg) as the succinylsuccinate, (R)-α-methylbenzylamine (191.5 mg) as the chiral amine, and anhydrous methanol as the solvent. Recrystallization from 96% ethanol yielded red needles. (81 mg, 18.2 %) **^{1}H NMR** (400 MHz, Chloroform-*d*) δ 7.46 – 7.18 (m, 10H), 7.12 (s, 2H), 4.53 (p, *J* = 6.6 Hz, 2H), 3.81 (s, 6H), 1.55 (d, *J* = 6.7 Hz, 6H). **^{13}C{^{1}H} NMR** (100 MHz, $CDCl_3$) δ 168.35, 145.44, 139.94, 128.42, 126.67, 125.76, 116.30, 115.07, 77.22, 76.90, 76.58, 53.05, 51.63, 24.88. **HRMS** (ESI/Q-TOF) m/z: [M + H]+ Calcd. for $C_{23}H_{29}N_2O_4$ 433.2122; Found 433.2122. **IR** 1684, 2361, 2963, 3374 cm^{-1}. **Melting point**: 118-120 °C.

5.2.3 TP-AMBA-S

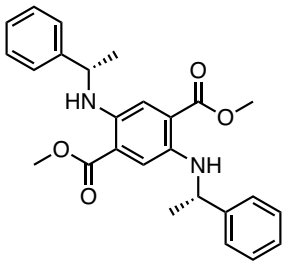

The general procedure for the synthesis of chiral DATs was followed using dimethyl succinylsuccinate (180.3 mg) as the succinylsuccinate, (S)-α-methylbenzylamine (191.5 mg) as the chiral amine, and anhydrous methanol as the solvent.

Recrystallization from 96% ethanol yielded red needles. (90 mg, 26.3 %) **^{1}H NMR** (400 MHz, Chloroform-*d*) δ 7.46 – 7.18 (m, 10H), 7.12 (s, 2H), 4.53 (p, *J* = 6.6 Hz, 2H), 3.81 (s, 6H), 1.55 (d, *J* = 6.7 Hz, 6H). **^{13}C{^{1}H} NMR** (100 MHz, $CDCl_3$) δ 168.35, 145.44, 139.94, 128.42, 126.67, 125.76, 116.30, 115.07, 77.22, 76.90, 76.58, 53.05, 51.63, 24.88. **HRMS** (ESI/Q-TOF) m/z: [M + H]+ Calcd. for $C_{23}H_{29}N_2O_4$ 433.2122; Found 23.2123. **IR** 1684, 2361, 2963, 3374 cm^{-1}. **Melting point**: 116-118 °C.

5.2.4 TP-ALA-R

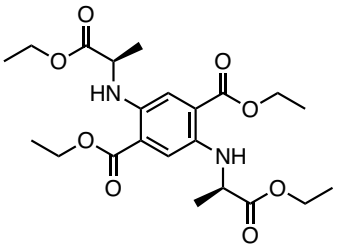

The general procedure for the synthesis of chiral DATs was followed using diethyl succinylsuccinate (202.4 mg) as the succinylsuccinate, *d*-alanine ethyl ester hydrochloride (242.7 mg) as the chiral amine, and anhydrous ethanol as the solvent. Recrystallization from a mixture of ethanol and water yielded orange needles. (63.6 mg, 17.8%) **^{1}H NMR** (400 MHz, Chloroform-*d*) δ 7.29 (s, 2H), 4.37 (q, *J* = 7.1, 1.3 Hz, 4H), 4.27 – 4.14 (m, 8H), 1.56 (d, *J* = 6.9 Hz, 6H), 1.42 (t, *J* = 7.1 Hz, 6H), 1.28 (t, *J* = 7.1 Hz, 6H). **^{13}C{^{1}H} NMR** (101 MHz, $CDCl_3$) δ 174.23, 167.41, 140.03, 117.42, 114.63, 60.86, 60.74, 51.93, 18.61, 14.14, 14.08. **HRMS** (ESI/Q-TOF) m/z: [M + H]+ Calcd. for $C_{22}H_{33}N_2O_8$ 453.2131; Found 453.2232. **IR** 1684, 1741, 2359, 2982, 3349 cm^{-1}. **Melting point**: 94-96 °C.

5.2.5 TP-ALA-S

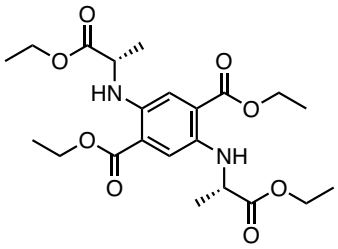

The general procedure for the synthesis of chiral DATs was followed using diethyl succinylsuccinate (202.4 mg) as the succinylsuccinate, *l*-alanine ethyl ester hydrochloride (242.7 mg) as the chiral amine, and anhydrous ethanol as the solvent. Recrystallization from a mixture of ethanol and water yielded orange needles. (108.9 mg, 30.5%) **^{1}H NMR** (400 MHz, Chloroform-*d*) δ 7.29 (s, 2H), 4.37 (q, *J* = 7.1, 1.3 Hz, 4H), 4.27 – 4.14 (m, 8H), 1.56 (d, *J* = 6.9 Hz, 6H), 1.42 (t, *J* = 7.1 Hz, 6H), 1.28 (t, *J* = 7.1 Hz, 6H). **^{13}C{^{1}H} NMR** (101 MHz, $CDCl_3$) δ 174.23, 167.41, 140.03, 117.42, 114.63, 60.86, 60.74, 51.93, 18.61, 14.14, 14.08. **HRMS** (ESI/Q-TOF) m/z: [M + H]+ Calcd. for $C_{22}H_{33}N_2O_8$ 453.2231; Found 453.2231. **IR** 1684, 1741, 2359, 2982, 3349 cm^{-1}. **Melting point**: 96-98 °C.

5.2.6 TP-PHE-R

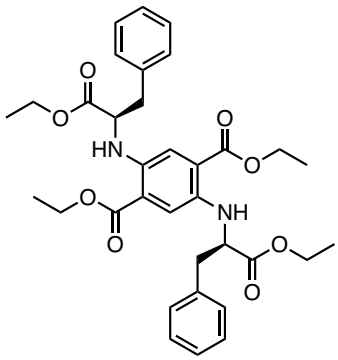

The general procedure for the synthesis of chiral DATs was followed using diethyl succinylsuccinate (202.4 mg) as the succinylsuccinate, *d*-phenylalanine ethyl ester hydrochloride (362.9 mg) as the chiral amine, and anhydrous ethanol as the solvent. Recrystallization from a mixture of ethanol and water yielded reddish-orange needles. (43.0 mg, 9.0 %) **^{1}H NMR** (400 MHz, Chloroform-*d*) δ 7.33 – 7.06 (m,

12H), 4.44 – 4.24 (m, 6H), 4.16 – 4.03 (m, 4H), 3.14 (dd, *J* = 6.8, 2.5 Hz, 4H), 1.37 (t, *J* = 7.1 Hz, 6H), 1.15 (t, *J* = 7.2 Hz, 6H). **^{13}C{^{1}H} NMR** δ 172.92, 167.23, 139.78, 136.66, 129.20, 128.28, 126.71, 117.57, 114.74, 60.86, 60.76, 58.23, 38.88, 14.17, 13.99. **HRMS** (ESI/Q-TOF) m/z: [M + H]+ Calcd. for $C_{34}H_{41}N_2O_8$ 605.2857; Found 605.2858. **IR** 1684, 1741, 2362, 2980, 3347 cm^{-1}. **Melting point**: 124-126 °C.

5.2.7 TP-PHE-S

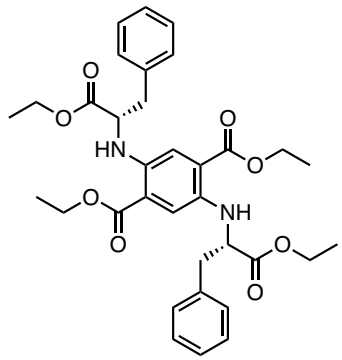

The general procedure for the synthesis of chiral DATs was followed using diethyl succinylsuccinate (202.4 mg) as the succinylsuccinate, *d*-phenylalanine ethyl ester hydrochloride (362.9 mg) as the chiral amine, and anhydrous ethanol as the solvent. Recrystallization from a mixture of ethanol and water yielded reddish-orange needles. (57.8 mg, 12.1 %) **^{1}H NMR** (400 MHz, Chloroform-*d*) δ 7.33 – 7.06 (m, 12H), 4.44 – 4.24 (m, 6H), 4.16 – 4.03 (m, 4H), 3.14 (dd, *J* = 6.8, 2.5 Hz, 4H), 1.37 (t, *J* = 7.1 Hz, 6H), 1.15 (t, *J* = 7.2 Hz, 6H). **^{13}C{^{1}H} NMR** δ 172.92, 167.23, 139.78, 136.66, 129.20, 128.28, 126.71, 117.57, 114.74, 60.86, 60.76, 58.23, 38.88, 14.17, 13.99. **HRMS** (ESI/Q-TOF) m/z: [M + H]+ Calcd. for $C_{34}H_{41}N_2O_8$ 605.2857; Found 605.2857. **IR** 1684, 1741, 2362, 2980, 3347 cm^{-1}. **Melting point:** 126-128 °C.

5.2.8 General Procedure for the Esterification of Aminoacids

To a suspension of aminoacid (12.5 mmol) in 25 mL of dry ethanol, $SOCl_2$ (5.34 g, 2.0 eq.) was added dropwise over the course of 10 minutes. All of the solids had dissolved by the end of the addition of $SOCl_2$. The resulting solution was then refluxed for 2 hours. The mixture was then concentrated *in vacuo*. To the oily residue, Et_2O was added until turbidity was observed, and the mixture was chilled to -18°C in the freezer to facilitate crystallization. A liquid phase separation was observed instead. The biphasic mixture was shaken vigorously until solids started to form and then left overnight in the freezer. In each case, the bottom layer had completely solidified by morning. The solids were then collected by filtration, washed thoroughly with Et_2O, and air dried to yield clear needle crystals.

5.2.9 D-Alanine Ethyl Ester Hydrochloride[68,69]

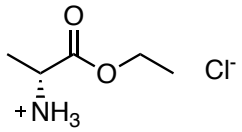

The general procedure for the esterification of aminoacids was followed using *d*-alanine (1.00 g) as the aminoacid. (1.82 g, 94.5 %) **^{1}H NMR** (400 MHz, Chloroform-*d*) δ 8.73 (s, 3H), 4.35 - 4.16 (m, 3H), 1.74 (d, J = 7.2 Hz, 3H), 1.31 (t, J = 7.1 Hz, 3H).

5.2.10 L-Alanine Ethyl Ester Hydrochloride[68,69]

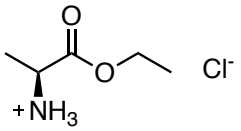

The general procedure for the esterification of aminoacids was followed using *d*-alanine (1.00 g) as the aminoacid. (1.87 g, 96.9 %) **^{1}H NMR** (400 MHz, Chloroform-*d*) δ 8.73 (s, 3H), 4.35 - 4.16 (m, 3H), 1.74 (d, *J* = 7.2 Hz, 3H), 1.31 (t, *J* = 7.1 Hz, 3H).

5.2.11 D-Phenylalanine Ethyl Ester Hydrochloride[70,71]

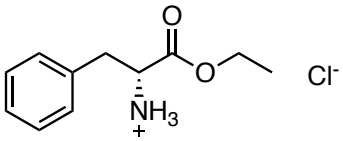

The general procedure for the esterification of aminoacids was followed using *d*-phenylalanine (2.06 g) as the aminoacid. (3.67 g, 97.8 %) **^{1}H NMR** (400 MHz, Chloroform-*d*) δ 8.81 (s, 3H), 7.33 (m, 5H), 4.38 (q, *J* = 6.3 Hz 1H), 4.16 (qd, *J* = 7.2, 1.7 Hz, 2H), 3.48 (dd, *J* = 5.9, 14.5 Hz, 1H), 3.37 (dd, *J* = 7.1, 14.0 Hz, 1H), 1.18 (td, *J* = 7.2, 1.1 Hz, 3H).

5.2.12 L-Phenylalanine Ethyl Ester Hydrochloride[70,71]

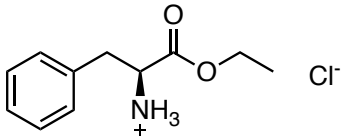

The general procedure for the esterification of aminoacids was followed using *d*-phenylalanine (2.06 g) as the aminoacid. (3.25 g, 87.0 %) **^{1}H NMR** (400 MHz, Chloroform-*d*) δ 8.81 (s, 3H), 7.33 (m, 5H), 4.38 (q, *J* = 6.3 Hz 1H), 4.16 (qd, *J* = 7.2, 1.7 Hz, 2H), 3.48 (dd, *J* = 5.9, 14.5 Hz, 1H), 3.37 (dd, *J* = 7.1, 14.0 Hz, 1H), 1.18 (td, *J* = 7.2, 1.1 Hz, 3H).

5.2.13 General Procedure For the Synthesis of Succinylsuccinates

To a suspension of NaH (2.0 g of 60% in mineral oil) in 50 mL of still-dried THF, dialkyl succinate (22.5 mmol) was added at once. The mixture was stirred at reflux for 5 hours. The reaction was then quenched with addition of 20 mL of water, followed by 5 mL of concentrated HCl solution. The resulting solids were collected by filtration. Solids were washed thoroughly with hexanes. Recrystallization from a mixture of EtOH and H_2O gave clear needle crystals.

5.2.14 Dimethyl succinylsuccinate (8)[72]

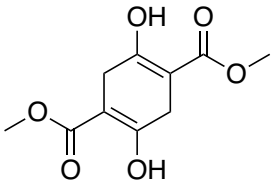

The general procedure for the synthesis of succinylsuccinates was followed using dimethyl succinate (3.30 g). (1.23 g, 47.7%) **^{1}H NMR** (400 MHz, Chloroform-*d*) δ 12.13 (s, 2H), 3.79 (s, 6H), 3.19 (s, 4H)

5.2.15 Diethyl succinylsuccinate (9)[73]

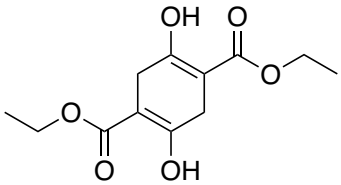

The general procedure for the synthesis of succinylsuccinates was followed using dimethyl succinate (3.92 g). (1.41 g, 48.9%) **^{1}H NMR** (400 MHz, Chloroform-*d*) δ 12.20 (s, 2H), 4.23 (q, *J*=7.1 Hz, 4H), 3.17 (s, 4H), 1.30 (t, *J*=7.1 Hz, 6H)

REFERENCES

(1) Mezey, P. G. *A Global Approach to Molecular Chirality*; New Developments in Molecular Chirality; **1991**.

(2) Voet, D.; Voet, J. G.; Pratt, C. W. *Fundamentals of Biochemistry*, 5th Edition.; Applied Biochemistry and Biotechnology; Wiley: USA, **2016**.

(3) Zhou, S.-F.; Zhong, W.-Z. *Molecules* **2017**, *22*, 279.

(4) Loue, S.; Sajatovic, M. *Encyclopedia of Women's Health*, 1st Edition.; **2004**.

(5) Vargesson, N. *Birth Def. Res.* **2015**, *105*, 140–156.

(6) Tokunaga, E.; Yamamoto, T.; Ito, E.; Shibata, N. *Sci. Rep.* **2018**, *8*, 17131.

(7) Smith, M. L.; Nichols, D. C.; Underwood, P.; Fuller, Z.; Moser, M. A.; Flegel, R.; Gorelick, D. A.; Newmeyer, M. N.; Concheiro, M.; Huestis, M. A. *J. Anal. Toxicol.* **2014**, *38*, 524–527.

(8) Berova, N.; Polavarapu, P. L.; Nakanishi, K.; Woody, R. W. *Comprehensive Chiroptical Spectroscopy*; Wiley: New Jersey, **2018**.

(9) Condon, E. U.; Altar, W.; Eyring, H. *J. Chem. Phys.* **1937**, *5*, 753–775.

(10) Caldwell, D. J.; Eyring, H. *Theor. Chem.* **1975**, *1*, 53–113.

(11) Pflantz, R.; Christoffers, J. *Chem. Eur. J.* **2009**, *15*, 2200–2209.

(12) Baeyer, A. *Ber. Dtsch. Chem. Ges.* **1886**, *19*, 428–433.

(13) Magalhães, A. L. de; Pinto, M. L. S.; Ribeiro, D.; Moreira, C.; Ferreira, M.; Martins, M. E. G.; Fernandes, R. F.; Lima, L. S.; Dias, A. G.; Freitas, M. C.; Guedes, F.; Bastos, M. C.; Ramos, F.; Pinto, J. R.; Sousa, J. A. de; Fernandes, F. M. S. S.; Abrantes, L. M.; Oliveira, E.; Dourado, D.; Gesto, D.; Coimbra, J.; Porto, F. de C. da U. do. *Rev. Cien. Elem.* **2015**, *3*.

(14) Liebermann, H.; Schulze, B. *Liebigs Ann. Chem.* **1934**, *508*, 144–153.

(15) Liebermann, H. *Liebigs Ann. Chem.* **1935**, *518*, 245–259.

(16) Liebermann, H. *Liebigs Ann. Chem.* **1914**, *404*, 272–321.

(17) Uhlig, E.; Richter, K. *Z. Anorg. Allg. Chem.* **1962**, *316*, 34–40.

(18) Uhlig, E. *Z. Anorg. Allg. Chem.* **1956**, *288*, 24–27.

(19) Uhlig, E.; Berndt, H. *Fresenius Z. Anal. Chem.* **1964**, *203*, 241–252.

(20) Labana, S. S.; Labana, L. L. *Chem. Rev.* **1967**, *67*, 1–18.

(21) Lomax, S. Q. *Stud. Conserv.* **2013**, *50*, 19–29.

(22) Christie, R.; Abel, A. *Encyclopedia of Colors, Dyes, Pigments* **2022**, *1*, 61–68.

(23) Freimuth, L.; Rozzi, C.; Lienau, C.; Christoffers, J. *Synthesis* **2015**, *47*, 1325–1328.

(24) Wallisch, M.; Sulmann, S.; Koch, K.-W.; Christoffers, J. *Chem. Eur. J.* **2017**, *23*, 6535–6543.

(25) Freimuth, L.; Christoffers, J. *Chem. Eur. J.* **2015**, *21*, 8214–8221.

(26) Pittalis, S.; Delgado, A.; Robin, J.; Freimuth, L.; Christoffers, J.; Lienau, C.; Rozzi, C. A. *Adv. Funct. Mater.* **2015**, *25*, 2047–2053.

(27) Schröder, N.; Schmidtmann, M.; Christoffers, J. *Eur. J. Org. Chem.* **2021**, *2021*, 4244–4244.

(28) Markovic, A.; Buschbeck, L.; Klüner, T.; Christoffers, J.; Wittstock, G. *Chemistryopen* **2019**, *8*, 1152–1152.

(29) Christoffers, J. *Eur. J. Org. Chem.* **2018**, *2018*, 2366–2377.

(30) Wache, N.; Schröder, C.; Koch, K.-W.; Christoffers, J. *ChemBioChem* **2012**, *13*, 993–998.

(31) Buschbeck, L.; Markovic, A.; Wittstock, G.; Christoffers, J. *Beilstein J. Org. Chem.* **2019**, *15*, 981–991.

(32) Markovic, A.; Buschbeck, L.; Brand, I.; Dosche, C.; Christoffers, J.; Wittstock, G. *Langmuir* **2020**, *36*, 14623–14632.

(33) Markovic, A.; Buschbeck, L.; Klüner, T.; Christoffers, J.; Wittstock, G. *ChemistryOpen* **2019**, *8*, 1176–1182.

(34) Zhang, Y.; Starynowicz, P.; Christoffers, J. *Eur. J. Org. Chem.* **2008**, No. 20, 3488–3495.

(35) Wallisch, M.; Sulmann, S.; Koch, K.-W.; Christoffers, J. *Chem. Eur. J.* **2017**, *23*.

(36) Koch, K.-W.; Christoffers, J. *Meth. Mol. Bio.* **2019**, *1929*, 583–594.

(37) Sulmann, S.; Wallisch, M.; Scholten, A.; Christoffers, J.; Koch, K.-W. *Biochemistry* **2016**, *55*, 2567–2577.

(38) Rogez, B.; Horeis, R.; Moal, E. L.; Christoffers, J.; Al-Shamery, K.; Dujardin, G.; Boer-Duchemin, E. *J. Phys. Chem. C* **2015**, *119*, 22217–22224.

(39) Buschbeck, L.; Christoffers, J. *J. Org. Chem.* **2018**, *83*, 4002–4014.

(40) Segelken, J.; Wallisch, M.; Schultz, K.; Christoffers, J.; Janssen-Bienhold, U. *ACS Chem. Neurosci.* **2018**, *9*, 858–867.

(41) Schröder, N.; Christoffers, J. *Synthesis* **2022**, *10*, 2511–2515.

(42) Zhang, Y.; Christoffers, J. *Synthesis* **2007**, *2007*, 3061–3067.

(43) Wache, N.; Scholten, A.; Klüner, T.; Koch, K.; Christoffers, J. *Eur. J. Org. Chem.* **2012**, *2012*, 5712–5722.

(44) Huang, R.; Tang, B.; Ye, K.; Wang, C.; Zhang, H. *Adv. Opt. Mater.* **2019**, *7*, 1900927.

(45) Zhang, X.; Wang, J.; Liu, H.; Yu, F.; Wang, T.; Huang, X.; Hao, H. *Dyes Pigm.* **2022**, *197*, 109903.

(46) Shimizu, M.; Asai, Y.; Takeda, Y.; Yamatani, A.; Hiyama, T. *Tetrahedron Lett.* **2011**, *52*, 4084–4089.

(47) Sambiagio, C.; Marsden, S. P.; Blacker, A. J.; McGowan, P. C. *Chem. Soc. Rev.* **2014**, *43*, 3525–3550.

(48) Zhang, X.-T.; Fan, L.-M.; Fan, W.-L.; Li, B.; Liu, G.-Z.; Liu, X.-Z.; Zhao, X. *Cryst. Gr. Des.* **2016**, *16*, 3993–4004.

(49) Liu, K.; Deng, L.; Zhang, Y.; Jiao, S.; Geng, Y.; Wang, L. *Crystals* **2018**, *8*, 236.

(50) Wang, J.; Gao, L.; Zhang, J.; Zhao, L.; Wang, X.; Niu, X.; Fan, L.; Hu, T. *Cryst. Gr. Des.* **2018**, *19*, 630–637.

(51) Chapman, A. W. *J. Chem. Soc.* **1927**, 1743–1751.

(52) Hojo, N.; Yoneno, H. *J. Chem. Soc. (A)* **1970**, *772*, 2387–2389.

(53) Hahm, H.; Yoo, K.; Ha, H.; Kim, M. *Inorg. Chem.* **2016**, *55*, 7576–7581.

(54) Zhao, X.; Lu, Z.; Zhang, Y.; Zhou, M.; Xu, S.; Li, Z. *J. Mater. Sci.* **2022**, *33*, 4737–4754.

(55) Liu, W.; Zhong, Y.; Wang, X.; Zhuang, C.; Chen, J.; Liu, D.; Xiao, W.; Pan, Y.; Huang, J.; Liu, J. *Inorg. Chem. Comm.* **2020**, *111*, 107675.

(56) Hendrickx, K.; Vanpoucke, D. E. P.; Leus, K.; Lejaeghere, K.; Deyne, A. V. Y.-D.; Speybroeck, V. V.; Voort, P. V. D.; Hemelsoet, K. *Inorg. Chem.* **2015**, *54*, 10701–10710.

(57) Zhang, S.; Rong, F.; Guo, C.; Duan, F.; He, L.; Wang, M.; Zhang, Z.; Kang, M.; Du, M. *Coordin. Chem. Rev.* **2021**, *439*, 213948.

(58) Guo, X.; Liu, L.; Xiao, Y.; Qi, Y.; Duan, C.; Zhang, F. *Coordin. Chem. Rev.* **2021**, *435*, 213785.

(59) Li, K.; Fong, D.; Meichsner, E.; Adronov, A. *Chem. Eur. J.* **2021**, *27*, 5057–5073.

(60) Xu, M.; Han, J.-M.; Wang, C.; Yang, X.; Pei, J.; Zang, L. *ACS Appl. Mater. Inter.* **2014**, *6*, 8708–8714.

(61) Akdag, A.; Wahab, A.; Beran, P.; Rulíšek, L.; Dron, P. I.; Ludvík, J.; Michl, J. *J. Org. Chem.* **2015**, *80*, 80–89.

(62) Liu, B.; Di, Q.; Liu, W.; Wang, C.; Wang, Y.; Zhang, H. *J. Phys. Chem. Lett.* **2019**, *10*, 1437–1442.

(63) Shimizu, M.; Tamagawa, T. *Eur. J. Org. Chem.* **2014**, *2015*, 291–295.

(64) Tang, B.; Wang, C.; Wang, Y.; Zhang, H. *Angew. Chem. Int. Ed.* **2017**, *56*, 12543–12547.

(65) Ünay, G. Ç. **2022**.

(66) Frisch, M. J.; Trucks, G. W.; Schlegel, H. B.; Scuseria, G. E.; Robb, M. A.; Cheeseman, J. R.; Scalmani, G.; Barone, V.; Mennucci, B.; Petersson, G. A.; Nakatsuji, H.; Caricato, M.; Li, X.; Hratchian, H. P.; Izmaylov, A. F.; Bloino, J.; Zheng, G.; Sonnenberg, J. L.; Hada, M.; Ehara, M.; Toyota, K.; Fukuda, R.; Hasegawa, J.; Ishida, M.; Nakajima, T.; Honda, Y.; Kitao, O.; Nakai, H.; Vreven, T.; Montgomery, J. A.; Jr.; Peralta, J. E.; Ogliaro, F.; Bearpark, M.; Heyd, J. J.;

Brothers, E.; Kudin, K. N.; Staroverov, V. N.; Kobayashi, R.; Normand, J.; Raghavachari, K.; Rendell, A.; Burant, J. C.; Iyengar, S. S.; Tomasi, J.; Cossi, M.; Rega, N.; Millam, J. M.; Klene, M.; Knox, J. E.; Cross, J. B.; Bakken, V.; Adamo, C.; Jaramillo, J.; Gomperts, R.; Stratmann, R. E.; Yazyev, O.; Austin, A. J.; Cammi, R.; Pomelli, C.; Ochterski, J. W.; Martin, R. L.; Morokuma, K.; Zakrzewski, V. G.; Voth, G. A.; Salvador, P.; Dannenberg, J. J.; Dapprich, S.; Daniels, A. D.; Farkas, O.; Foresman, J. B.; Ortiz, J. V.; Cioslowski, J.; Fox, and D. J.; Gaussian; Inc.; CT, W. *Gaussian 09, Revision A.02*; **2009**.

(67) Liu, H.; Zhang, S.; Ding, L.; Fang, Y. *Chem. Commun.* **2021**, *57*, 4011–4014.

(68) Yao, P.; Marshall, J. R.; Xu, Z.; Lim, J.; Charnock, S. J.; Zhu, D.; Turner, N. J. *Angew. Chem. Int. Ed.* **2021**, *60*, 8717–8721.

(69) Habata, Y.; Kizaki, J.; Hosoi, Y.; Ikeda, M.; Kuwahara, S. *Dalton Trans.* **2014**, *44*, 1170–1177.

(70) Almansour, A. I.; Arumugam, N.; Kumar, R. S.; Menéndez, J. C.; Ghabbour, H. A.; Fun, H.-K.; Kumar, R. R. *Tetrahedron Lett.* **2015**, *56*, 6900–6903.

(71) Banerjee, P. K.; Amidon, G. L. *J. Pharm. Sci.* **1981**, *70*, 1299–1303.

(72) Yang, Z.; Liu, J.; Li, Y.; Zhang, G.; Xing, G.; Chen, L. *Angew. Chem. Int. Ed.* **2021**, *60*, 20754–20759.

(73) John, J.; Hopf, H. *Eur. J. Org. Chem.* **2013**, *2013*, 841–845.

APPENDICES

A. NMR Spectra

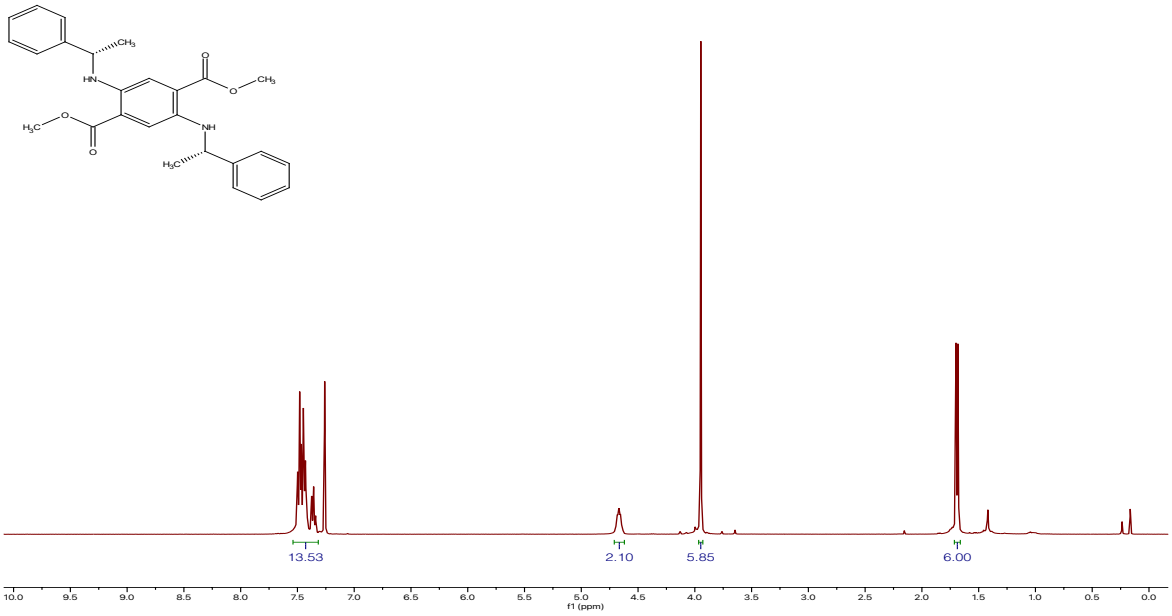

Figure 25 1H NMR Spectrum of **TP-AMBA-S**

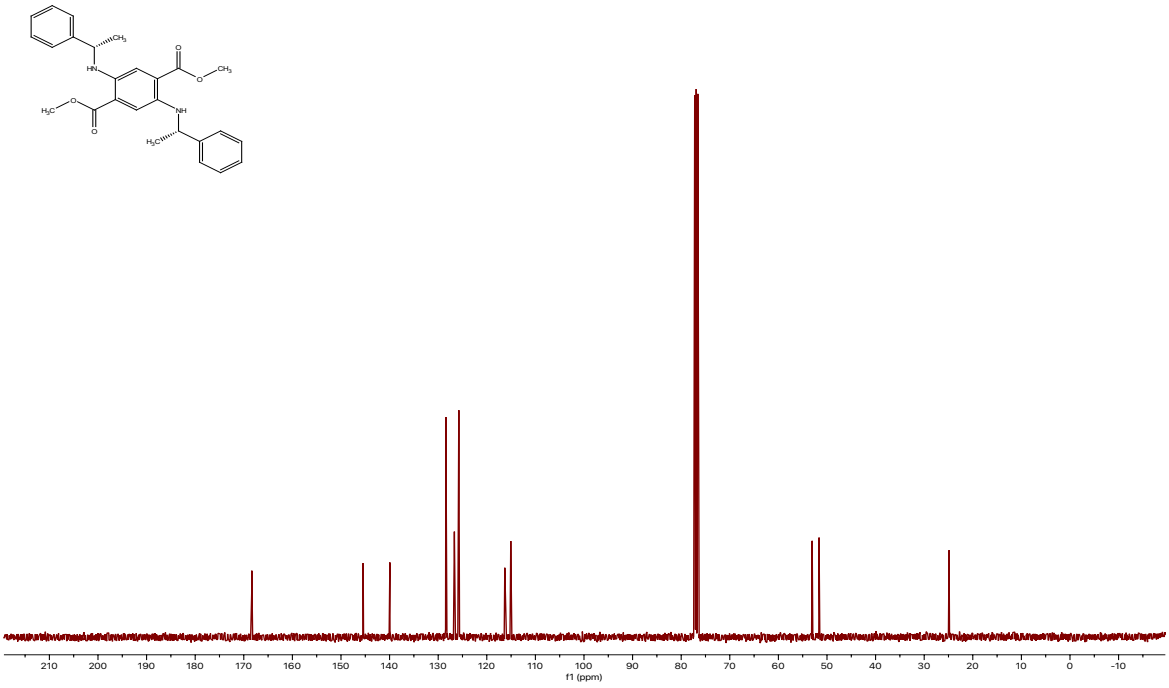

Figure 26 13C NMR Spectrum of **TP-AMBA-R**

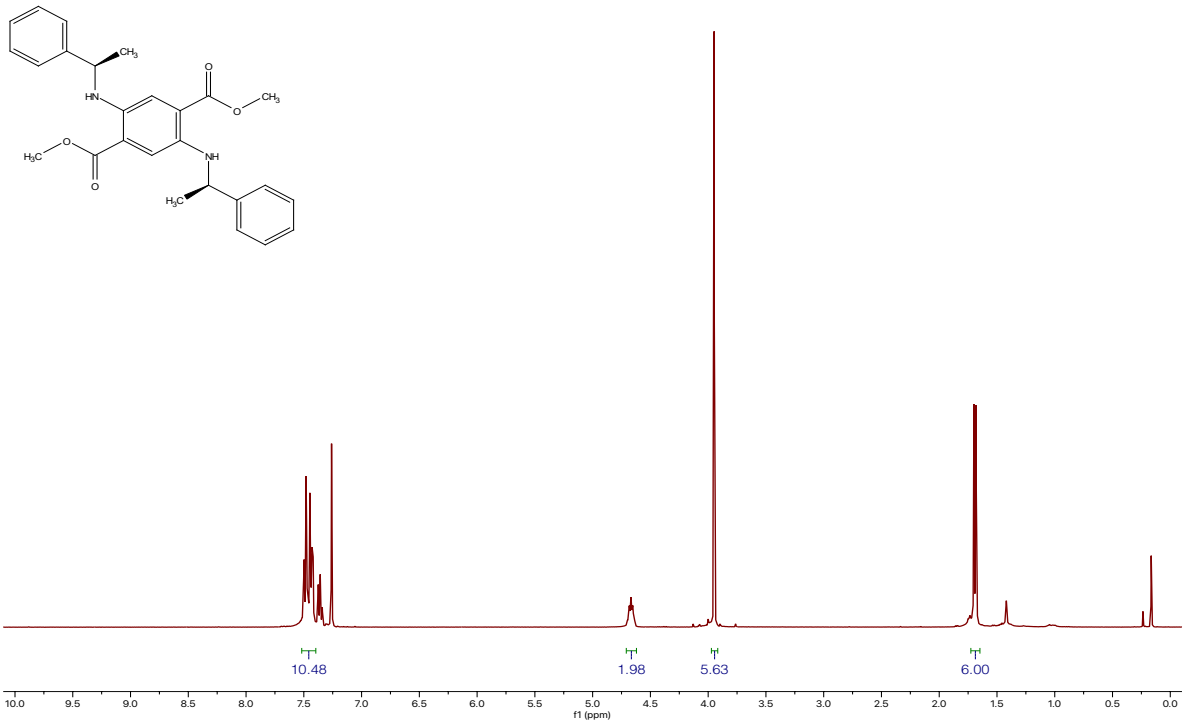

Figure 28 1H NMR Spectrum of **TP-AMBA-R**

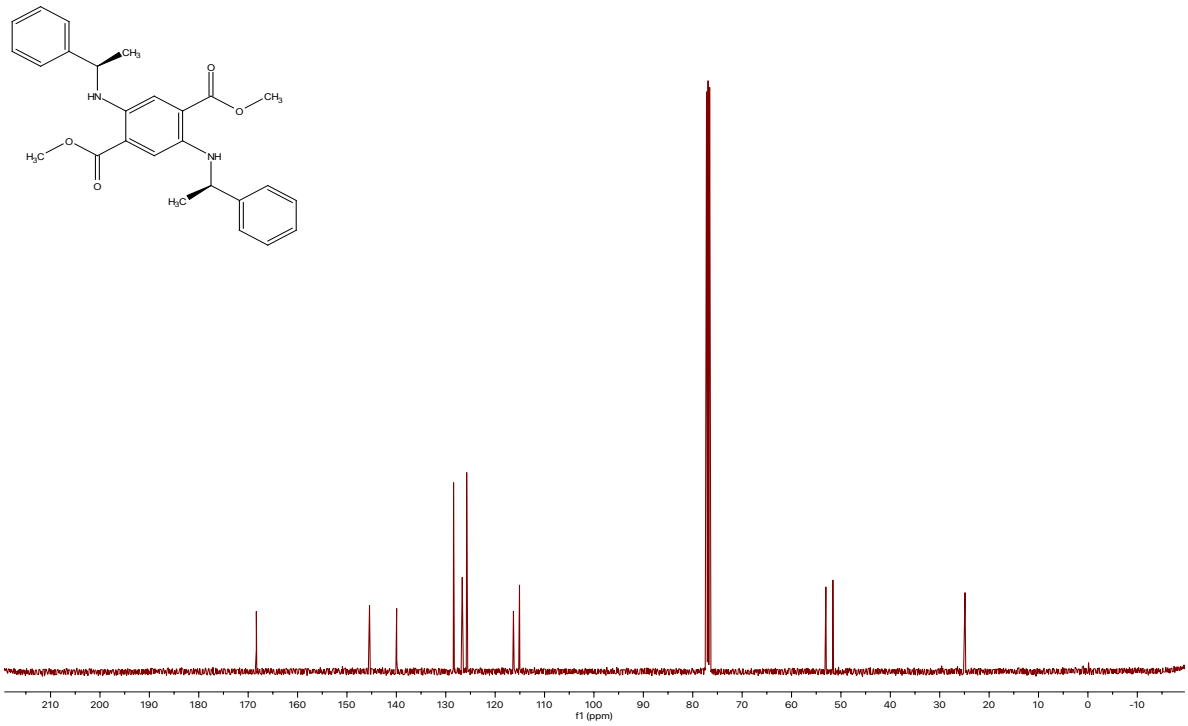

Figure 27 13C NMR Spectrum of **TP-AMBA-R**

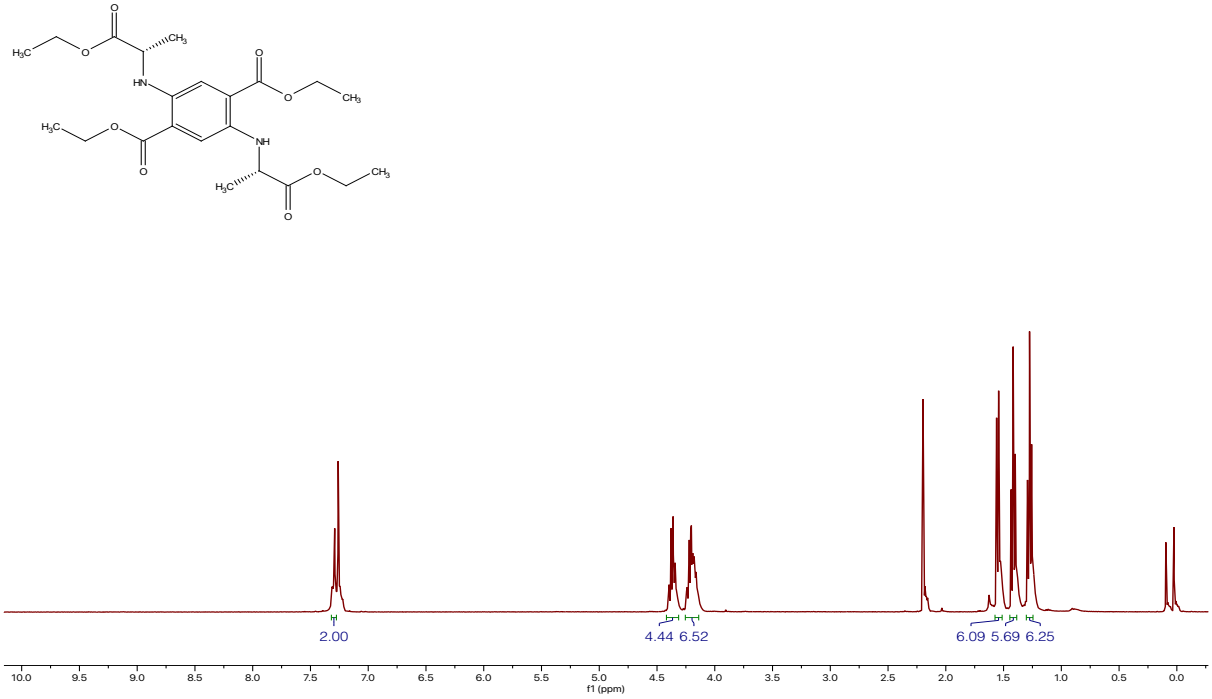

Figure 29 1H NMR Spectrum of **TP-ALA-S**

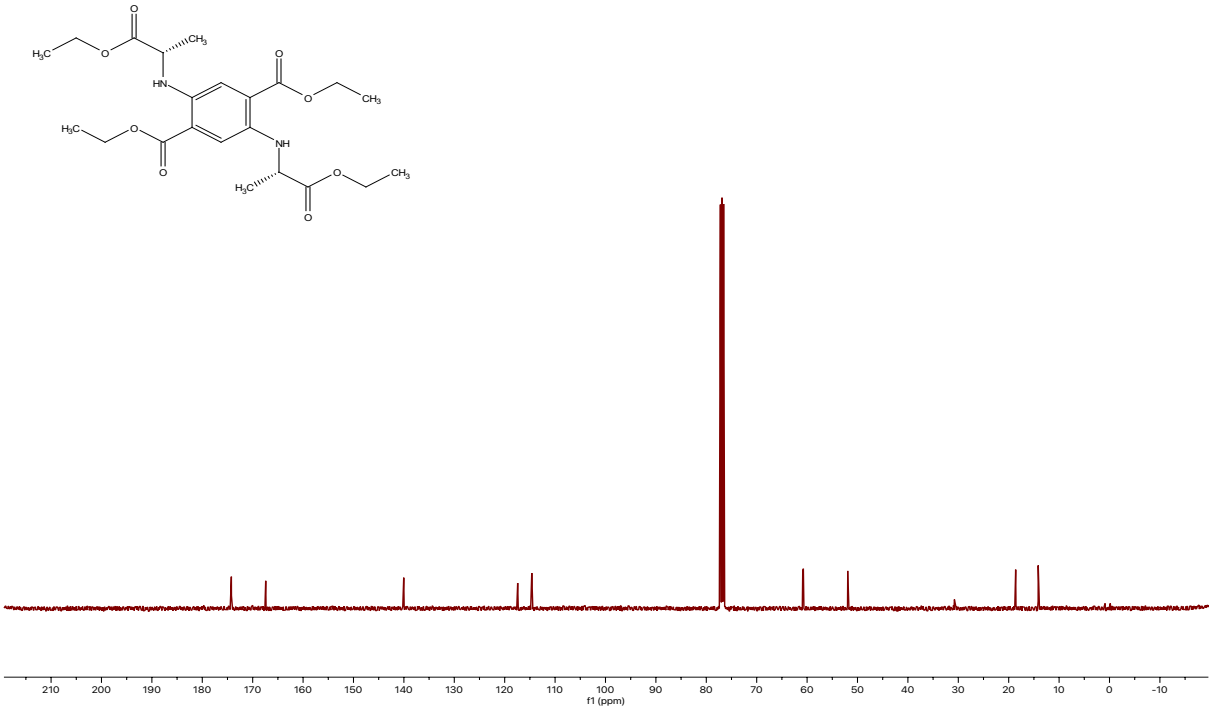

Figure 30 13C NMR Spectrum of **TP-ALA-S**

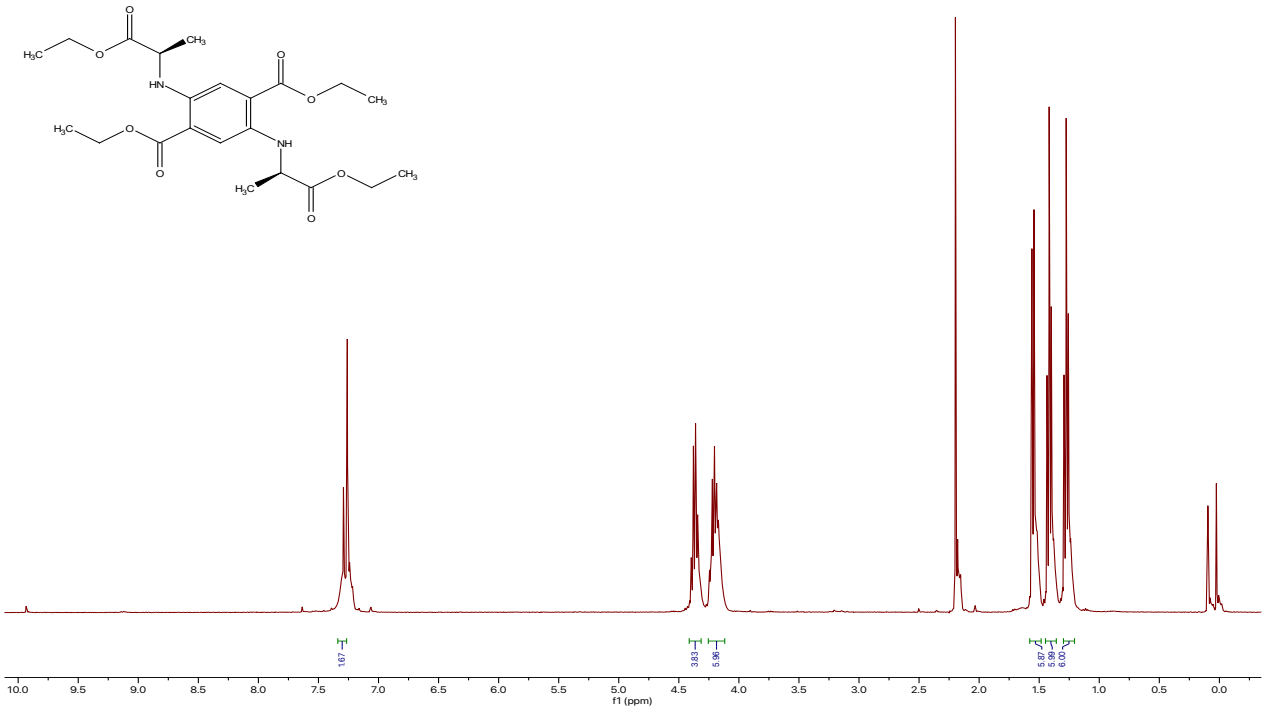

Figure 32 1H NMR Spectrum of **TP-ALA-R**

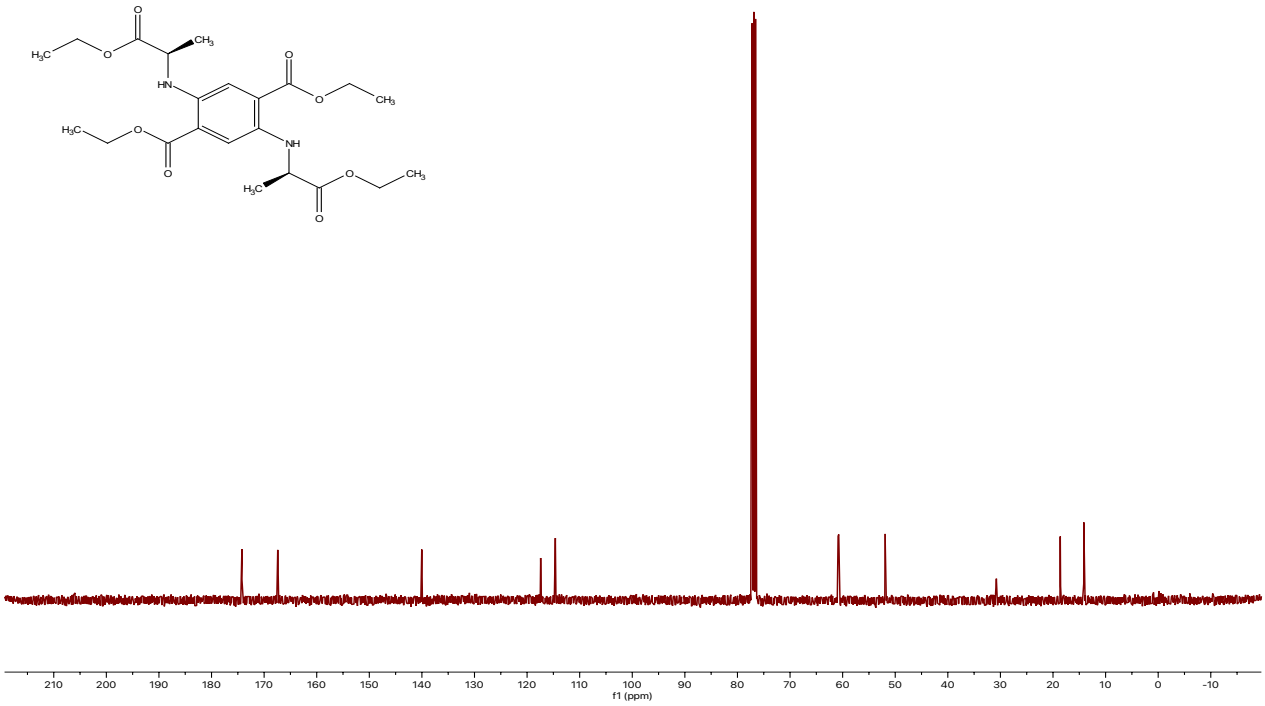

Figure 31 13C NMR Spectrum of **TP-ALA-R**

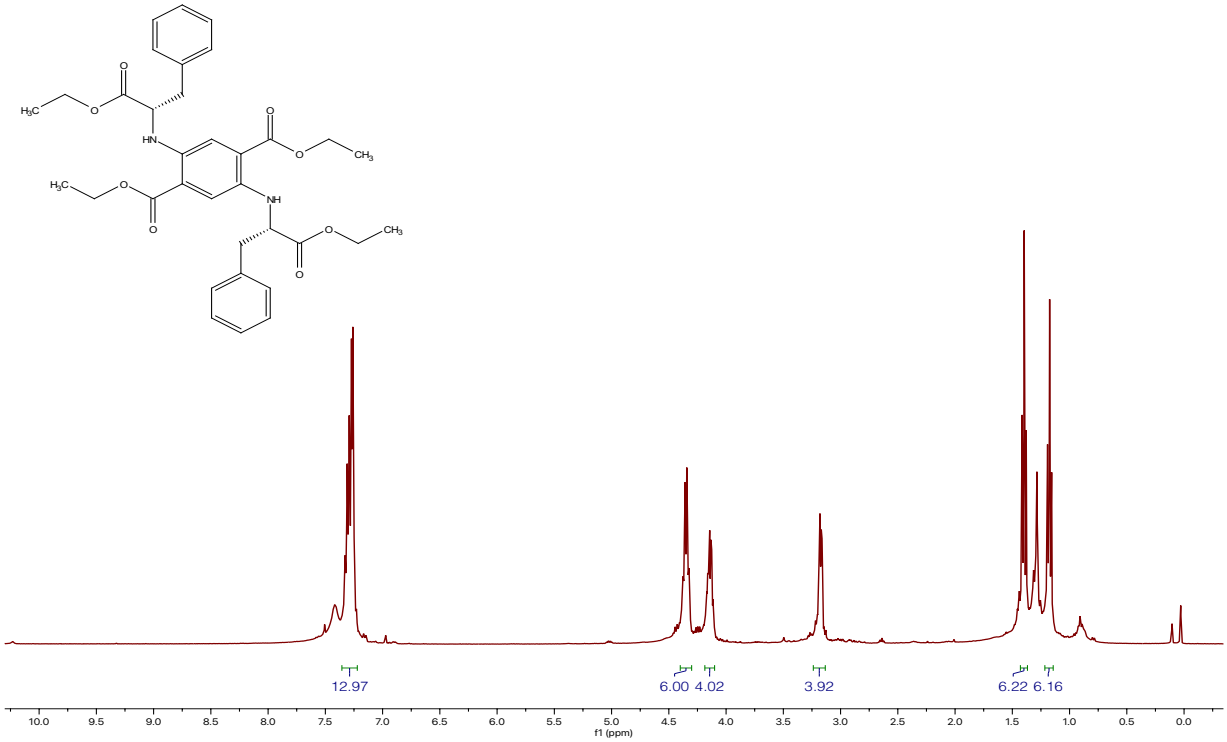

Figure 34 1H NMR Spectrum of **TP-PHE-S**

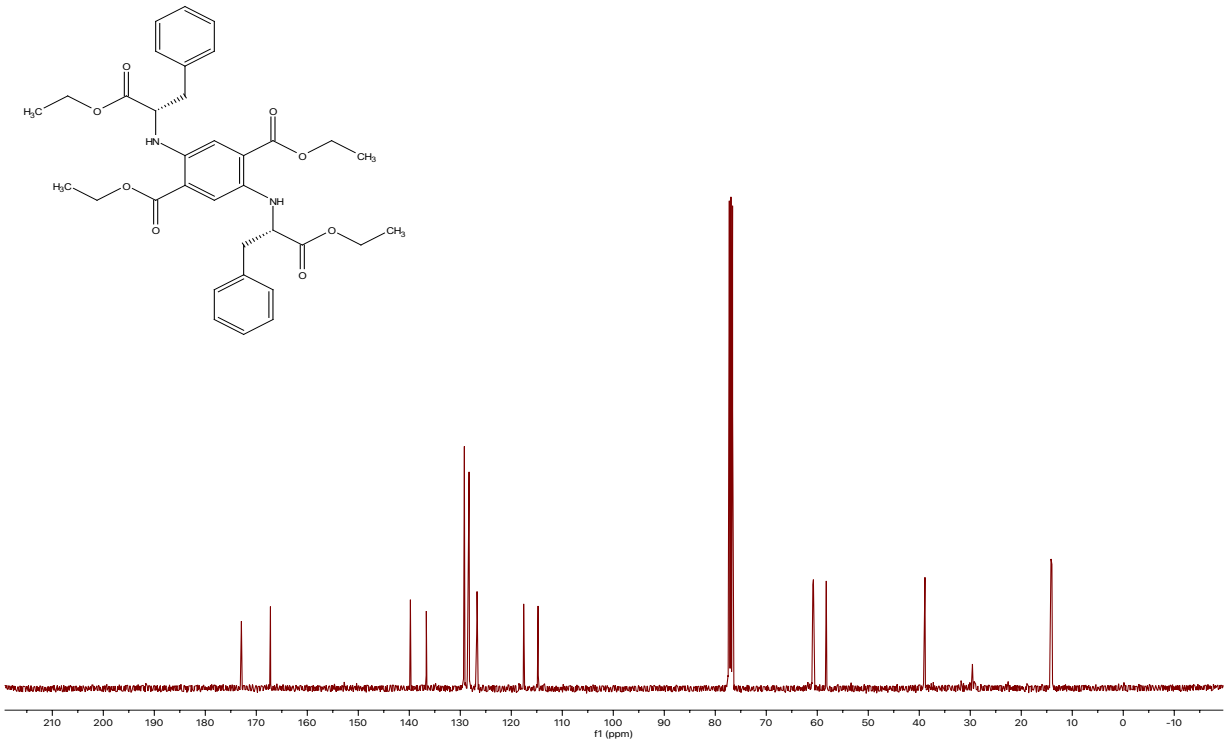

Figure 33 13C NMR Spectrum of **TP-PHE-S**

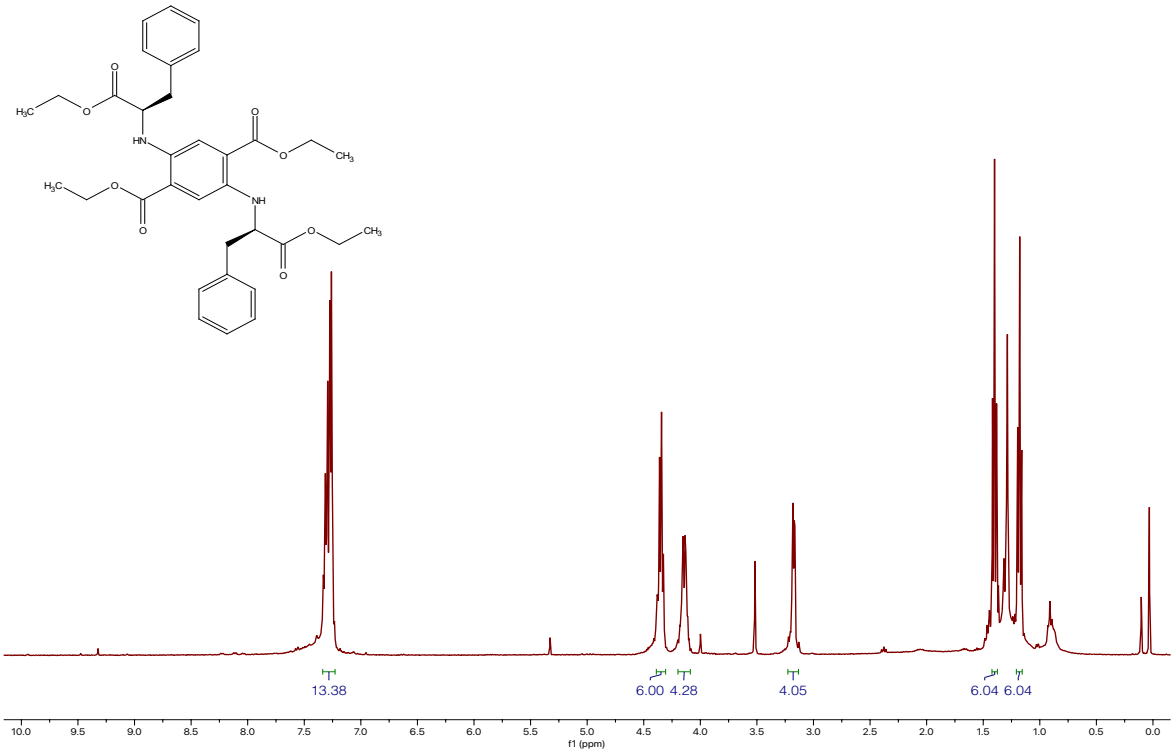

Figure 36 1H NMR Spectrum of **TP-PHE-R**

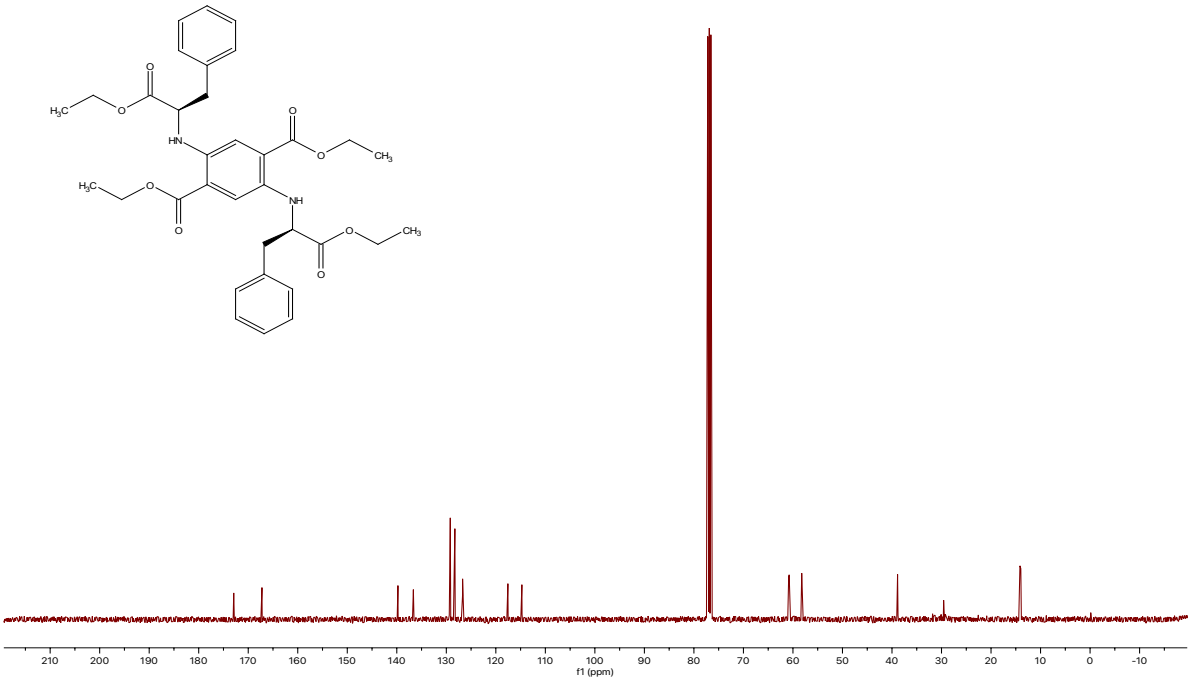

Figure 35 13C NMR Spectrum of **TP-PHE-R**

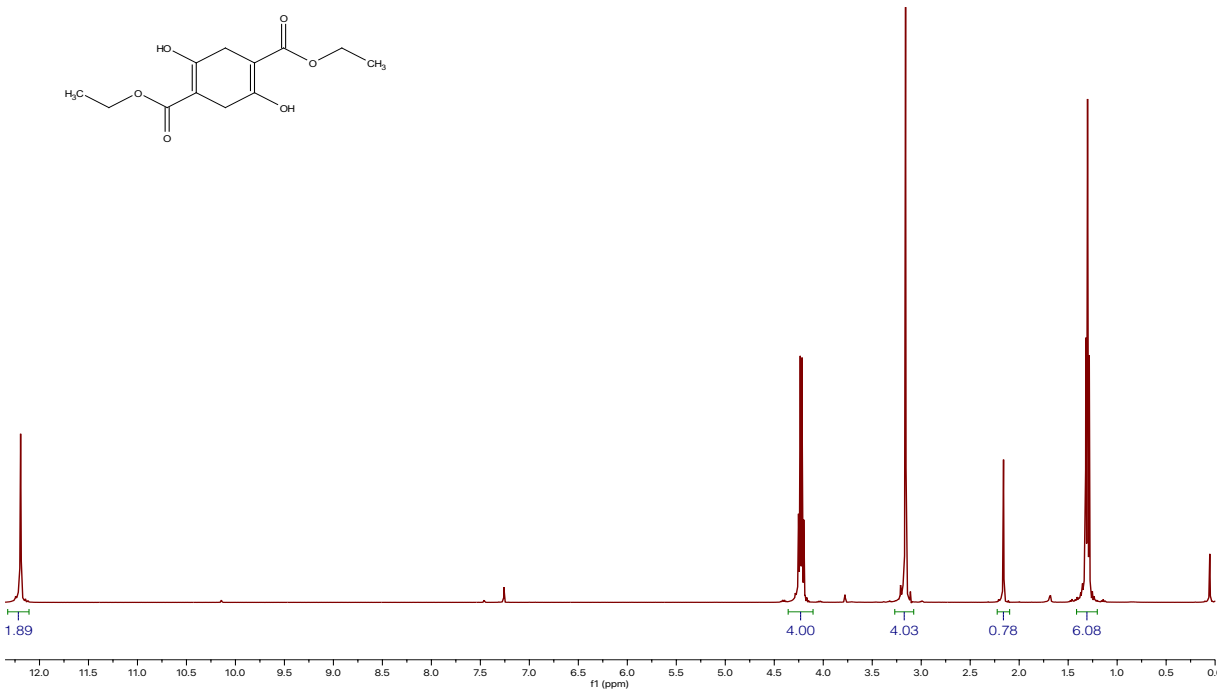

Figure 38 1H NMR Spectrum of **8** (diethyl succinylsuccinate)

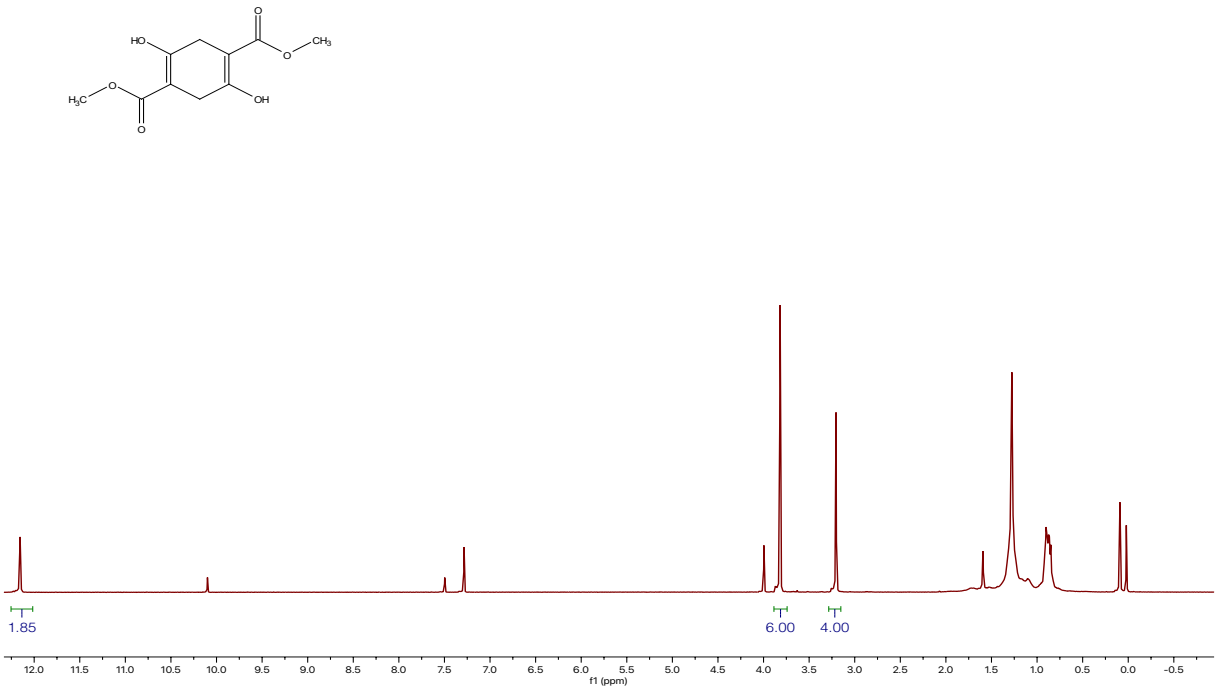

Figure 37 1H NMR Spectrum of **9** (diethyl succinylsuccinate)

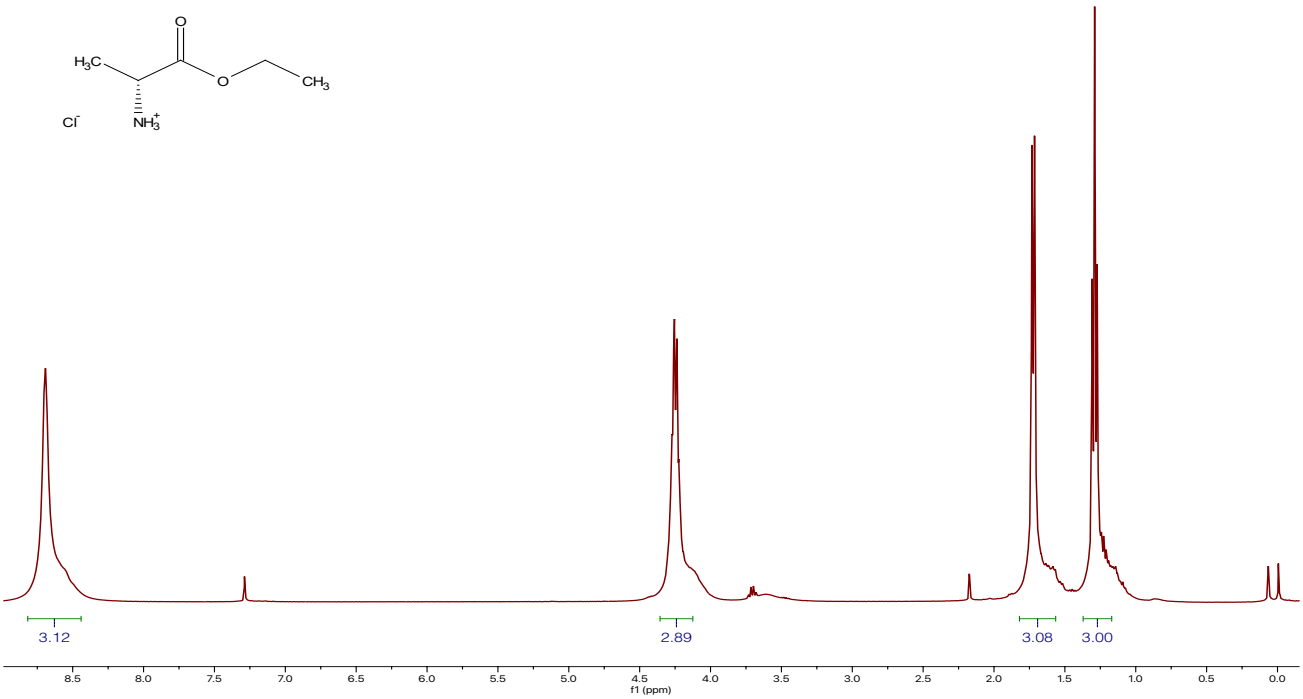

Figure 39 1H NMR Spectrum of L-alanine Ethyl Ester Hydrochloride

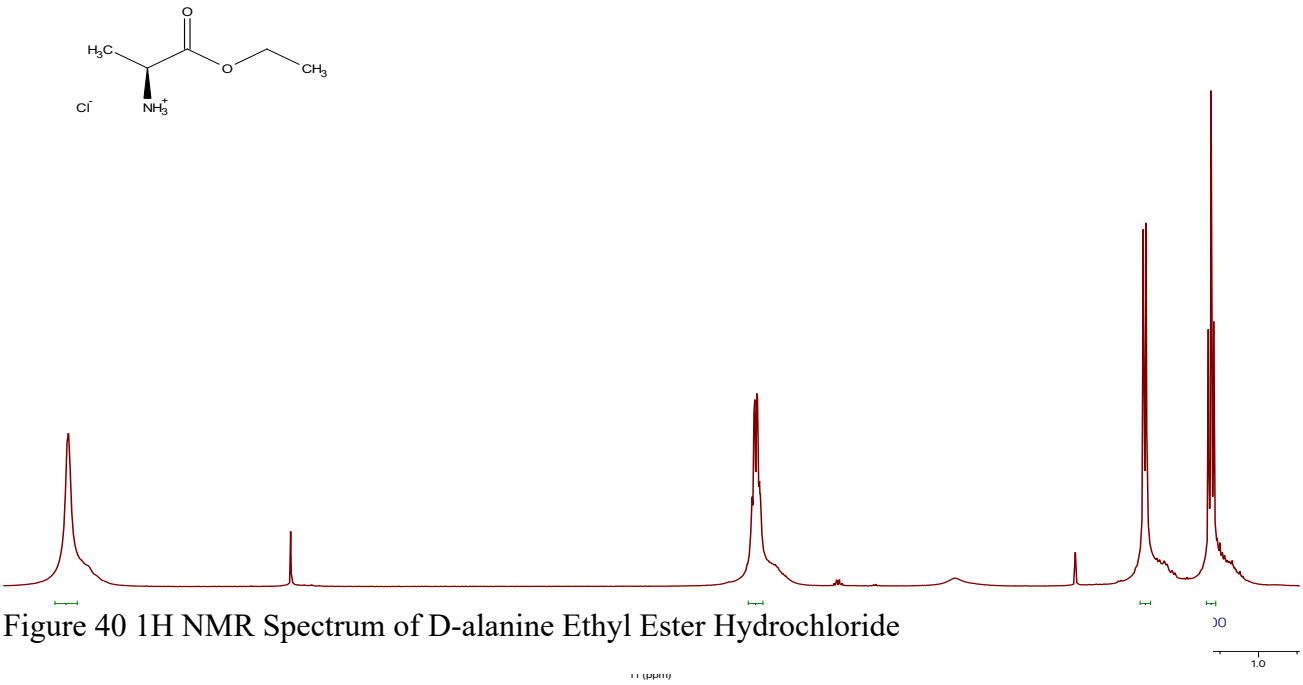

Figure 40 1H NMR Spectrum of D-alanine Ethyl Ester Hydrochloride

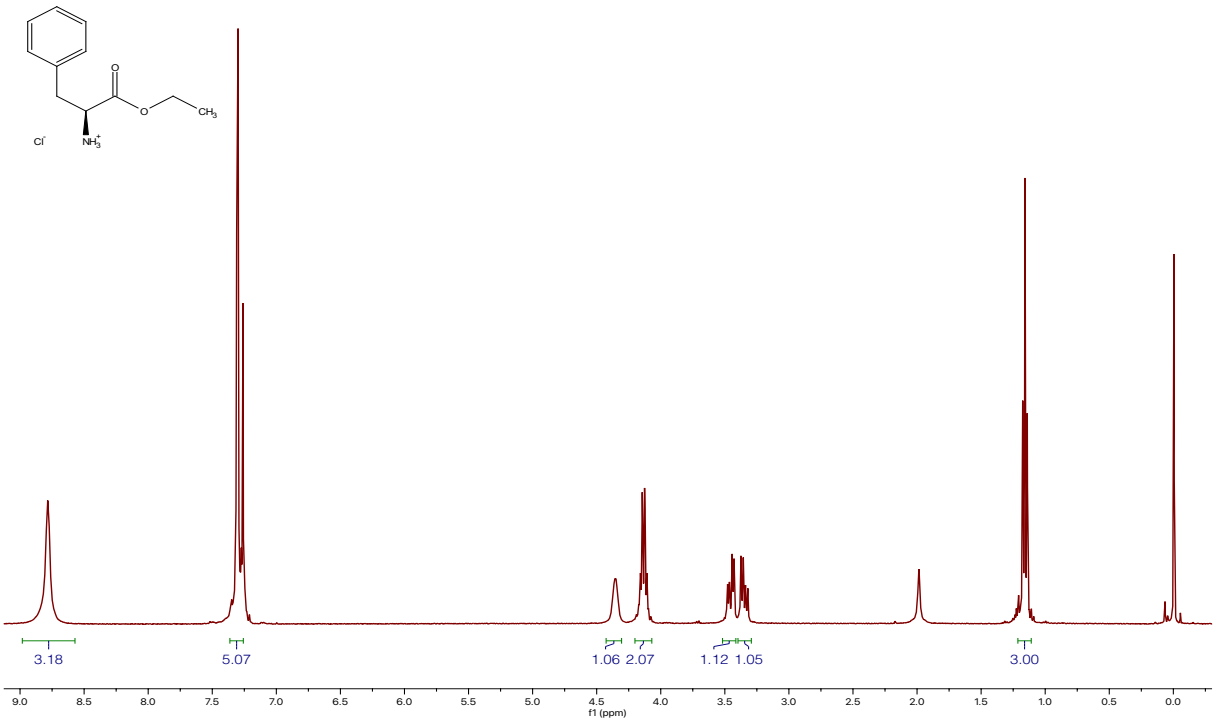

Figure 42 1H NMR Spectrum of D-phenylalanine Ethyl Ester Hydrochloride

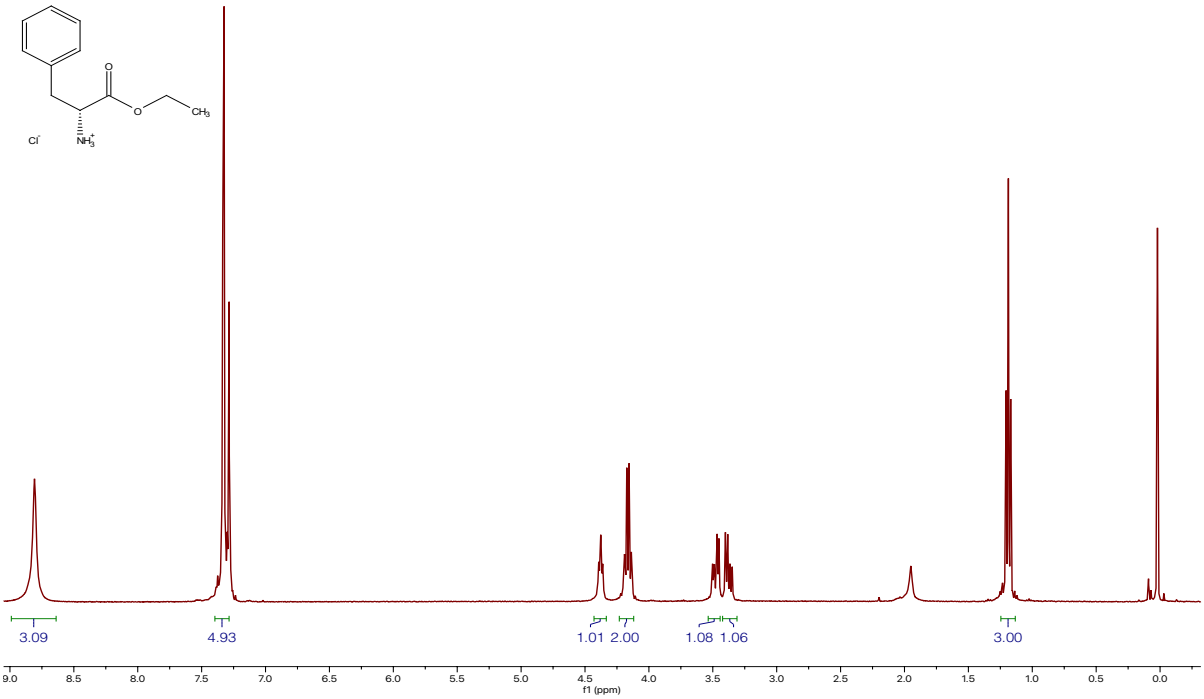

Figure 41 1H NMR Spectrum of L-phenylalanine Ethyl Ester Hydrochloride

B. HRMS Spectra

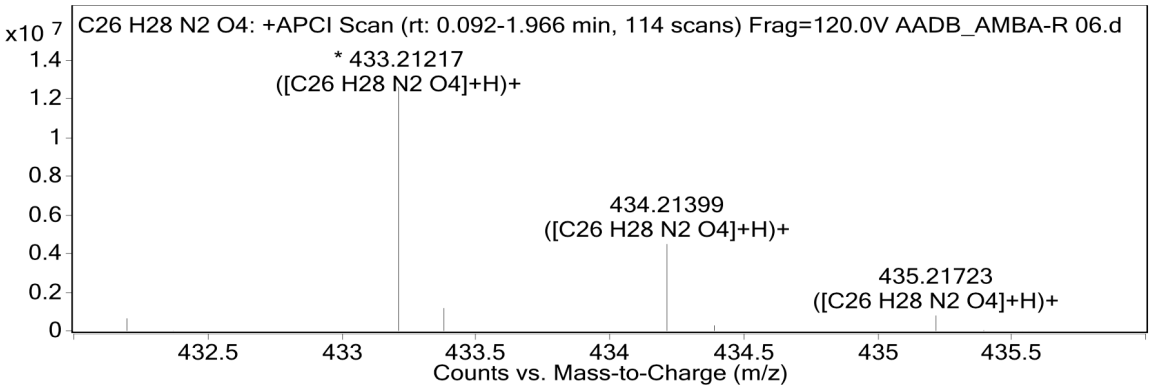

Figure 43 HRMS Spectrum of **TP-AMBA-R**

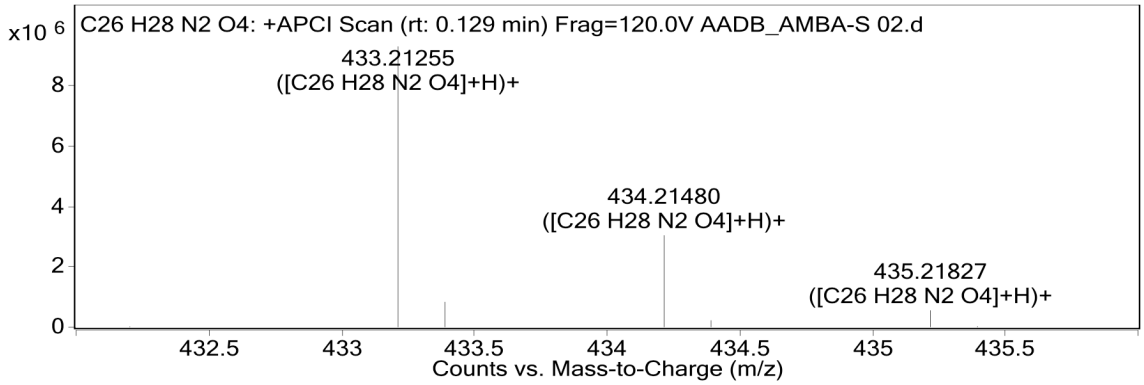

Figure 45 HRMS Spectrum of **TP-AMBA-S**

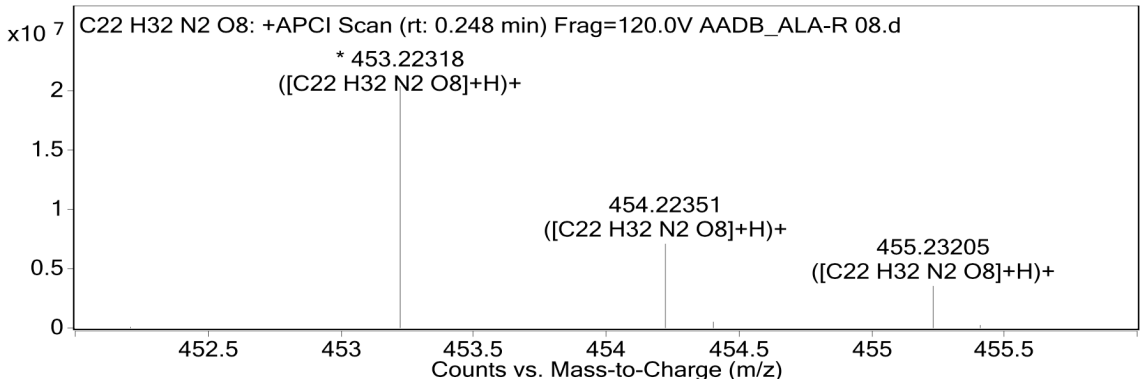

Figure 44 HRMS Spectrum of **TP-ALA-R**

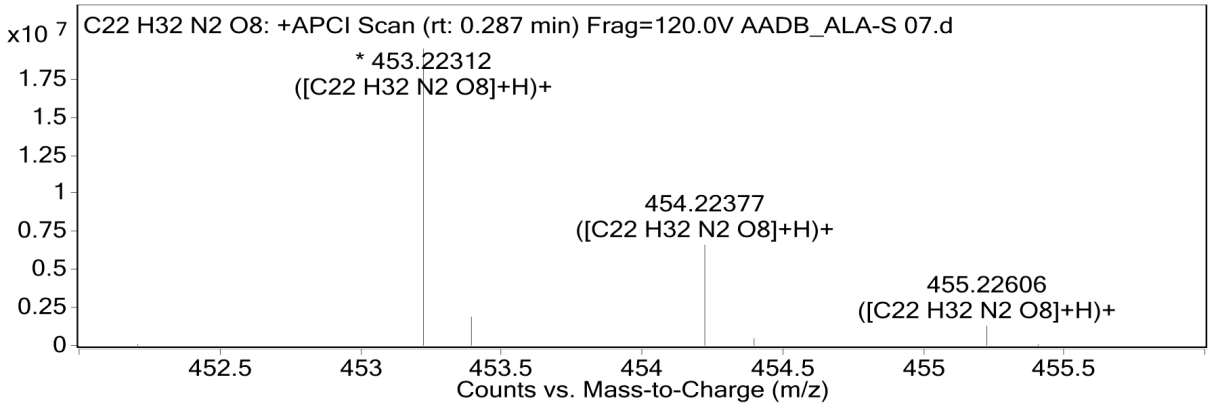

Figure 46 HRMS Spectrum of **TP-ALA-S**

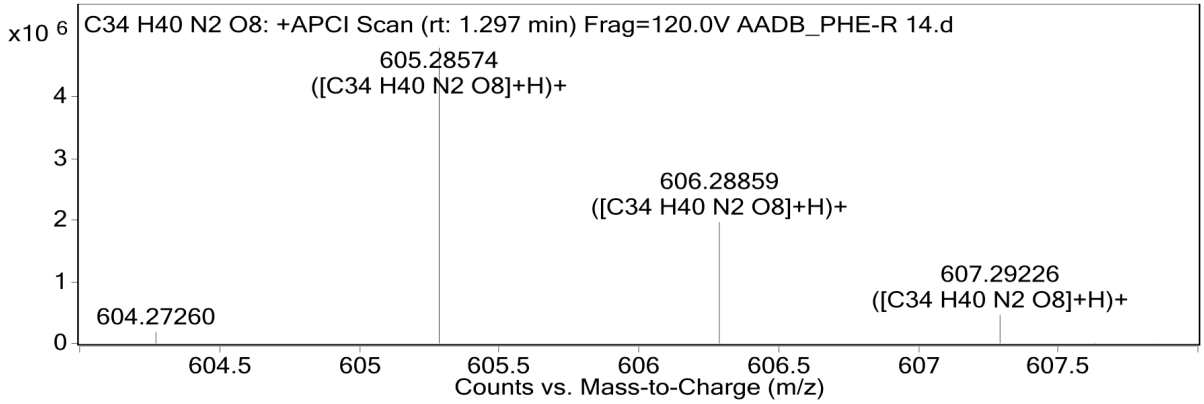

Figure 48 HRMS Spectrum of **TP-PHE-R**

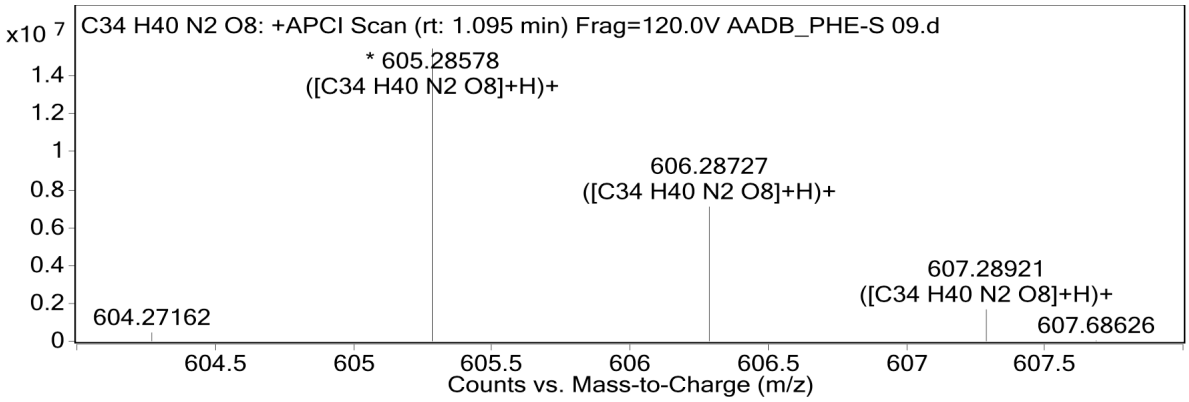

Figure 47 HRMS Spectrum of **TP-PHE-S**

C. IR Spectra

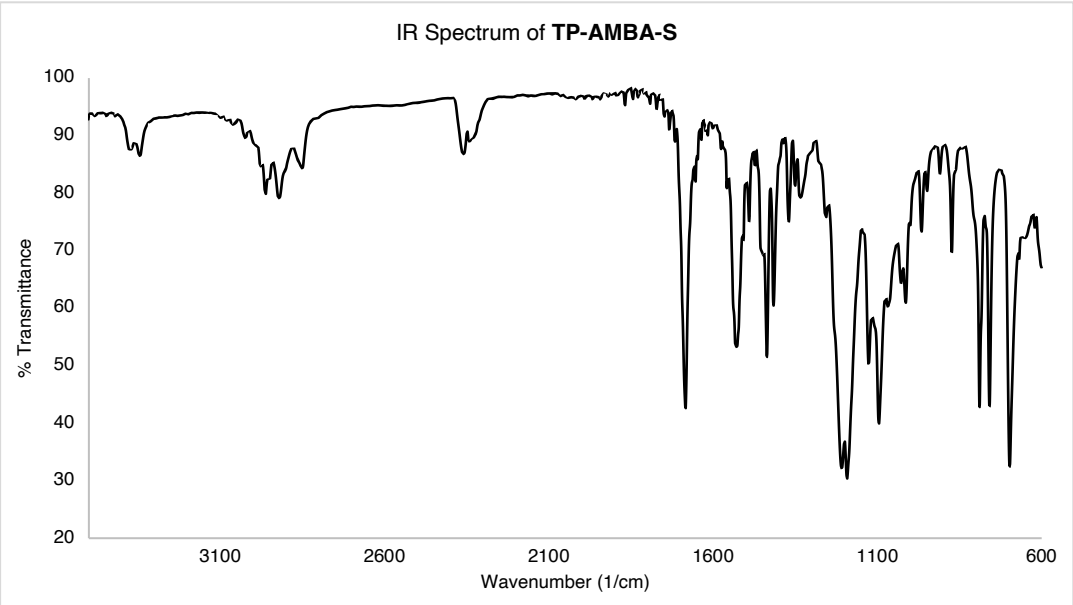
IR Spectrum of **TP-AMBA-S**
% Transmittance
100
90
80
70
60
50
40
30
20
3100
2600
2100
1600
1100
600
Wavenumber (1/cm)

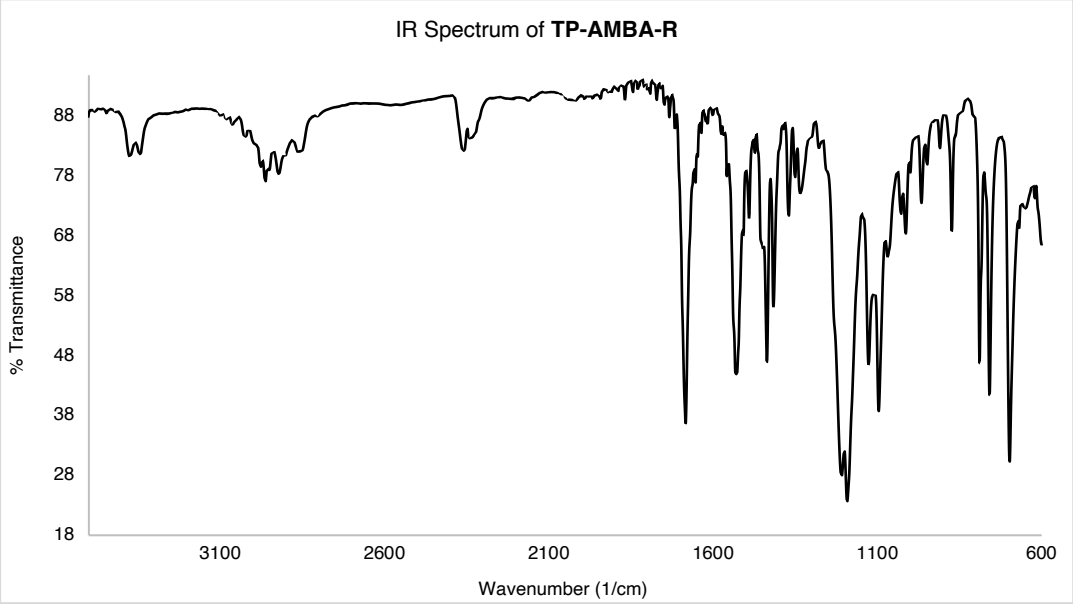
IR Spectrum of **TP-AMBA-R**
% Transmittance
88
78
68
58
48
38
28
18
3100
2600
2100
1600
1100
600
Wavenumber (1/cm)

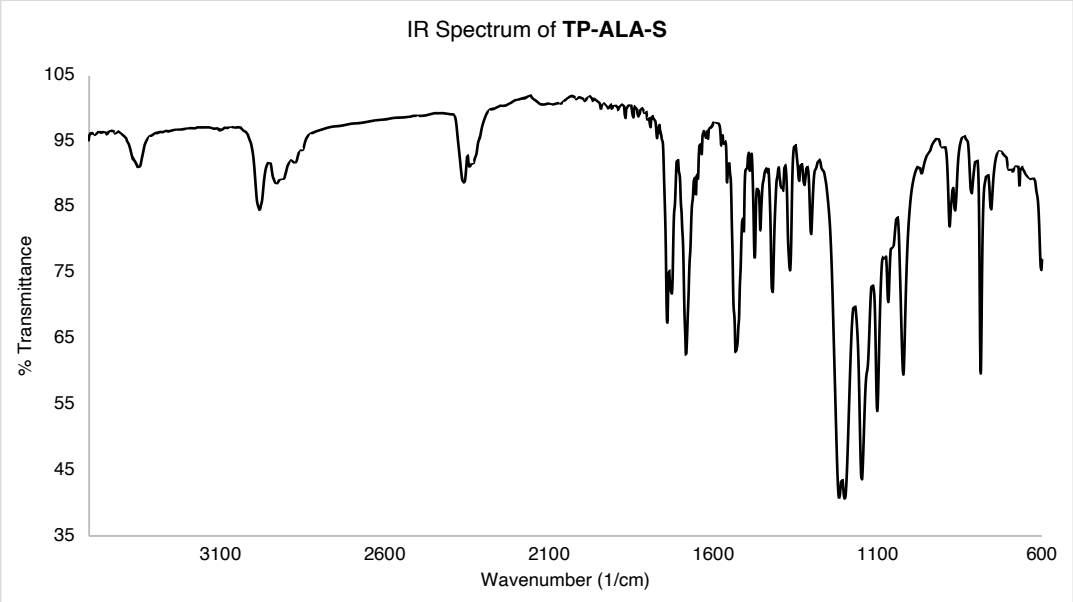
IR Spectrum of **TP-ALA-S**
105
95
85
75
65
55
45
35
% Transmittance
3100
2600
2100
1600
1100
600
Wavenumber (1/cm)

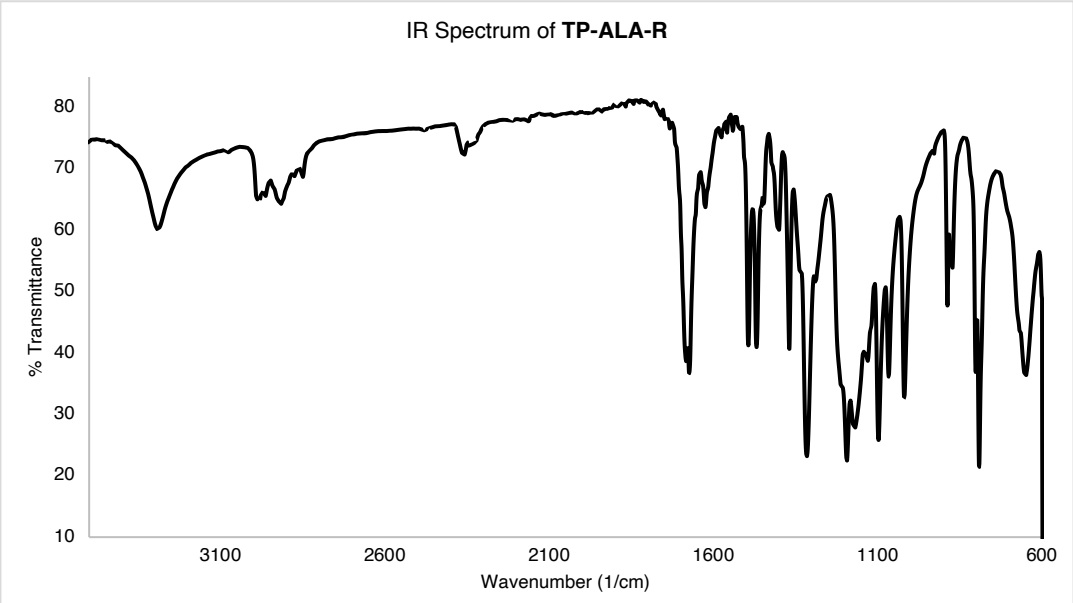
IR Spectrum of **TP-ALA-R**
80
70
60
50
40
30
20
10
% Transmittance
3100
2600
2100
1600
1100
600
Wavenumber (1/cm)

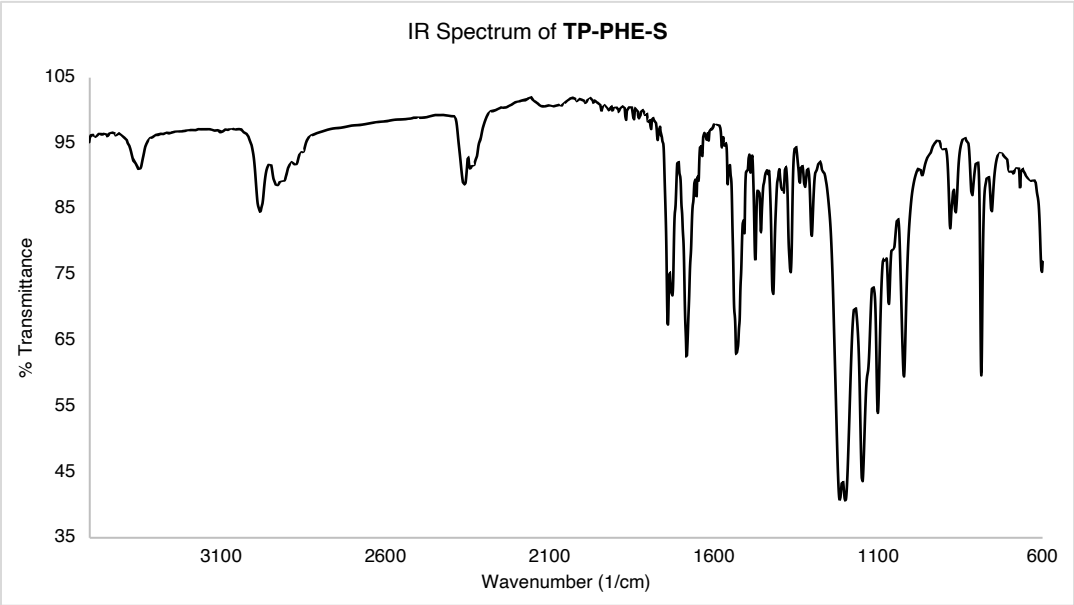
IR Spectrum of **TP-PHE-S**
% Transmittance
105
95
85
75
65
55
45
35
3100
2600
2100
1600
1100
600
Wavenumber (1/cm)

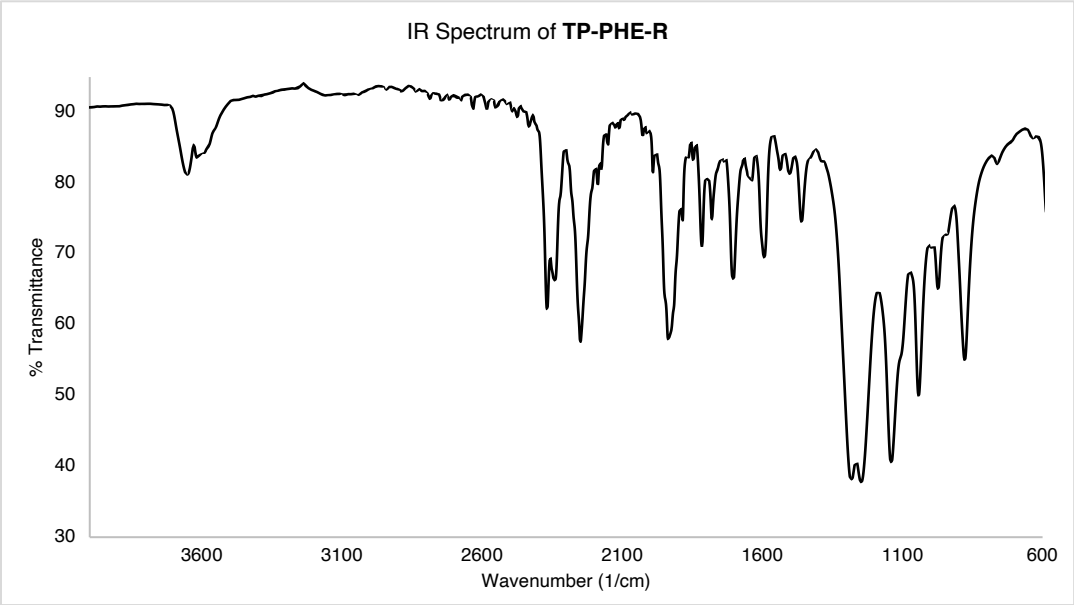
IR Spectrum of **TP-PHE-R**
% Transmittance
90
80
70
60
50
40
30
3600
3100
2600
2100
1600
1100
600
Wavenumber (1/cm)

D. XYZ Coordinates for Optimized Geometries

TP-AMBA-R

C	-1.445665	0.078738	-0.253918
C	-0.640407	1.251420	-0.231414
C	-0.764561	-1.143428	-0.236437
C	0.627024	-1.240015	-0.213920
C	1.432274	-0.067412	-0.210844
C	0.752082	1.154576	-0.212346
H	1.316399	2.080706	-0.180678
H	-1.327681	-2.070489	-0.228443
C	1.253061	-2.575142	-0.168998
O	0.364451	-3.578197	-0.288296
C	0.918574	-4.885324	-0.219842
O	2.444952	-2.798301	-0.034494
H	1.417681	-5.044481	0.742308
H	1.648460	-5.041567	-1.021429
N	2.802946	-0.139455	-0.210718
C	3.686574	1.007284	-0.168324
H	3.175752	-1.040564	0.065573
C	5.067990	0.574029	0.264624
H	3.317228	1.738626	0.576398
C	3.769807	1.699169	-1.531247
H	4.192762	1.005424	-2.269267
H	4.418533	2.583037	-1.475836
H	2.781832	2.014184	-1.889212
C	5.818074	1.387117	1.112881
C	5.644726	-0.602072	-0.221364
C	6.935163	-0.961682	0.150114
C	7.112618	1.034719	1.477647
C	7.673903	-0.144712	0.999650
H	8.684755	-0.427129	1.288889
H	7.365750	-1.887004	-0.229389
H	5.376625	2.308931	1.494749
H	7.682575	1.680022	2.144246
H	5.078186	-1.246970	-0.894638
C	-1.267817	2.585794	-0.194036
O	-2.465047	2.806997	-0.117382
O	-0.374494	3.590482	-0.245853
C	-0.931240	4.896362	-0.176413
H	-1.481464	5.033540	0.760892
H	-1.616669	5.073189	-1.012188
N	-2.815877	0.143035	-0.293864
C	-3.688262	-1.013549	-0.215768
H	-3.205673	1.052341	-0.070413
C	-5.058953	-0.585938	0.252455
H	-3.289171	-1.725264	0.531384
C	-3.791040	-1.730379	-1.563477
H	-4.229404	-1.056558	-2.310724
H	-4.432215	-2.617521	-1.481063
H	-2.806408	-2.044784	-1.931130
C	-5.706463	-1.285845	1.268566
C	-6.987466	-0.928201	1.675638
C	-7.637023	0.141787	1.070533
C	-6.999005	0.848251	0.055400
C	-5.722040	0.483997	-0.354173
H	-5.229988	1.039934	-1.153610
H	-5.196053	-2.120830	1.750293
H	-7.476915	-1.483724	2.474049
H	-8.637962	0.426957	1.389886
H	-7.499734	1.688235	-0.423493
H	0.077603	-5.572726	-0.331297
H	-0.084756	5.584316	-0.225504

TP-ALA-R

C	-1.442902	-0.034702	0.253953
C	-0.764659	1.187464	0.223322
C	0.624271	1.309218	0.249195
C	1.440182	0.148855	0.326151
C	0.762775	-1.073690	0.338727
C	-0.626182	-1.195973	0.295380
H	-1.315918	2.122364	0.168645
C	1.105505	2.711647	0.164796
N	2.813968	0.197866	0.402603
H	1.314977	-2.009052	0.375962
C	-1.105011	-2.600943	0.275811
N	-2.818301	-0.078510	0.260434
O	-2.438692	-2.716129	0.111996
O	-0.387468	-3.572724	0.375138
C	-2.954791	-4.052511	0.043892
O	2.447629	2.818800	0.098627
O	0.383708	3.684921	0.138302
C	2.976948	4.144978	-0.034248
C	-3.657962	1.069444	0.065847
H	-3.262400	-0.974443	0.097531
C	3.664705	-0.954117	0.295897
H	3.260817	1.081004	0.185021
C	-4.444367	-3.942307	-0.145908
H	-2.462069	-4.575790	-0.785918
H	-2.683535	-4.582168	0.966288
H	-4.891221	-4.940576	-0.220959
H	-4.909520	-3.415247	0.695535
H	-4.682654	-3.382757	-1.058082
C	4.477342	4.018273	-0.058051
H	2.576586	4.589694	-0.954786
H	2.617723	4.754787	0.804409
H	4.939091	5.002671	-0.197874
H	4.847838	3.591780	0.881824
H	4.801679	3.355832	-0.868944
C	5.002600	-0.477685	-0.239255
C	3.861426	-1.675457	1.632055
H	3.270694	-1.676056	-0.443571
O	5.828442	-1.504371	-0.455341
O	5.297256	0.679517	-0.435393
C	7.132724	-1.162844	-0.953369
C	7.913622	-2.443255	-1.076881
H	7.015182	-0.649439	-1.916573
H	7.599421	-0.451894	-0.259792
H	8.917608	-2.238148	-1.465651
H	8.015655	-2.933969	-0.102086
H	7.415636	-3.140150	-1.760650
H	4.489481	-2.564909	1.514491
H	4.330220	-0.996880	2.355683
H	2.892272	-1.981406	2.041267
C	-4.987679	0.575410	-0.470459
C	-3.893765	1.863189	1.355221
H	-3.238914	1.748554	-0.698901
O	-5.766746	1.602121	-0.823139
O	-5.309996	-0.588351	-0.550528
C	-7.085483	1.274126	-1.293913
H	-4.495138	2.758465	1.164269
H	-4.409424	1.233424	2.091317
H	-2.936042	2.169667	1.789997
H	-7.376637	2.133617	-1.906311
H	-7.023213	0.385395	-1.932237
C	-8.031563	1.061216	-0.137976
H	-9.050107	0.893011	-0.507601
H	-7.732334	0.185821	0.449236
H	-8.044902	1.939030	0.518771

TP-PHE-R

C	-1.266043	-0.515993	-0.661437
C	-0.090009	-1.313416	-0.636856
C	-1.077526	0.869802	-0.625858
C	0.181253	1.471378	-0.596894
C	1.356872	0.673849	-0.627134
C	1.167323	-0.711151	-0.636281
H	2.029484	-1.368882	-0.645706
H	-1.939090	1.529549	-0.623298
C	0.277226	2.942827	-0.513497
O	-0.919906	3.548021	-0.443860
O	1.316831	3.580512	-0.495460
C	-0.884073	4.979094	-0.367203
C	-2.302881	5.458592	-0.212468
H	-0.409694	5.368928	-1.277510
H	-0.250224	5.273648	0.478927
H	-2.922891	5.126922	-1.053848
H	-2.329805	6.553697	-0.177264
H	-2.745871	5.076041	0.714692
C	-0.176536	-2.786302	-0.579495
O	-1.207147	-3.435922	-0.631108
O	1.022929	-3.377710	-0.442867
C	1.009969	-4.809635	-0.391780
C	2.422021	-5.261497	-0.128197
H	0.621155	-5.193572	-1.344368
H	0.316044	-5.132536	0.394524
H	3.103568	-4.890404	-0.903837
H	2.474840	-6.356229	-0.119186
H	2.774769	-4.894782	0.844354
N	2.617143	1.221491	-0.663347
C	3.807884	0.441863	-0.438869
C	5.025445	1.248531	-0.842274
H	3.817747	-0.439574	-1.096904
C	3.958873	-0.021278	1.030260
O	4.968916	2.480061	-0.308998
O	5.942536	0.839083	-1.506847
C	6.065939	3.352683	-0.616348
C	5.755059	4.688250	0.004383
H	6.173867	3.411676	-1.706901
H	6.989139	2.906893	-0.221886
H	4.811589	5.085160	-0.388649
H	6.553493	5.406376	-0.214635
H	5.659097	4.600143	1.092846
N	-2.521789	-1.072214	-0.737083
C	-3.729165	-0.327900	-0.480515
C	-3.924360	0.007453	1.015494
C	-4.922307	-1.116099	-0.985466
H	-3.735931	0.601578	-1.068065
O	-5.792910	-0.681379	-1.694585
O	-4.903226	-2.365609	-0.492205
C	-6.001844	-3.204912	-0.878826
C	-5.772964	-4.554858	-0.253779
H	-6.041244	-3.251278	-1.974544
H	-6.934922	-2.734511	-0.540323
H	-4.826935	-4.986574	-0.600473
H	-6.585676	-5.240037	-0.520698
H	-5.731991	-4.477246	0.839023
H	2.668931	2.223817	-0.506386
H	-2.561385	-2.081627	-0.623898
C	5.053782	-1.029319	1.207454
H	2.993833	-0.447063	1.340443
H	4.129593	0.870428	1.650325
C	4.813191	-2.378157	0.935054
C	6.336974	-0.641258	1.591346
C	7.357568	-1.578224	1.708131
C	5.830907	-3.317526	1.048363
C	7.106589	-2.919079	1.437241
H	7.903883	-3.654480	1.530308
H	8.353424	-1.259820	2.011912
H	6.534009	0.412099	1.801457
H	3.807963	-2.690206	0.637659
H	5.629323	-4.366818	0.835039
C	-5.162451	0.815561	1.266195
H	-3.028318	0.549979	1.350809
H	-3.952565	-0.941339	1.569617
C	-6.332589	0.215982	1.731931
C	-7.491737	0.963787	1.909319
C	-7.496268	2.323500	1.617785
C	-6.335471	2.931831	1.148796
C	-5.179857	2.180971	0.975230
H	-4.266879	2.655836	0.609242
H	-8.403371	2.909183	1.756003
H	-6.330646	3.996184	0.918278
H	-6.328605	-0.850990	1.962570
H	-8.396135	0.482313	2.277967

11

C	-1.425282	1.483125	0.134979
C	-1.469312	0.065112	0.241862
C	-0.158219	2.063581	0.015839
C	1.021454	1.318195	-0.000502
C	0.977422	-0.099812	0.106320
C	-0.289652	-0.680274	0.225451
H	-0.375788	-1.758578	0.309774
N	2.106778	-0.872569	0.094533
H	-0.072076	3.141874	-0.068626
N	-2.554670	2.255843	0.146432
C	2.313902	2.015475	-0.129358
O	2.188024	3.350400	-0.220274
C	3.412037	4.081443	-0.347415
O	3.409424	1.477106	-0.155208
H	3.946211	3.730800	-1.240236
H	4.051523	3.860130	0.517161
C	3.053491	5.541438	-0.433404
H	2.412052	5.734935	-1.301115
H	3.959794	6.149776	-0.532585
H	2.518120	5.865146	0.466817
C	-2.761748	-0.632145	0.371035
O	-3.857240	-0.093733	0.397334
O	-2.635894	-1.967074	0.461813
C	-3.859902	-2.698082	0.589307
C	-3.501372	-4.158080	0.675288
H	-4.499576	-2.476818	-0.275145
H	-4.393852	-2.347349	1.482221
H	-2.966165	-4.481810	-0.225021
H	-4.407673	-4.766396	0.774628
H	-2.859793	-4.351587	1.542893
H	2.985045	-0.377872	0.006925
C	2.084976	-2.301010	0.203811
H	-3.432849	1.761231	0.235386
C	-2.532681	3.684521	0.040313
H	-1.976355	4.158716	0.865757
H	-3.561489	4.054713	0.076065
H	-2.084586	4.028898	-0.906451
H	1.529614	-2.777139	-0.621158
H	1.635960	-2.643399	1.150871
H	3.113896	-2.671064	0.169914

12

C	0.119768	-1.427127	-0.133897
C	-1.149744	-0.798007	-0.013612
C	1.239116	-0.588710	-0.115835
C	1.149870	0.798269	0.013697
C	-0.119637	1.427389	0.134028
C	-1.238986	0.588978	0.115921
H	-2.227997	1.024759	0.218587
N	-0.263312	2.780954	0.274638
H	2.228124	-1.024487	-0.218542
N	0.263500	-2.780688	-0.274392
C	2.383808	1.603213	0.025583
O	3.496031	0.850327	-0.040665
C	4.734453	1.556390	0.000229
O	2.441181	2.820156	0.090023
C	-2.383672	-1.602958	-0.025557
O	-2.441030	-2.819899	-0.089994
O	-3.495938	-0.850100	0.040637
C	-4.734287	-1.556290	-0.000209
H	0.584557	3.328408	0.207829
C	-1.541718	3.429869	0.307478
H	-0.584358	-3.328191	-0.207959
C	1.541919	-3.429555	-0.307562
H	2.136377	-3.129660	-1.185295
H	1.386690	-4.510746	-0.364428
H	2.145854	-3.218716	0.591811
H	-2.136374	3.129982	1.185076
H	-2.145464	3.219063	-0.592034
H	-1.386468	4.511054	0.364415
C	-5.854381	-0.561609	-0.020299
H	-4.805287	-2.225337	0.868799
H	-4.740993	-2.199894	-0.892467
C	-7.072127	-0.888501	0.573902
C	-5.720118	0.670924	-0.659838
C	-6.788444	1.559083	-0.701984
C	-8.144319	-0.004886	0.523292
C	-8.004057	1.223240	-0.113841
H	-4.767699	0.934005	-1.118053
H	-8.839631	1.920112	-0.148349
H	-6.670543	2.521327	-1.197882
H	-7.179462	-1.846518	1.084331
H	-9.089131	-0.272911	0.993145
C	5.854381	0.561516	0.020308
H	4.741190	2.199958	0.892512
H	4.805561	2.225448	-0.868761
C	5.720021	-0.670757	0.660350
C	6.788103	-1.559198	0.702417
C	8.003589	-1.223908	0.113683
C	8.143957	0.003955	-0.523927
C	7.071990	0.887858	-0.574456
H	7.179405	1.845657	-1.085276
H	8.838976	-1.921007	0.148120
H	9.088666	0.271543	-0.994237
H	4.767698	-0.933406	1.119013
H	6.670123	-2.521235	1.198697

E. Comparison of Calculated Oscillator Strengths against Experimental UV-Vis Spectra

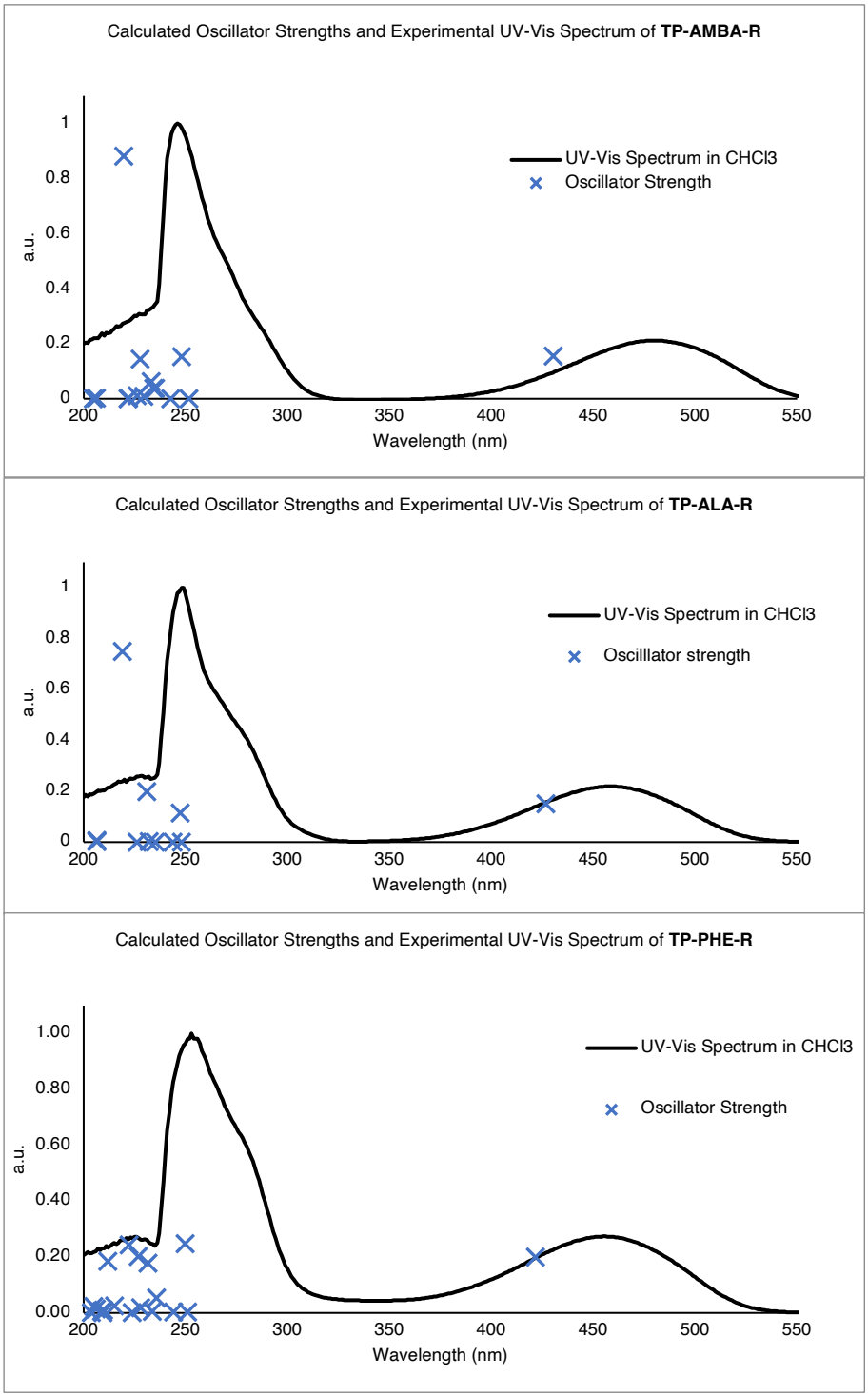

F. Comparison of Calculated Rotatory Strengths against Experimental CD Spectra